

Grant agreement no: 101097101

TERahertz ReconfigurAble METAsurfaces for ultra-high rate wireless communications

TERRAMETA

Deliverable D2.1

Requirements, use cases, and scenario specifications

Technical Manager: George Alexandropoulos

Organization: NKUA

Project Coordinator: Luís Pessoa

Organization: INESC TEC

Start date of project: 01-01-2023

Date of issue: 07-07-2023

Due date: 30-06-2023

Document Reference:

TERRAMETA Deliverable 2.1 - Requirements, use cases, and scenario specifications

Leader in charge of deliverable: Ryan Husbands, BT

<i>Dissemination level</i>		
PU	Public	X
CO	Confidential, only for members of the consortium (including the Commission Services)	

The TERRAMETA project has received funding from the Smart Networks and Services Joint Undertaking (SNS JU) under the European Union's Horizon Europe research and innovation programme under Grant Agreement No 101097101, including top-up funding by UK Research and Innovation (UKRI) under the UK government's Horizon Europe funding guarantee.



Views and opinions expressed are however those of the authors only and do not necessarily reflect those of the European Union, SNS JU or UKRI. The European Union, SNS JU or UKRI cannot be held responsible for them.

Table of Contents

1.	Statement of independence.....	6
2.	Abbreviations	7
3.	Executive summary.....	10
4.	Introduction	11
4.1.	WP2 approach and relation to other WPs.....	11
4.2.	Identified use cases and mapping to WPs	12
5.	THz and RISs in 6G Networks	14
5.1.	Introduction to THz.....	14
5.1.1.	THz-enabled Use Cases.....	15
5.1.2.	Relevance of THz in 6G Requirements.....	16
5.1.3.	Challenges in THz.....	16
5.2.	Definition of RISs.....	17
5.2.1.	DMAs.....	22
5.2.2.	T-RIS: Conformal Array	23
5.2.1.	Holographic MIMO	24
5.3.	THz RISs in 6G	25
6.	Deployment Scenarios and Use Cases.....	26
6.1.	Different Kinds of Scenarios under 6G	26
6.2.	Indoor and Outdoor Deployment Strategies	27
6.3.	Overview of the TERRAMETA Scenarios and Use Cases.....	28
6.4.	High-Capacity Communications.....	30
6.4.1.	Coverage Extension.....	30
6.4.2.	Multi-Carrier/Multit-Band RIS Operation.....	32
6.4.3.	Infrastructure Sharing	33
6.4.4.	Backhaul and Integrated Access.....	35
6.4.5.	Direct Short-Range Links.....	43
6.4.6.	Ultra-Directive Short Haul and Mid-Haul.....	44
6.5.	High-Resolution Localisation, Sensing, and 3D Mapping	45
6.5.1.	RIS-aided Backhaul Link Sensing and Localisation.....	46
6.5.2.	RIS-aided Multi-Access Sensing.....	46
6.5.3.	RIS-aided Outdoor-to-Indoor Sensing	47
6.5.4.	Full-Duplex Enabled Simultaneous Communications and Sensing.....	47
6.5.5.	Environmental Mapping and Imaging	48
6.6.	Industrial Environments	48

6.6.1.	Enhancing Throughput, Localisation, and Mapping in Factory Settings	48
6.6.2.	Software Defined Networking Enhancement in Data Centres	53
6.6.3.	Large-Scale Distributing Sensing in Factory Environments.....	55
7.	KPI Definitions and Requirements for THz	57
7.1.	KPI definitions	57
7.2.	6G Requirements	59
7.2.1.	Generic Requirements	59
7.2.2.	Requirements and KPIs for Manufacturing Use-Cases	60
8.	THz Link Budget Analysis and System Design Challenges.....	61
8.1.	Preliminary Link Budget Analysis for THz.....	61
8.1.1.	Models and Definitions	61
8.1.2.	Example I - Outdoor Use Case.....	64
8.1.3.	Example II – Industrial Factory Use Case	66
8.2.	RIS Beamforming Challenges.....	68
8.3.	THz Hardware Components	70
8.3.1.	RIS Element and Structure Design.....	70
8.3.1.1.	CMOS-based Technology for THz	70
8.3.1.2.	Microfluidic-based technology for THz.....	71
8.3.1.3.	A High-power THz Transceiver Option.....	71
8.3.2.	BBU Architecture for THz Communications.....	72
8.4.	RISs in Existing Network Architectures	73
8.4.1.	Integration in O-RAN.....	73
8.4.2.	Integration in Industrial Networks	74
9.	Conclusion.....	76
10.	References.....	77

List of Figures

Figure 4-1 WP Mapping	11
Figure 5-1 Attenuation by atmospheric gases and related effects on the propagation channel over TH/sub-THz frequency ranges.	14
Figure 5-2 Specific attenuation caused by gaseous and water molecule [ITU-P.676] and rain [ITU-P.838].	15
Figure 5-3 Schematic drawings of different operations with an RIS.....	18
Figure 5-4 Schematic drawings of different types of EM control.	19
Figure 5-5 a) Far field and b) near field regimes of RIS operation.	20
Figure 5-6 a) Passive element with only phase shifting capability, b) phase shifting and amplifying capabilities enabled by an active unit with a passive phase shifter.	21
Figure 5-7 Criteria for RIS classification.	21
Figure 5-8 Schematic drawing of DMAs and Spatially-Fed RISs.	22
Figure 5-9 Small printed unit cells assembled to form flexible and extendable diode array.	23
Figure 5-10 Flexible array overlaid on parabolic frame to produce enhanced dish antenna.	23
Figure 5-11 Transmissive RIS Techniques.	24
Figure 6-1 Deployment scenarios for future communication networks (adapted from [GGJ23]).	27
Figure 6-2 Blind spot coverage enhancement.....	30
Figure 6-3 Blindspot Indoor Coverage	31
Figure 6-4 Hybrid Outdoor/Indoor RIS repeater	31
Figure 6-5 Non cooperative deployment	33
Figure 6-6 BS station sharing.....	34
Figure 6-7 BS station and RIS sharing.....	34
Figure 6-8 The THz network as a shared “Network of Networks” where a network of UAVs is also shared.	35
Figure 6-9 An RIS's use case of increasing THz backhaul connectivity using the relay concept.	36
Figure 6-10 An RIS's use case of relaxing high interference caused by in-line backhaul links.....	37
Figure 6-11 An RIS's use case of managing THz backhaul links' beam alignment.	37
Figure 6-12 An RIS's use case of beam-splitting.	38
Figure 6-13 Cell deployment scenario in the city centre of Berlin	39
Figure 6-14 Example of a wireless backhaul network using a star topology based automatic planning algorithm considering only LoS link connectivity.	40
Figure 6-15 Example of a wireless backhaul network using a star topology based automatic planning algorithm considering both LoS and NLoS link connectivity.....	40
Figure 6-16 Example of a wireless backhaul network using a ring topology based automatic planning algorithm considering only LoS link connectivity.	41
Figure 6-17 Example of a wireless backhaul network using a ring topology based automatic planning algorithm considering both LoS and NLoS link connectivity.....	41
Figure 6-18 5G-NR IAB network architecture.....	42
Figure 6-19 Indoor direct short-range link for immersive data analysis and exchange	43
Figure 6-20 Ultra-directive short-haul	44

Figure 6-21 Outdoor mid-haul	44
Figure 6-22 THz RIS-aided backhaul links based JSAC.....	46
Figure 6-23 THz RIS-aided multi-access based JSAC	46
Figure 6-24 THz RIS aided indoor localisation and sensing.....	47
Figure 6-25 Full duplex holographic MIMO system enabling sensing and beamforming.....	48
Figure 6-26 Example of a software-defined factory.....	49
Figure 6-27 Example diagram showing the overall network throughput available per local cell for WiFi, 5G, and THz and number of high bitrate robots are supported.....	50
Figure 6-28 Diagram showing robot to server communication utilizing a THz RIS and server-server connection between local cells using THz RIS MIMO.....	51
Figure 6-29 Factory floor design	52
Figure 6-30 Possible THz RIS deployment strategy	53
Figure 6-31 Using THz RIS links to augment optical network throughput.....	54
Figure 6-32 THz communications using TDMA and RIS.....	55
Figure 6-33 using a RIS for human detection [ESN21].....	56
Figure 8-1 T-RIS and the primary source (Base Station) acting as an antenna (case i).....	61
Figure 8-2 RIS acting as a dynamic target (case ii)	62
Figure 8-3: The coordinate system used for link budget calculation. Cited from [WT2021].....	63
Figure 8-4 Telcom outdoor use case.....	64
Figure 8-5: Calculated UE received power and SNR ($f=140\text{GHz}$) at varied distances (d_2) between UE and RIS.	65
Figure 8-6: SNR at UEs with varied incident and reflection angles to/from the RIS.....	65
Figure 8-7: Factory floor use case.....	67
Figure 8-8: Calculate the SNR and received power at the data server with the machine or robot in different locations (d_1).....	67
Figure 8-9: The SNR at the server when the machine is in varied locations.....	68
Figure 8-10: Directivity of an idealize RIS aperture that redirects the incoming beam (considered as plane wave) to a 45-degree plane wave as function of frequency.	69
Figure 8-11: Directivity of an idealize RIS aperture that redirects the incoming beam (considered as plane wave) to a 45-degree plane wave for different phase quantization step.	69
Figure 8-12 Reconfigurable technologies for implementing RIS versus operating.	70
Figure 8-13 Output Power @150 GHz.....	71
Figure 8-14 Output Power @285 GHz.....	72
Figure 8-15 The architecture of BBU.....	73
Figure 8-16 Hosted O-RAN solution for Neutral Hosts [SCF22].	74
Figure 8-17 Possible Network architecture using pillar RIS deployment strategy.....	75

Change register

Version	Date	Author	Organization	Changes
A	12-06-2023	Ryan Husbands	BT	First draft consolidating partner inputs
B	28-06-2023	Ryan Husbands	BT	Second draft after internal review by Sérgio Matos and Sean Ahearne
C	30-06-2023	Sérgio Matos	IT	Inputs in sections 5 & 6
D	05-07-2023	George Alexandropoulos	NKUA	Restructured sections 5 & 6
E	06-07-2023	Kyriakos Sytlianopoulos	NKUA	Review and corrections
F	07-07-2023	Ryan Husbands	BT	Review and formatting
G	07-07-2023	Luis Pessoa	INESC TEC	Review and formatting

1. Statement of independence

The work described in this document is genuinely a result of efforts pertaining to the TERRAMETA project: any external source is properly referenced.

Confirmation by Authors:

Ryan Husbands
 Sean Ahearne
 Bo Kum Jung
 Qi Luo
 Sérgio Matos
 Luís Pessoa
 George Alexandropoulos
 Kyriakos Stylianopoulos
 Panagiotis Gavriilidis
 Tung Phan
 Georgios Ropokis
 Dimitrios Kritharidis
 Pan Cao
 Antonio Clemente
 Zaid Abdullah
 Verónica Lain-Rubio
 Jack Soh
 Konstantinos Katsanos
 Aristeides Papadopoulos
 Evangelos Pikasis
 Jose Luis Gonzalez

2. Abbreviations

3D	Three Dimensional
3GPP	Third Generation Partnership Project
4G	Fourth Generation
5G	Fifth Generation
5G-NR	Firth Generation – New Radio
6G	Sixth generation
AI	Artificial Intelligence
ACM	Adaptive Coding and Modulation
ASE	Area Spectral Efficiency
BAP	Backhaul Adaptation Protocol
BS	Base Station
CN	Core Network
CU	Central Unit
DL	Down Link
DMA	Dynamic Metasurface Antenna
DU	Distributed Unit
EM	Electromagnetic
FDD	Frequency Division Duplex
FEC	Forward Error Correction
FSO	Free Space Optics
H-RIS	Hybrid RIS
HMIMO	Holographic Multiple-Input Multiple-Output
IAB	Integrated Access and Backhaul
IB	In-Band
IoT	Internet of Things
ITU	International Telecommunication Union

JSAC	Joint Sensing and Communication
ISAC	Integrated Sensing and Communication
KPI	Key Performance Indicator
LoS	Line-of-Sight
LTE	Long Term Evolution
MCS	Macro Cell Site
MIMO	Multiple-Input Multiple-Output
MNO	Mobile Network Operator
MT	Mobile Termination
NLoS	Non-Line-of-Sight
NR	New Radio
OB	Out-of-Band
O-RAN	Open Radio Access Network
PoC	Proof of Concept
QAM	Quadrature Amplitude Modulation
QoS	Quality of Service
R-RIS	Receiving RIS
RAN	Radio Access Network
RF	Radio Frequency
RF-SOI	Radio-Frequency Silicon-On-Insulator
RIS	Reconfigurable Intelligent Surface
RU	Radio Unit
RX	Receiver
SCS	Small Cell Site
SDN	Software Defined Network
SE	Spectral Efficiency
SEE	Spectral and Energy Efficiency
SiGe	Silicon-Germanium

SINR	Signal to Interference plus Noise Ratio
SLAM	Simultaneous Localization and Mapping
SNS JU	Smart Networks and Services Joint Undertaking
STAR-RIS	Simultaneous Transmitting And Reflecting RIS
T-RIS	Transmissive RIS
Tbps	Terabits per second
TDD	Time Division Duplex
TDMA	Time Division Multiple Access
THz	Terahertz
TX	Transmitter
UAV	Unmanned Aerial Vehicle
UE	User Equipment
WP	Work Package
WLAN	Wireless Local Area Network
WRC	World Radiocommunication Conference

3. Executive summary

This document defines the scenarios, use cases and requirements that will drive the developments to be made in the project. The document starts by describing the approach of WP2 and the relation to other WPs as well as how the identified use cases map to the different work-packages. An introduction to THz and RISs in 6G networks is also given including a detailed definition of the different types of RIS. The core of this document is the description of the proposed scenarios and use cases, which include different kinds of scenarios aligned with 6G, including the possibility of indoor and outdoor deployment. The proposed scenarios and use cases have been grouped along 3 main categories: a) High-Capacity Communications, b) High-Resolution Localisation, Sensing, and 3D Mapping, c) Industrial Environments. The document also addresses KPI definitions and requirements for THz, including a specific analysis of requirements and KPIs for manufacturing use cases. Finally, the document addresses THz link budget analysis and system design challenges, including specific examples for outdoor and industrial factory use cases, analysis of specific RIS-based beamforming challenges, description of related THz hardware components and lastly, discusses aspects of integration of RISs in existing network architectures.

4. Introduction

4.1. WP2 approach and relation to other WPs

Work Package 2 (WP2) is responsible for defining the scenarios, use cases and requirements that will drive the developments to be made in the project. This includes specifying the requirements of the Reconfigurable Intelligent Surfaces (RIS) based THz systems and how such systems can be evaluated. These specifications will describe the artefacts that will be built (from scratch), enhanced (from existing artefacts) and/or combined in the project to achieve a practical THz communication system including Reconfigurable Intelligent Surfaces (RIS). Such artefacts can be either hard (such as components and sub-assemblies) or soft (such as models or characterisations). An iterative approach to the definition of requirements will be used, with the specifications themselves being enhanced over the three phases of the project (evaluation, design, and demonstration). The three phases of the project are: i) evaluation of the technologies and components for THz RIS; ii) design which refers to both the physical layer (WP3/4) and algorithmic designs (WP5), and iii) demonstration via testbeds (WP6). The scenarios used to evaluate the artefacts will be detailed in conjunction with the specifications of the artefacts themselves.

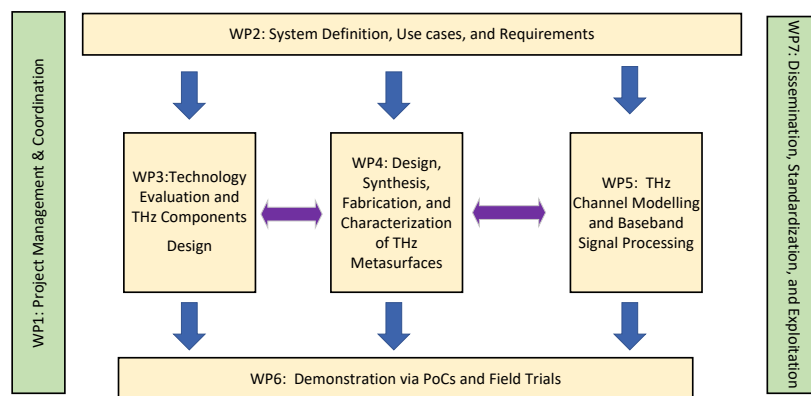


Figure 4-1 Work-package inter-relations.

WP2's work governs the work covered in WP3, WP4, and WP5, with all technical WP's contributing to WP6. WP2 will be closely interacting with WP3 and WP4 to receive as inputs the RIS design characteristics, and consequently the limitations of the investigated and proposed hardware architectures for the various available forms of reconfigurable metasurfaces. WP3 will develop new sub-THz and THz hardware solutions for some of the fundamental building blocks of the RIS design in WP4 as well as RIS demonstrators in WP6. WP4 will design, synthesise, fabricate, and characterise the THz metasurfaces developed in this project. The development of THz RIS elements will be carried out in WP3, where different hardware implementations of meta-elements (e.g. MEMS, CMOS, Microfluidic MEMS) will be tested and used as the foundation for realizing multiple types of RIS based on operation modes (Transmissive RIS (T-RIS), Reflecting RIS (commonly referred to simply as RIS), Receiving RIS (R-RIS), and H-RIS (e.g., simultaneous reflecting and sensing RIS) as well as simultaneous transmitting and reflecting (STAR-RIS)) or even metasurface-based antenna (this mode refers to using an RIS as the front-end of a transceiver) and functions (communication, sensing, localisation).

As far as WP4 is concerned, the scalability of the developed RIS technology will be studied, as well as the application of the proposed operation modes using the fabricated technology. Furthermore, the control unit of RIS will be designed and integrated to the prototype. WP5 will be responsible for the THz channel sounding and modelling activities of TERRAMETA, as well as the design of efficient algorithms for most of the envisioned functionalities with ultra-massive Multiple-Input Multiple-Output (MIMO) metasurface-based antenna arrays and any of the available types of RISs. WP6 will focus on demonstrating the effective exploitation of THz RIS wireless links through the use of simulations, lab-based testing, as well as integration and demonstration with "real-world" use cases and infrastructure.

An investigation to determine the compatibility of THz RIS components with use case network infrastructure will be performed, and a compatible signalling method and physical interface between these devices will be defined and implemented. In support of the development and integration of THz

RIS hardware, a simulation-based demonstrator will also be developed, based on the use-case environments, to both showcase the potential benefits of a large-scale THz RIS system beyond the scope of what can be demonstrated in the project and to provide results which can be directly compared against those collected in the lab and by the planned use-case demonstrators.

4.2. Identified use cases and mapping to WPs

The identified TERRAMETA use cases of RISs for THz wireless operations are listed in Table 1, including for each of them the WPs that will devote relevant effort. For example, a check at WP3 implies that the use case will be studied in terms of the building blocks of the RIS. A WP4 check means that an aperture will be built or simulated (scalability study) to be compatible with the particular use case. A check in WP5 means that channel modelling and signal processing will be carried out (from simulation or real data acquisition) for the corresponding use case. And finally, a WP6 check indicates that the use case will be experimentally tested by one of TERRAMETA's Proof-of-Concepts (PoCs) or field trials.

Table 1 highlights the use cases exemplified in this deliverable and their potential work package mappings.

Use Case / Work Package	WP2 (Use case/scenarios Definitions)	WP3 (Unit cell design)	WP4 (RIS design)	WP5 (Channel sounding and algorithms)	WP6 (PoCs & Field tests)
Blind Spot Coverage	✓	✓	✓	✓	✓
Hybrid Indoor/Outdoor Repeater	✓		✓	✓	
Multi-Carrier/Multi-RIS Operation	✓	✓		✓	
Infrastructure Sharing	✓	✓		✓	
Backhaul and Integrated Access	✓	✓	✓	✓	✓
Direct Short-Range Links	✓	✓	✓	✓	
Ultra-Directive Short-Haul and Mid-Haul	✓	✓	✓	✓	
THz RIS-aided Backhaul Link Sensing and Localisation	✓	✓	✓	✓	
THz RIS-aided Multi-Access Sensing	✓	✓	✓	✓	
THz RIS-aided Outdoor-to-Indoor Sensing	✓	✓	✓	✓	
Joint Communication and Sensing with Full	✓	✓	✓	✓	

Duplex Holographic DMAs					
Environmental Mapping and Imaging	✓	✓	✓	✓	
Enhancing Throughput, Localisation, and Mapping in Factory Settings	✓	✓	✓	✓	✓
Software Defined Networking Enhancement in Data Centres	✓	✓	✓	✓	
Large Scale Distributed Sensing in Factory	✓	✓	✓	✓	

5. THz and RISs in 6G Networks

5.1. Introduction to THz

As our insatiable thirst for connectivity grows, the sixth generation of wireless technology promises to redefine the limits of speed, responsiveness, and connectivity. The 6G wireless technology is envisioned to be available in 2030 [ZFW19]. It promises extreme data rates in the order of Terabits per second (Tbps) and ultra-low latency in the order of sub-milliseconds. In 6G, wireless connectivity will be expanded beyond traditional devices and networks, such as Internet of Things (IoT) devices, wearables and sensors. 6G will operate in higher frequency bands and in new spectrum ranges to cope with the increasing demand for wireless connectivity. The 6G networks will need to be integrated with AI for network management, personal user experience and smart resource localization. In addition, in 6G, energy consumption will be optimized for reduced environmental impact while on the same time the growing number of connected devices will be supported.

To enable the realisation of all the above 6G features, it is essential for 6G to operate at frequencies in the order of THz [0.1, 10] [HWL22]. This spectrum offers larger bandwidth than previous generation wireless networks and therefore allow higher data rates in the desirable order of Tbps, as well as ultra-low latency. As the frequency increases, free-space path loss represents an important challenge for long range communication. In addition, wave propagation at THz frequency spectrum is vulnerable to atmospheric conditions.

Nevertheless, there is a prevailed myth that wireless communication at THz frequency is not available due to the high attenuation of the atmospheric condition. While it is true that the strength of the signal will be more reduced than the wave propagation at frequencies below 100 GHz, the influence of the atmospheric condition may not be as strong as commonly thought. Specifically, in Figure 5-1 and Figure 5-2, the frequency dependent impact of atmospheric condition is visualized exploiting the results of [ITU-P.676] and [ITU-P.838].

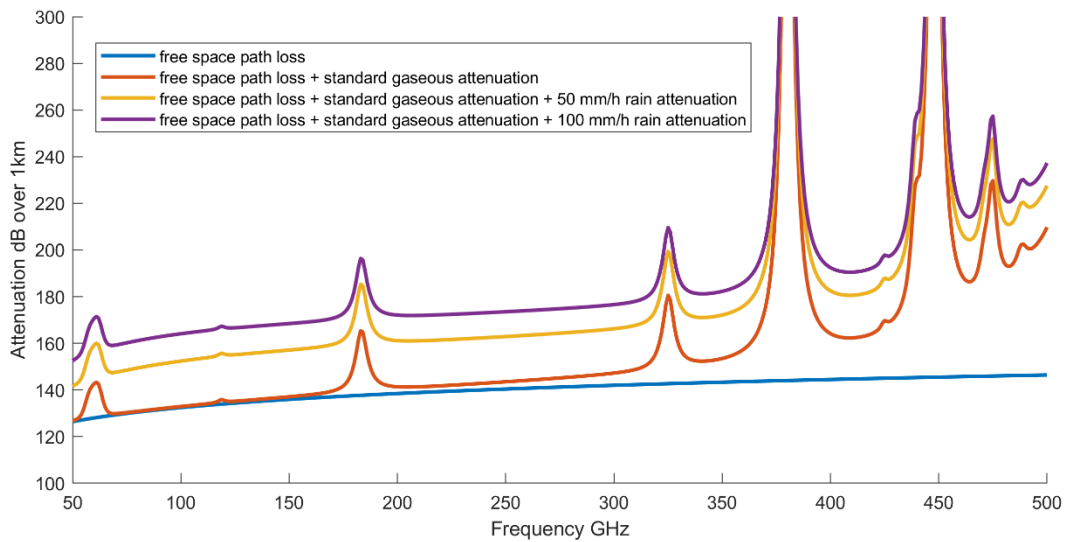


Figure 5-1 Attenuation by atmospheric gases and related effects on the propagation channel over THz/sub-THz frequency ranges.

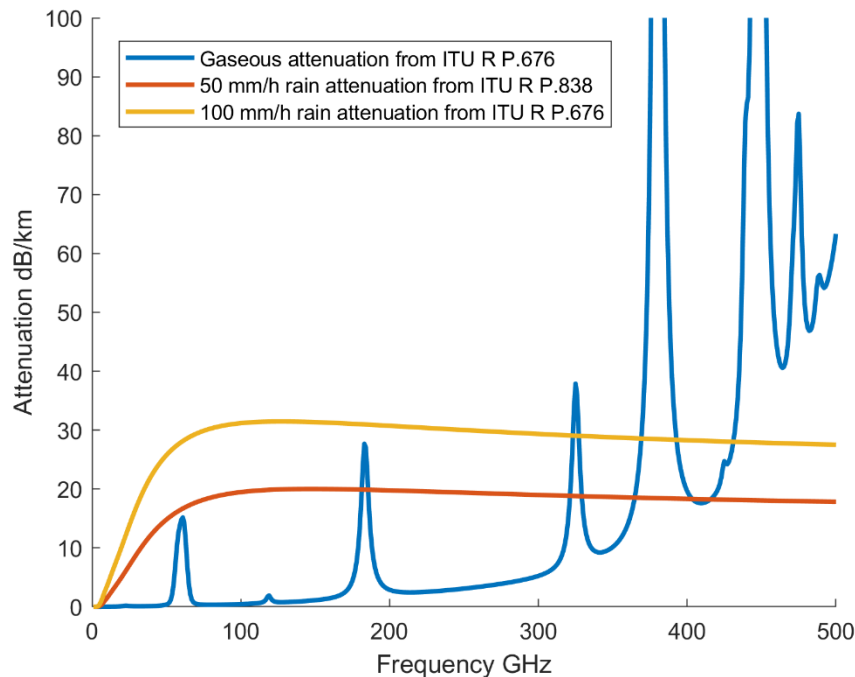


Figure 5-2 Specific attenuation caused by gaseous and water molecule [ITU-P.676] and rain [ITU-P.838].

Here the gaseous attenuation indicates the specific attenuation under the standard atmospheric condition given in [ITU-P.676]. Note that the gaseous attenuation is calculated with 1 GHz interval thus it may not include the peak of line centres where the molecules resonate. As it is possible to observe from both figures that the impact of atmospheric weather condition at the frequency bands of 150 GHz and 300 GHz is not dominant to the point that wireless communication will not be feasible. Moreover, the specific attenuation value is of the order of dB/km. This indicates that the impact of atmospheric condition can be scaled down by reducing the link distance.

5.1.1. THz-enabled Use Cases

THz bands can act as enablers of exotic innovations as well as amplifiers of existing technologies. Examples include, but are not limited to, holography, artificial intelligence (AI), microelectronics, optoelectronics, and space applications. In particular, the 6G high data rates and ultra-low latency can support the following:

- **Holographic-type Communications** [JHH21], such as holographic telepresence for online training, education and interaction with ultra-realistic objects.
- **Extended Reality (ER)** [JHH21] where augmented, virtual and mixed realities are combined producing high-resolution, data rate, color-depth and dynamic range video at a 360 degrees field of view experience.
- **Connected and Autonomous Vehicles** [AKP21] concept including autonomous driving, cooperative vehicle networks, Internet of Vehicles, Vehicular Ad-hoc Networks, air-to-ground networks, and space-air-ground interconnected networks.
- **Industry 5.0** [AKP21], where people are expected to be working alongside robots and smart machines to add a personal human touch to Industry and increase automation and efficiency. 6G is needed since a massive number of things in Industry 5.0 are connected either using wired or wireless technologies to provide various applications and services that are enabled by a complete integration of cloud/edge computing, big data, and AI.
- **Collaborative Robots** (or cobots) [AKP21] are robots designed to work collaboratively side-by-side with humans. Cobots need to perform tedious, repetitive, risky tasks, reliably, safely and

make real time decisions. These require demanding computing and network connections that can be supported by 6G.

- **Intelligent Healthcare** [AKP21] is an AI-driven concept, where it would be possible the real time monitoring and measurement of health data. These data, collected by wearables can be processed at edge nodes and sent to medical doctors that are located remotely to the patient. The realisation of holography, intelligent robots, and high data rates in 6G will enable the doctor to even perform remote surgery, avoiding disease transmission.

5.1.2. Relevance of THz in 6G Requirements

The aforementioned use cases envisioned in 6G networks are expected to demand unprecedented data rates, ultra-reliability, and low latency [JHH21]. To that end, THz communications arises as the most promising candidate to meet these requirements, mainly due to the large amount of unoccupied bandwidth. Conventional 5G networks have a typical available bandwidth up to 2 GHz, whereas in THz communications it can reach up to 69 GHz as stated in the first standardization efforts [PKH20]. In what follows, we list some of the difficulties that 6G networks will be met with, which can be tackled by transitioning to THz communications:

- Peak data rates will be hundreds of times higher than in 5G networks, ranging from 1 to 10 Tbps [JHH21].
- End-to-End Latency will be reduced at least by at least one order of magnitude compared with 5G standards and lie even beneath 0.1 ms [AKP], to support applications like autonomous vehicles which rely heavily on reliable and ultra-low latency networks.
- Traffic and connection density challenges, since due to the Internet of Things evolution, an exponential growth of connected devices to the network is projected. As a result, traffic density could be more than 100 Tb/s/km² [CLS20]. This spectrum congestion problem can be solved by exploiting the large available bandwidth in THz.
- Stringent positioning precision requirements, since 6G is expected to reduce the positioning error from the present metre level to the centimetre level [CLS20], thus enabling ultra-reliable sensing of the propagation environment. The THz electromagnetic waves have shorter wavelength leading to finer spatial resolution. This allows for the realisation of highly focused beams leading to both higher positioning precision and lower interference.

5.1.3. Challenges in THz

Although THz communications have been established as probably the most prominent enablers of 6G, there remain certain challenges to be dealt with. Specifically, we identify a few challenges, list them and propose ways to counter them in what follows:

- Propagation path loss. Compared to traditional communications frequencies, the propagation path loss of the THz electromagnetic signal decays proportionally with the square of the operating frequency following Friis' formula [B16]. This liability can be tackled with the use of extremely massive antennas, which are highly directive and boast large gains, with RIS technology, as will be further explained.
- Molecular absorption is a phenomenon present in THz frequencies due to molecules in the atmosphere resonating in frequencies included within this band. This can be dealt with, by carefully selecting the communication bandwidth to be outside of those specific resonant frequencies, as shown in [JA11]. Molecular absorption leads to the attenuation of the electromagnetic signal, since the photons that constitute the EM wave, are absorbed by the molecule, the number of photons decrease and consequently the amplitude of the EM wave is attenuated. The molecules that absorb this energy from the incoming signal are excited to higher vibrational and rotational energy states and will eventually drop to lower energy states by emitting additional photons. These photons generate the molecular noise which is linearly dependent on the transmitted power. Water-vapor molecules are the dominant contributors to the molecular absorption mechanism with oxygen being three orders of magnitude less significant. Eventually molecular absorption induces to frequency selection, distance dependence and environmental impact (water vapor is altitude dependent) to THz communications, as previously discussed.

- Blockage vulnerability/severe shadowing. THz EM waves heavily rely on Line-of-Sight (LoS) communication since they cannot penetrate through obstacles, and exhibit extreme attenuation in the reflective paths. To that end, RIS once again plays a major role of establishing a direct path from transmitter to receiver.
- High-Frequency Hardware Components. It is difficult to design efficient circuits such as THz mixers, THz oscillators, THz amplifiers and THz antennas [CLS20]. This challenge can be addressed with the use of simplified hardware such as metasurface-based antennas, and graphene-based THz modulators [HAC16].

Simply put, this project aims to assess new RIS-based approaches to counteract the inherent difficulties of the THz regime, and design THz RISs with different capabilities.

5.2. Definition of RISs

The concept of RISs has been established as a paradigm [DDP19] envisioning dynamic control of the radio propagation environment to improve, and even enable with reduced/efficient hardware [JAB22] infrastructure, a wide variety of wireless applications. While the readiness of this technology is still ongoing the transition from theoretical works and new ideas to precise definitions and boundaries, the key feature that characterises an RIS is its dynamic response reconfigurability that can be realised with low-cost hardware [LLM21] which has the potential to be very efficient in terms of energy consumption [HZA19]. The actual benefits of RIS technology in terms of cost and efficiency require rigorous quantification, potentially depend on the actual application, and are tightly coupled to other alternative existing technologies, such as active multi-antenna relays, and phase-arrays [BÖL20]. Nevertheless, theoretical [BDD19], algorithmic [HZA19], and experimental [CYZ23] works by the established community of the past years demonstrate clear advancements and value-propositions. In the current paragraph, we layout the adopted RIS taxonomy that will be used throughout this project based on existing literature [ETSI15, ETSI23], with the intention to capture the variety of RIS-based functionalities. Several criteria are used to classify an RIS, as summarised in Figure 5-7 and graphical illustrations of the various operating modes are provided in Figure 5-3. In particular, the RIS can be applied for communications applications [SAW21], sensing [ZDB22] (e.g., human activity recognition [SSK22] and digital twins [CLN23]) as well as localisation/tracking [WHD20] and detection of passive objects [dH20]. In what follows we distinguish RISs based on their operation modes:

- Signal reflection, where an RIS is conventionally used as a reconfigurable reflector (Figure 5-3 (a)), desirably steering impinging EM waves, thus the reflecting operation mode of RIS, is commonly referred to simply as RIS.
- Receiving signals (R-RIS) [LLM21] (Figure 5-3 (b)), enabling sensing of the environment, channel state information acquisition and localisation. Reception with R-RIS may include the typical Radio Frequency chain (RF chain) reception, but is not limited to this technology, for example signal intensity detectors can be implemented [AAI23].
- Signal transmission (T-RIS) [DMG23] (Figure 5-3 (c)), when used in conjunction with signal feeding units (e.g., through spatial feeding [DMG23] or RF chains [SAI21]).
- Simultaneous signal reflection and reception (Figure 5-3 (d)), in the H-RIS operation mode [AAS21], which integrates the benefits of two operation modes by allocating a portion of the impinging signal power for reception and favourably reflecting the rest.
- Simultaneous signal transmission and reflection by refracting impinged EM waves (STAR-RIS) [LMX21] (Figure 5-3 (e)), where there are 3 different operating modes; 1) a portion of the impinged EM wave's power is refracted while the rest is reflected, 2) different elements switch between reflecting and refracting modes, and 3) switching in time between reflecting and refracting.

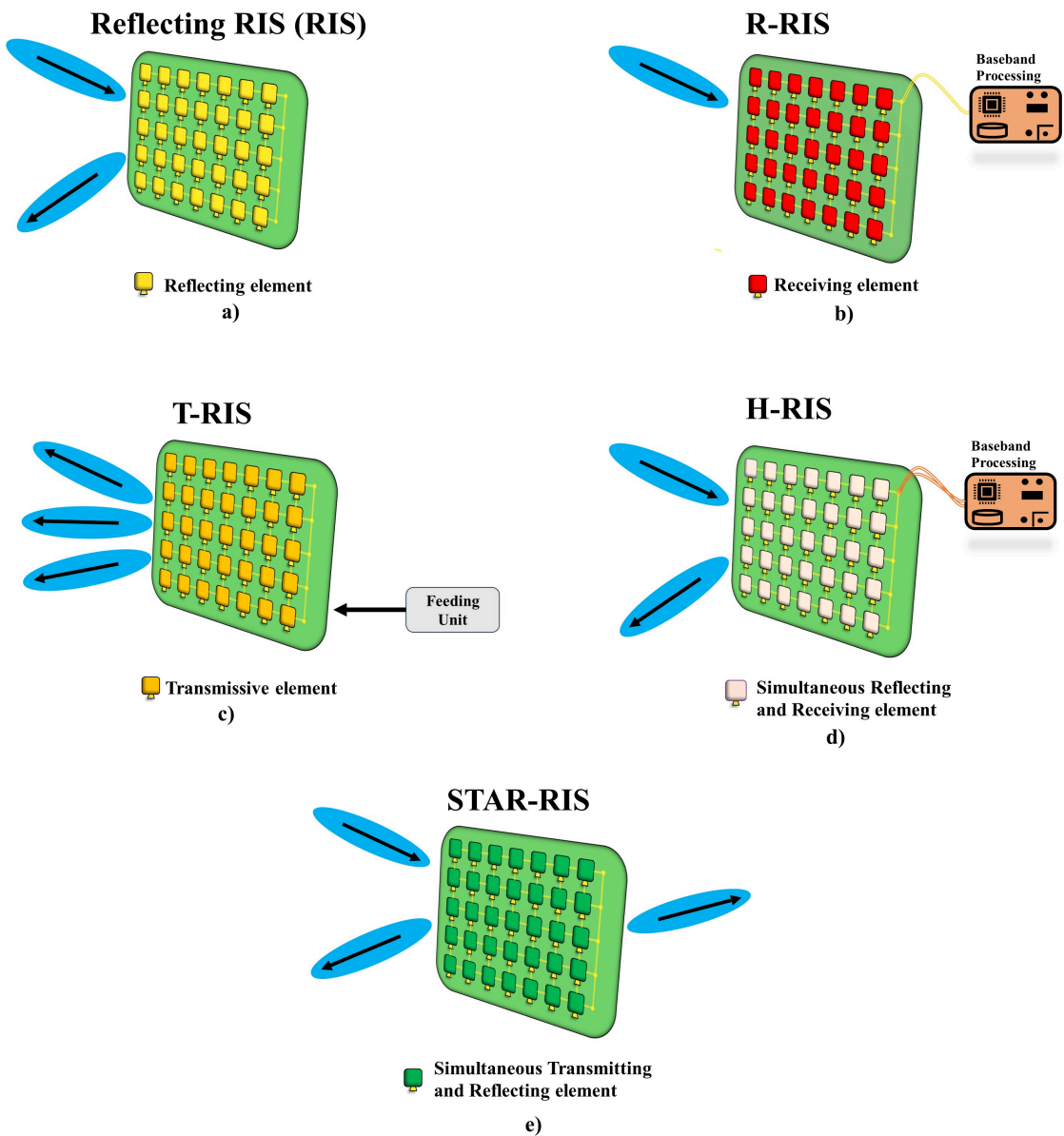


Figure 5-3 Schematic drawings of different operations with an RIS.

RISs can control the impinging EM waves in various ways (Figure 5-4), thus enabling exciting new applications. Here we list the most prominent control types in the following:

- Absorption of EM waves [AAS21], RISs can be used to completely absorb impinging EM waves, having ideally zero output, thus mitigating interference in wireless networks, as well as offering security enhancement [ETS123].
- Changing the polarization of EM waves [BBD19], offering a new degree of freedom in the manipulation of the propagation environment.
- Phase manipulation of EM waves, which depending on the considered hardware implementation can either be discrete (1bit, 2bits phase quantization) [ACL21], or continuous.
- Amplitude manipulation of EM waves, which if we refer to absorption can be implemented by nearly passive elements, however in most cases amplitude manipulation is considered as amplification of impinging signals which requires active elements [ZLX23].

Of course, all of these manipulations of EM waves require different hardware implementations [JAB22] and dedicated control units responsible for carrying out the RIS reconfigurability and the structure's interface (in- or out-of-band) with other network nodes.

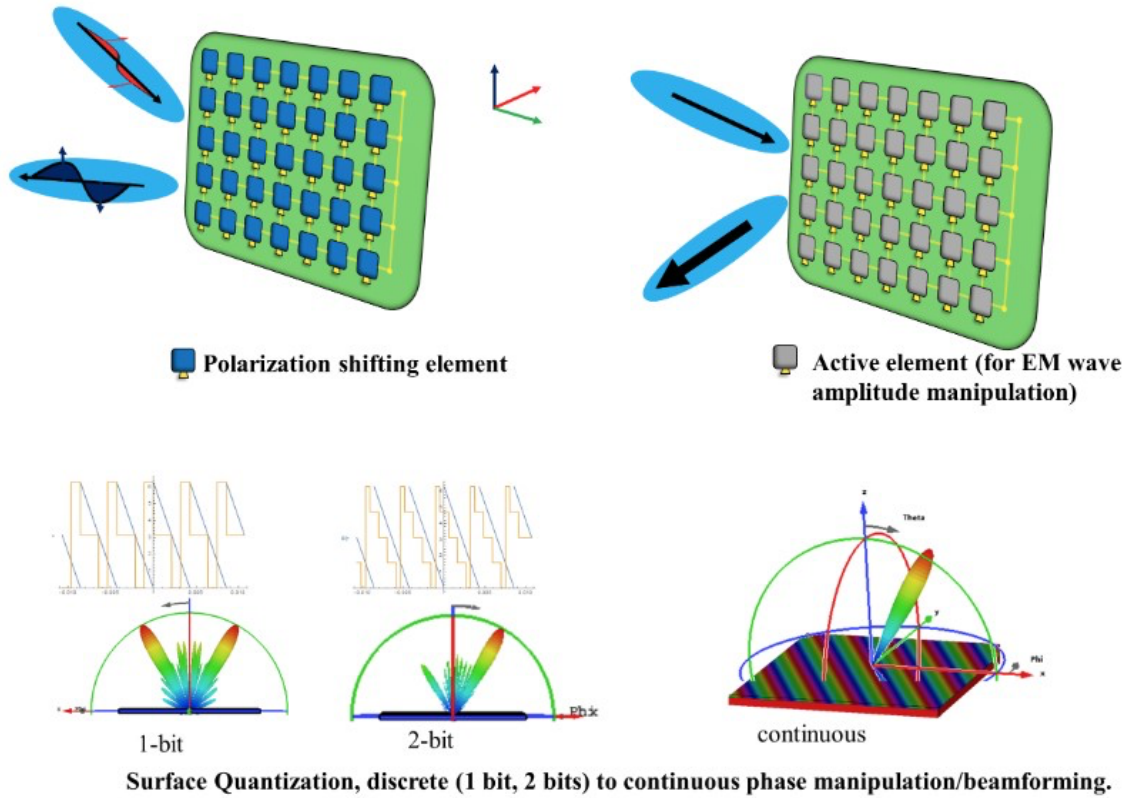
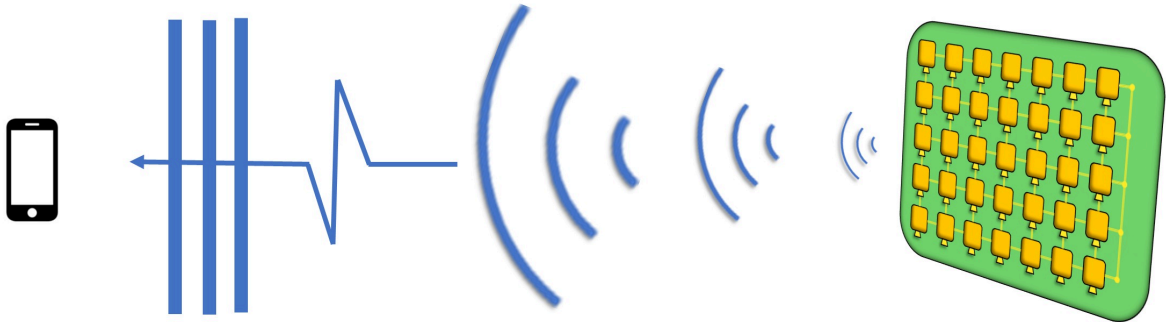


Figure 5-4 Schematic drawings of different types of EM control.

Furthermore, an RIS may operate in the near- or far-field region, depending on the frequency and its distance from the desired operation field. Their definition depends on the application, but in general the far-field region refers to the region of few wavelengths, usually two, or the Fraunhofer distance further away from the RIS [SJ17], which is proportional to the square of the aperture size and inversely proportional to wavelength of the operating frequency [BS20]. As demonstrated in Figure 5-5, the key difference of near- and far-field regimes is that in near field, the EM wave has a spherical wavefront compared to the typical planar wave assumption. Operating in the near field brings forth the possibility to focus signal transmission at a specific location, rather than at a specific direction, as happens with far-field beamforming. This feature enables multiple coexisting orthogonal links, even at very similar angles, thus improving the overall system capacity and sensing capabilities.

a) Far-Field



b) Near-Field

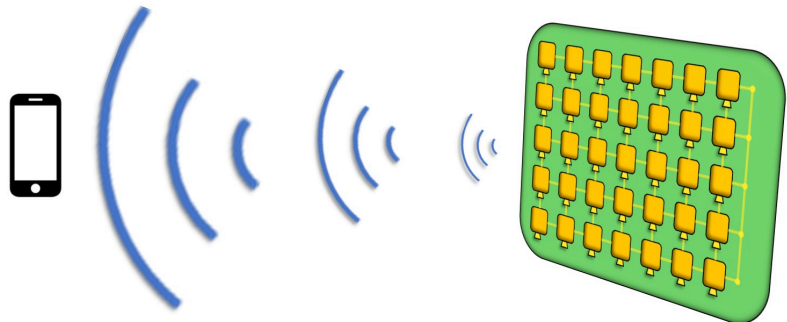


Figure 5-5 a) Far field and b) near field regimes of RIS operation.

In terms of power consumption, the RIS can be almost passive, in the sense that only the unit(s) responsible for its reconfigurability consume power, or include active components (e.g., amplifiers for signal or noise amplification) [ETSI23, JAB22]. An RIS with active elements offering reflection amplification contains a dedicated power source that allows it to amplify the reflecting electromagnetic signal. On the contrary, a nearly passive RIS (which we will term as passive from now on) has a much lower power consumption and simpler hardware components, as shown in Figure 5-6, a passive element can be implemented via a passive phase shifter, while amplification with any implementation (e.g. conventional amplifiers or negative resistance amplification [LLP21]) can be realised only by active units.

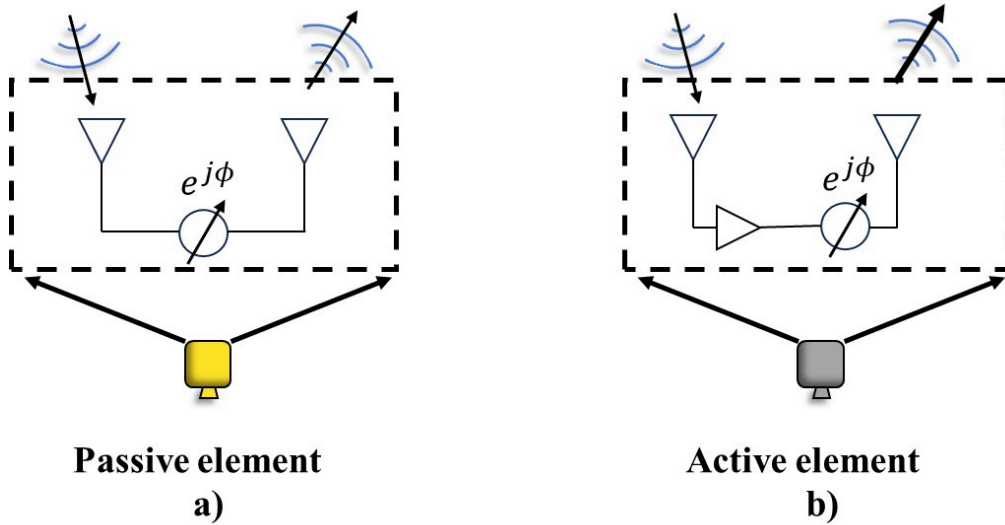


Figure 5-6 a) Passive element with only phase shifting capability, b) phase shifting and amplifying capabilities enabled by an active unit with a passive phase shifter.

Another feature that categorises an RIS is its channel access mode, which can be simplex, half-duplex, or full duplex. The radiation pattern is also a feature that is used for the RIS classification. In particular, the RIS can steer a beam across a target (pencil-beam scanning), shape the profile and phase of a beam (beam shaping), or generate multiple beams (multibeam) for MIMO and multi-user applications as is implied in the figure demonstrating the RIS operation modes and will be further showcased in some of the scenarios in Section 6. The various criteria for the classification of RISs are summarised in Figure 5-7.

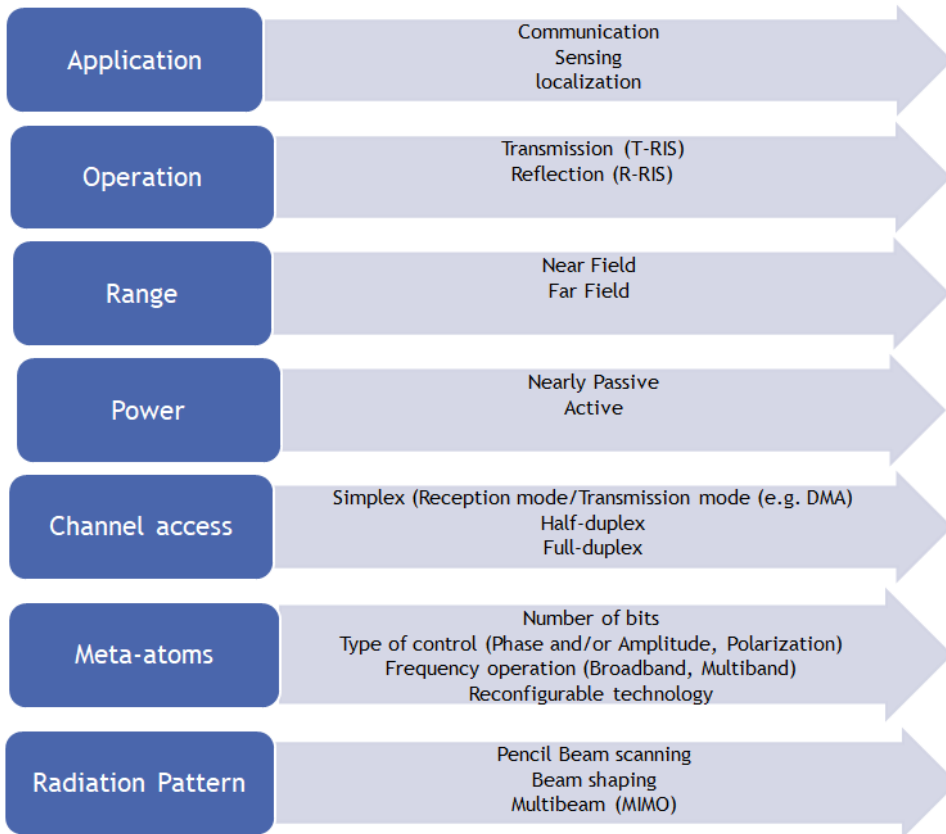


Figure 5-7 Criteria for RIS classification.

Two main approaches to implement RISs that have been mainly discussed in the literature, which are either based on traditional *antenna arrays* or *metasurfaces*. The antenna-array-based RIS uses unit cells that have resonant size close to half-wavelength while the metasurface-based RISs are composed of a large number of closely spaced sub-wavelength unit cells (e.g., 1/10 of the wavelength). The operation of metasurface-based RISs is based on diffraction to split the incident Electromagnetic (EM) wave into several components whose directions depend on the periodicity, operating frequency, and incident angle [AVA17]. It is obvious that the metasurface-based RIS is a sophisticated concept which requires a complex fabrication process. Recently, metagrating based-RIS has been introduced [LKT23] using a periodic array of scatters. Compared to the metasurface, only the scatterers of the metagrating are sub-wavelength, while the distance between them is comparable to wavelength. This allows it to be significantly simpler to fabricate and can afford broader bandwidths because of the larger footprint of the constituent elements.

5.2.1. *DMA*s

DMA are transceiver architectures that use meta-elements as the RF front end [SAI21]. In this paradigm as shown in Figure 5-8, each row of elements composes a microstrip antenna, where impinging or transmitting signals propagate, each microstrip antenna is also connected with an RF chain to support either of the two schemes, i.e., reception or transmission. The row-by-row distinction isn't necessary but was demonstrated this way for illustrative purposes.

When DMA are deployed as receivers, the EM wave impinged on each meta-element propagates via its respective waveguide to the output of the microstrip antenna connected to an RF chain, where it is down converted to baseband and processed by the baseband unit. On the other hand, when DMA are used as transmitters, the baseband unit acts as a source feeding digitally processed signals to the RF chains, where they are up converted, fed to each waveguide and then radiated from the metamaterial elements which process the signals in an analogue form. Thus DMA, from a signal processing perspective offer Hybrid beamforming, i.e., both analogue and digital.

Nevertheless, DMA, aren't the only transmitting architecture enabling the operation mode T-RIS, as mentioned before in Figure 5-7, feeding can be done spatially as proposed in [DMG23], which also limits the necessity for multiple RF chains. These two different feeding mechanisms are showcased in the following Figure 5-8.

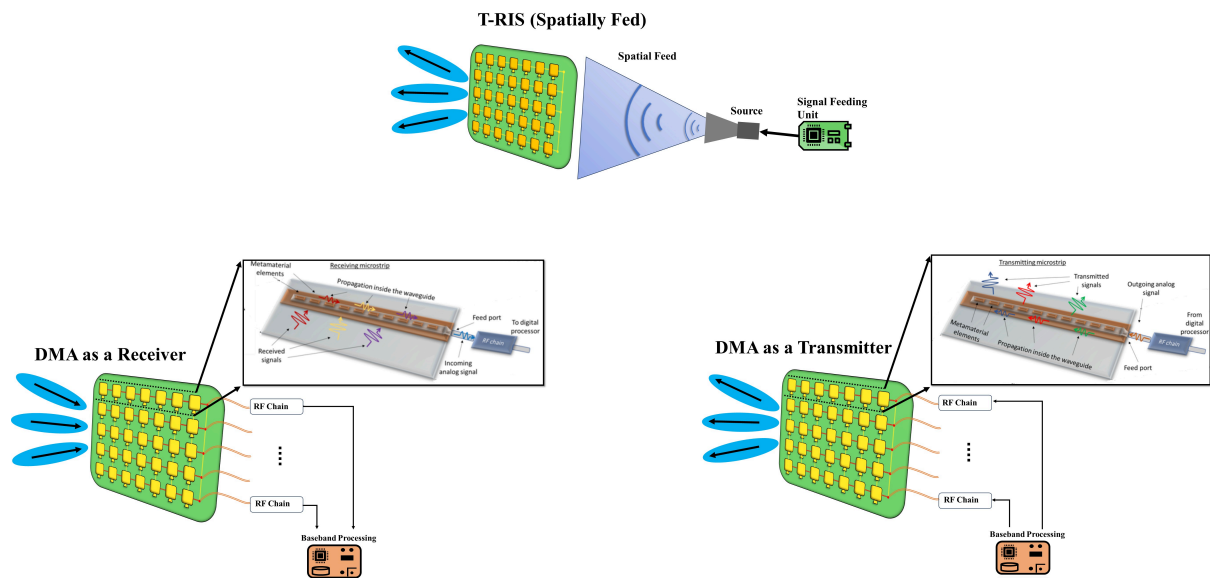


Figure 5-8 Schematic drawing of DMA and Spatially-Fed RISs.

5.2.2. *T-RIS: Conformal Array*

The ambition behind the conformal array architecture is to produce the “proof of physics” for a large scale programmable reflective surface to enhance THz transmitters via parabolic dish type implementation. Large-aperture antennas can be built only with reflectors or arrays and reflectors are far simpler than arrays. Although arrays give more degrees of freedom, this in general isn’t necessary in many applications. However, with plenty of room and slow scan rates, a reflector becomes a better design than an array. There can be many valid reasons for using an array in an application, but a reflector should always be considered. When considering THz transmissions, an array needs an elaborate feeding network, whereas a reflector uses a simple feed and free space as its feeding network.

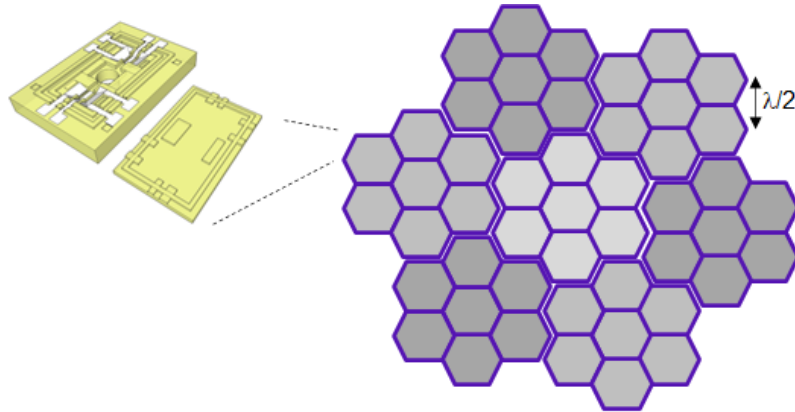


Figure 5-9 Small printed unit cells assembled to form flexible and extendable diode array.



Figure 5-10 Flexible array overlaid on parabolic frame to produce enhanced dish antenna.

The radiation pattern or antenna pattern is the angular dependence of the strength of the radio waves from the antenna dish. The sensitivity as a function of direction of an antenna when used for receiving is identical to the radiation pattern of the antenna when used for transmitting.

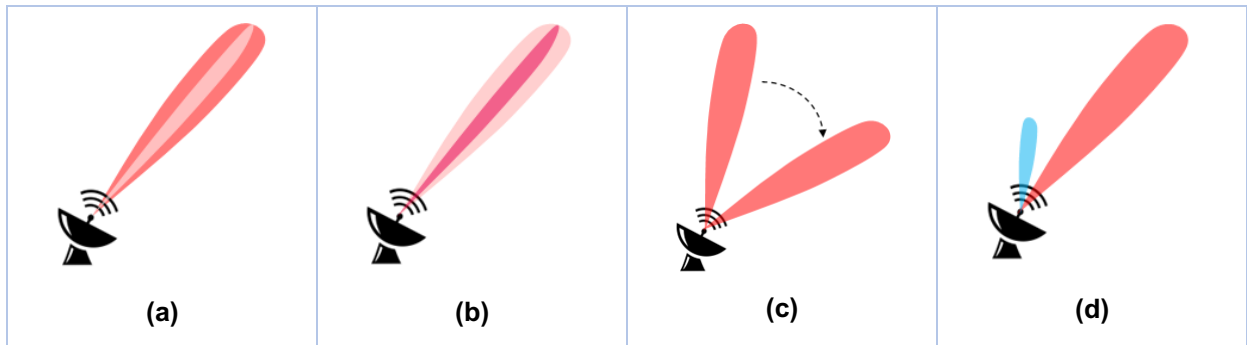


Figure 5-11 Transmissive RIS Techniques.

- (a) Adaptive nulling: Shape the antenna pattern to avoid producing interference and compensate for an interferer or jammer.
- (b) Reduce the beamwidth to make a smaller dish perform like a larger dish.
- (c) Reduce the need for moving the dish when steering the beam.
- (d) Enhance frequency/time slot selectivity and select unique doppler signatures.

5.2.1. Holographic MIMO

The enabling technology of RISs, namely meta-elements, has shown to be a promising candidate for implementing future Holographic MIMO (HMIMO) communications, paving the way for a low-cost efficient programmable wireless environment. In addition to the passive paradigm of RISs, meta-materials can be used in transceiver architectures as was previously demonstrated through the DMA paradigm, which is considered to be one of the most auspicious HMIMO enablers, bringing forth programmable control of the transmit/receive beam patterns with advanced hybrid analogue/digital signal processing capabilities. Compared with conventional antennas implemented by patch arrays and phase shifters, HMIMO architectures are envisioned to be low power consuming and cost efficient, while naturally implementing transmit/receive RF chain reduction [H20]. Additionally, RF chains can be completely eliminated through new energy efficient ways of realising transmission such as Leaky Wave antennas [AKX21] and photodiode coupled antenna arrays [ZFW19].

In general, the HMIMO paradigm, includes all the passive or active architectures that have the following characteristics: 1) have a large number of elements; and 2) have sub-wavelength inter-element distance. In order further clarify the meaning of holographic communications, the following definition is proposed in [GGJ23]: holographic wireless communications perform realistic and complete restoration of the Three-Dimensional (3D) target scenery with the help of new holographic-type antenna technologies and electromagnetics-based signal processing. In other words, HMIMO studies the asymptotic limit of numerous closely spaced elements (in less than half a wavelength distance) creating a nearly continuous surface, thus enabling a precise manipulation of the EM waves (both in phase and in amplitude) to the point of completely sensing or recreating the wireless propagation environment, in an EM manner. This paradigm is envisioned to be used for realising 3D remote dynamic interactions with people, objects, and their surrounding environment. There is a variety of use cases that arise, which relies on the super directivity concept brought by the mutual coupling effects [HYM22], the high precision manipulation of EM waves in phase and amplitude, and the ability to recreate object waves with unprecedented precision, leading to efficient localisation, massive gain beamforming and even 3D imaging of the wireless environment.

The interplay of holographic architectures and THz frequencies is of great interest, since at those bands there exists large available bandwidth for boosting data rates and the massive numbers of antenna elements can be used to compensate for the severe pathloss. A by-product of utilising large-scale transceiving arrays in sub-THz and THz frequency bands is that communication may take place in the

near-field (Fresnel) region, as opposed to 5G systems that typically operate in the far field, thus paving the way for near field beamforming [BDS21].

5.3. THz RISs in 6G

6G envisions a transformative shift in mobile networks, driven by the need to accommodate expanding services and use cases, as well as advancements in technology. With the aim of tightly coupling and enhancing interactions between the human world, digital world, and physical world, 6G seeks to create a cyber-physical continuum that improves the quality of our lives. This vision aligns with the objectives of the Smart Networks and Services Joint Undertaking (SNS JU) initiative, and the guidelines set by its flagship HEXA-X project [URB21], as well as those of International Telecommunication Union (ITU) and World Radiocommunication Conference (WRC).

The development of 6G is motivated by a combination of technology push and societal as well as industry pull factors. Key technologies, including sub-THz/THz access, network virtualisation, architectural disaggregation, meta-material surfaces, and AI/machine learning are driving the technology push. Meanwhile, societal challenges such as climate change, pandemics, digital divide, and social inequalities, as well as the European Green Deal [EC19], are exerting a pull on both the industry and academia to ensure the integration of core values, like sustainability and trustworthiness, which have been included in the design and purpose of 6G networks. As a result, a fundamental shift is envisioned in the design of mobile networks to meet the increasing demands of traffic, devices, sub-networks, and markets, while upholding the highest standards of energy efficiency, security, privacy, and reliability.

The deployment of THz RISs in 6G is crucial for achieving the extreme radio performance required to enable novel applications and services. While current communication systems operate in lower frequency bands, with the sub-THz band (100-300 GHz) being under preparation, the THz band (300 GHz - 1 THz) is poised to offer abundant spectral resources. These bands allow for high spectrum utilisation. Due to the very short wavelengths, massive arrays can be packed in a very small form factor providing potential for high-gain beamforming and fine angular resolvability – which can compensate the higher attenuation of signal propagation. Although 6G will leverage a combination of different frequency bands, the scientific, engineering, and commercialisation challenges associated with radio technology in the 100 GHz - 1 THz range demand careful investigation.

However, the implementation of THz RISs in 6G faces certain constraints, including hardware limitations and propagation challenges. Current technologies and techniques used in commercial 4th Generation (4G)/5th Generation (5G) radios, particularly in antennas, packaging, integrated circuits, and massive-MIMO beamforming, are not fully mature for large-scale systems, which motivates the objectives of TERRAMETA. Furthermore, the scalability of radio electronics to the THz range remains a challenge that will be partially tackled by the project. Addressing these challenges and advancing those technologies and algorithms will be crucial for harnessing the full potential of sub-THz and THz frequency bands for 6G.

6. Deployment Scenarios and Use Cases

A set of scenarios and use cases have been identified for the deployment of THz RIS technology. Although not all these scenarios and use cases will be developed in following work packages, it shows the potential societal impacts of the technological developments planned for TERRAMETA. In addition, this global perspective on THz RIS applications will be used to provide an initial set of top-down requirements that will guide the following WPs. This section first gives a top level overview of different categories of scenarios relevant to 6G (Section 6.1), and includes a discussion on deployment strategies from the perspective of network operators (Section 6.2). An overview of the scenarios and use cases is given in Section 6.3, before their presentation under Sections 6.4 to 6.6.

6.1. Different Kinds of Scenarios under 6G

6G is envisioned as a way of boosting the capacity of 4G/5G networks for enabling or augmenting new or existing services. This vision implicitly assumes a seamless integration of 6G on existing networks, which requires that THz RIS can reach most of the defined scenarios for lower frequencies. The 3GPP TR 38.901 report, which encompasses frequencies from 0.5 to 100 GHz, provides a general set of 5 scenarios that can be adapted for our 6G vision, namely:

- **Indoor open spaces, (InOp)**, aimed for indoor scenarios such as offices, schools, houses, where high-capacity communication, high-definition sensing and localization may be required. The typical deployment would be done using several radio access points located at ceiling or walls assisted by RIS (see Figure 6-1). The definition of whether the area is open plan office or mixed office space is included in the statistical assumptions of the path loss models.
- **Indoor factory (InFac)** where a large open area contains a variety of industrial machines (that can be mobile) communicating cooperatively as well as with radio access points. The flexibility provided by these smart high-capacity wireless links will assist on creating advance factory floors capable of self-reconfigurability and autonomous operation. This scenario has been identified by the consortium partners of great interest for industry and for this reason is seen in TERRAMETA as an important application for THz RIS. For this reason, we will further develop this scenario in a specific use case that will be used latter on the project for our demonstrator activity (WP6).
- **Outdoor urban microcell (OutUrMi)**, composed of radio units typically located on items of street furniture (e.g. lamp posts), below the height of the surrounding buildings that can communicate with mobile users (e.g. cars) and with the backhaul network.
- **Outdoor urban macrocell (OutUrbMa)** with antennas placed on rooftops and high masts with a mix of indoor and outdoor users at different levels of mobility. This scenario contains a wide range of use cases that are based on large size THz RIS deployment to counteract the expect free-space path loss and atmospheric attenuations. Application can range from communication, but as well as sensing and localization based for example in UAV units (see Figure 6-1).
- **Outdoor rural macrocell (OutRurMa)** referring to areas where typically there is a significant lower traffic density and higher mobility. This scenario is where RIS THz general deployment seems to be less likely to be competitive comparative exiting 4G and 5G technology. However, long range THz links can still make sense for specific cases where an exceptional increase on data rate demand may occur. This could happen for some localized events, such as a festival gathering or some emergency communication trigger by a disaster that can benefit of high-date rate transmission or high-resolution sensing.

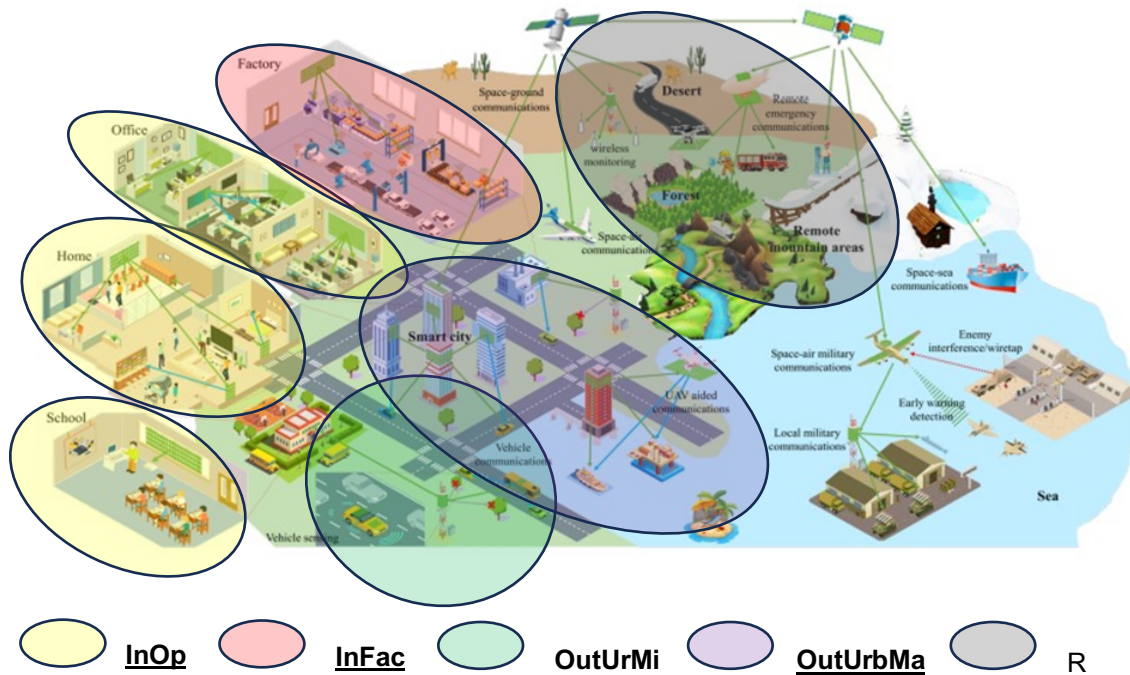


Figure 6-1 Deployment scenarios for future communication networks (adapted from [GGJ23]).

6.2. Indoor and Outdoor Deployment Strategies

Communications service providers are challenged on footprint, rent, and OPEX of macro sites, and those challenges are even more present at street level. New outdoor deployments will require creative solutions to meet these demands. Projections of increasing demand for wide-area communications supporting new applications requiring high data rates and reliable coverage necessitates the study of the terahertz frequency range. Given that THz communications have large bandwidths, this allows for the use of single carrier and multi-carrier techniques in wide area deployments. Single carrier frequency configuration denotes that each cell is only configured with one carrier frequency. Two main issues with single carrier deployments are high interference and small coverage due to high bandwidths. Multi-carrier configurations denotes that several carrier frequencies belong to the cell, and all the carrier frequencies can carry different data information. This is typically achieved with parts of the deployed frequency band. 5G introduced flexible numerology on a given carrier and this is expected to continue in 6G wireless communications. Due to the large bandwidths of THz deployments, it is possible to assign certain frequency spectrum within the overall carrier bandwidths in either direction (uplink or downlink). This assignment is known as a bandwidth part. In accordance with TS 38.211, a bandwidth part is a subset of contiguous common resource blocks. Flexible bandwidths allow for specific state and service requirements of the User Equipment (UE).

The continuous support for the growing diversity of wireless services and providers can be facilitated by considering further options for localised spectrum access when the use of THz is authorised. This allows for continuous competition among Mobile Network Operators (MNOs), and will drive the delivery of good outcomes for customers over the years to come, which will be supported by a range of public policy interventions. This competition is a key driver of good outcomes for technological and market developments that will take place. Network quality is always of a growing importance to customers, making for a more competitive dynamic. This competition is also likely to be driven by potential new applications that entail higher data consumption, such as augmented and virtual reality, as well as commercial or industrial applications like machine-to-machine communications.

MNOs are likely to use a range of approaches to deliver more capacity to meet this demand, including technology upgrade, leveraging the extensive use of their spectrum holdings, and increasing the number of sites where additional capacity is needed. Significant investment in mobile networks will be required to increase capacity and provide the network quality needed to meet future customer needs. In addition to this, there is a need to deliver shared network access in some cases, this is usually when it is not physically or financially viable for any individual or single operator solution. Neutral hosts can provide commercial, mobile access solutions to several operators via a single, shared network solution that is open to all operators.

A wider issue is whether quality of experience in areas where people and businesses go is sufficient to meet people's needs, although competition among MNOs has helped drive improvements in quality. Evidence suggests that quality of experience is generally good for most customers but can be patchy in localized regions.

Critical areas in which MNOs could meet growing demand for data:

- more extensive deployment of existing spectrum holdings and making use of planned spectrum releases.
- investment in technology upgrades to increase the amount of data that can be carried over a given amount of spectrum.
- increasing the number of sites in areas where additional capacity is needed (network densification).

These areas can be addressed with the deployment of THz base stations and a densification with THz RIS. Terahertz spectrum has the potential to allow very high throughput and a very low latency due to its extremely high bandwidth. Therefore, it is expected that THz RIS will be able to serve for coverage extension, throughput enhancement, and enable resilient networks.

At the same time, indoor environments provide a wide variety of use cases that can benefit for the THz RIS deployment for enhancing the user experience. Such scenarios are less affected by the THz path loss restrictions of the outdoor case, hence, in principle, smaller RIS dimensions could be used, impacting the cost and power consumption of the indoor devices. On the other hand, multiple path propagation caused by specular reflections needs to be properly accounted that otherwise would be the dominate effect for the fading of the channel. In a later stage of the project (WP5), these complex scenarios will be simulated accounting more realistic models of THz-RIS provided by WP3.

6.3. Overview of the TERRAMETA Scenarios and Use Cases

In this Deliverable, 15 use cases have been formulated that exemplify the benefits, deployment, and operation of THz RIS networks. The use cases are presented under three umbrella scenarios, namely *High-Capacity Communications* (Section 6.4), *High-Resolution Localisation, Sensing, and 3D Mapping* (Section 6.5), as well as *Industry 4.0* (Section 6.6). While the first two scenarios are based on the goal of the underlying use cases, the latter contains use cases arising from important considerations in industrial settings and treat a wide range of objectives.

To provide a clear view of the most important aspects of the envisioned cases, a taxonomy is given in Table 2 below. The use cases cover a wide range of applications from coverage enhancement to sensing and mapping. Different use cases are more applicable to outdoor scenarios, others are designed specific for indoor in mind, while some are applicable to both settings. In a similar manner, some use cases may be better suited to near field or far field communications, even though the majority of them can be applied to both cases. Apart from the network and deployment aspects that characterise each use case, a key piece of information is the kind of RIS hardware required for it to be implemented. While many of the use cases can be accommodated by low-cost and low-power reflective, or even fixed-beam RISs, more advanced cases may require or be better facilitated by elaborate operations performed by the surfaces, such as reception and transmission. Attaining successful trade-offs in terms of potential gains of such solutions over the associated (expected) design, manufacturing, deployment, and controlling overheads in each case will be a focal point throughout the lifetime of this Project.

Table 2 Taxonomy and characteristics of the TERRAMETA use cases.

Use Case	Application type	Indoor / Outdoor	Near-Field / Far-Field	RIS Types and Operation Modes	Key use case and network aspects
Blind Spot Coverage	Coverage extension	Both	Both	Reflective	Blocked LoS
Hybrid Indoor/Outdoor Repeater	Coverage extension	Indoor-to-Outdoor	Both	Reflective, Transmissive, Reconfigurable	Either static or reconfigurable repeater
Multi-Carrier/Multi-RIS Operation	Network interoperation	Outdoor	Far-Field	Reflective, Reconfigurable	Multiple network operators
Infrastructure Sharing	Network Interoperation	Outdoor	Far-Field	Reflective, Reconfigurable	Multiple network operators
Backhaul and Integrated Access	Backhaul planning	Outdoor	Far-Field	Reflective	Backhaul topologies
Direct Short-Range Links	High-Capacity connectivity	Indoor	Near Field (mainly) / Both	Reflective, Reconfigurable	Multiple user terminals
Ultra-Directive Short-Haul and Mid-Haul	High-Capacity connectivity	Both	Both	Transmissive, Reconfigurable	Even fixed beam antennas may be used
THz RIS-aided Backhaul Link Sensing and Localisation	Localisation and sensing	Outdoor	Both	Reflective, Reconfigurable, Receiving	Inter-base station, NLoS
THz RIS-aided Multi-Access Sensing	Localisation and sensing	Both	Both	Reflective, Reconfigurable, Receiving	Multiple targets
THz RIS-aided Outdoor-to-Indoor Sensing	Localisation and sensing	Outdoor-to-Indoor	Both	Reflective, Reconfigurable, Receiving, STAR RIS	Can be integrated to existing WLAN infrastructure
Joint Communication and Sensing with Full Duplex Holographic DMAs	Joint sensing and communications	Both	Near Field	Receiving, DMA, Holographic	Can serve multiple users

Environmental Mapping and Imaging	RF mapping	Both	Near Field	Receiving, DMA, Holographic	3D reconstruction of targets
Enhancing Throughput, Localisation, and Mapping in Factory Settings	Throughput enhancements / Simultaneous localisation and mapping	Indoor	Near Field	Reflective, Reconfigurable, Receiving, Transmissive	Mobility and blockage scenarios
Software Defined Networking Enhancement in Data Centres	Network resilience / Multiple Access	Indoor	Both	Reflective, Reconfigurable, Transmissive	Dynamic management of multiple server nodes
Large Scale Distributed Sensing in Factory	Sensing	Indoor	Near Field	Receiving	Detection of passive objects

6.4. High-Capacity Communications

Under this scenario different use cases are proposed that illustrate the benefits of THz RIS in terms of capacity improvements in envisioned 6G communication networks. All use cases of this section work by carefully designed beams toward target users or network transceivers. Various RIS types and operation modes are considered and appropriate far-field beamforming or near-field beam focusing policies are given at a high level.

6.4.1. Coverage Extension

Blind Spot Coverage

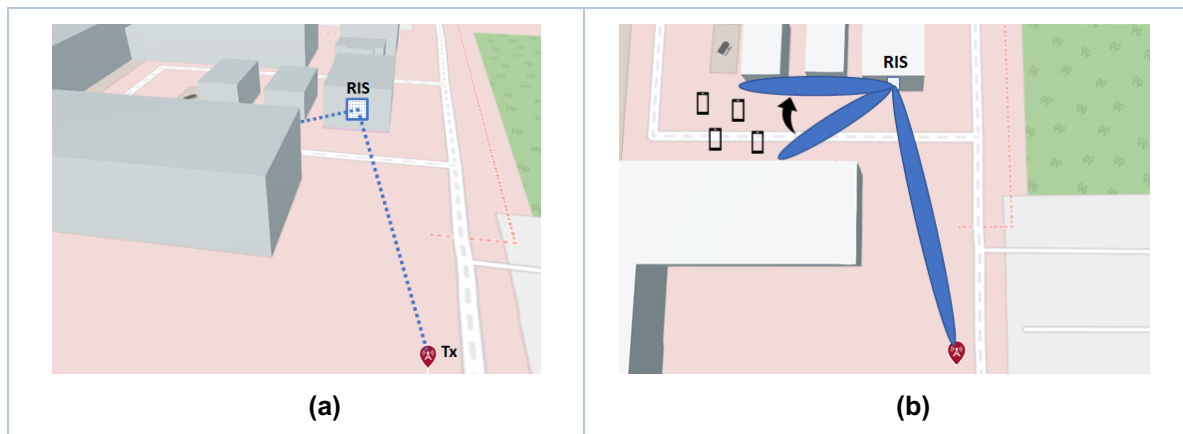


Figure 6-2 Blind spot coverage enhancement

This use case looks at the outdoor deployment of THz RIS and conventional THz transmitters. In this deployment scenario the THz RIS is placed at a distance, D , in the far field of the base station antenna in order to alter the propagation environment in a controlled manner. The expectation is that the use of such surfaces can provide coverage enhancement and spectral efficiency improvement.

Furthermore, similar to the case of the blind spot coverage enhancement use case, RISs can be used in indoor scenarios to cover blind regions due to the presence of corridors or to guarantee connectivity in the case when the LoS path is blocked as shown in Figure 6-3. These characteristics became extremely important at THz frequencies where the electromagnetic waves are highly attenuated when impinging obstacles. In this case, passive or electronically reconfigurable RISs can be used to extend the coverage.

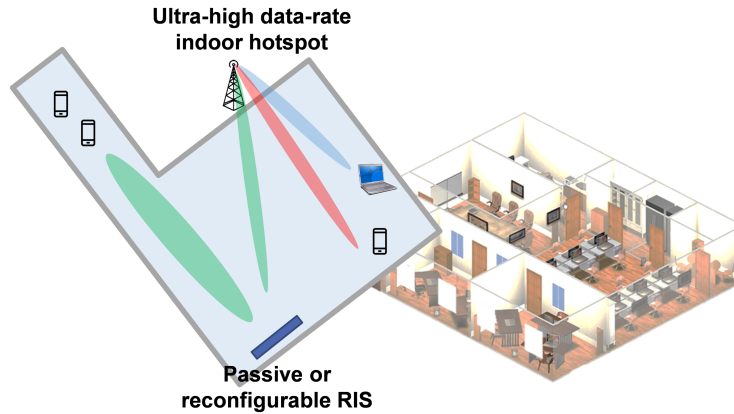


Figure 6-3 Blindspot Indoor Coverage

This use case variation considers a sub-THz point-to-point connection (Figure 6-3 (a)) with a single beam and is most relevant for stationary outdoor connections with large range and high-capacity requirements. In this case, the sub-THz beam needs no or only limited steering capability to compensate the misalignment between two antennas in direct link.

Hybrid Outdoor/Indoor Repeater

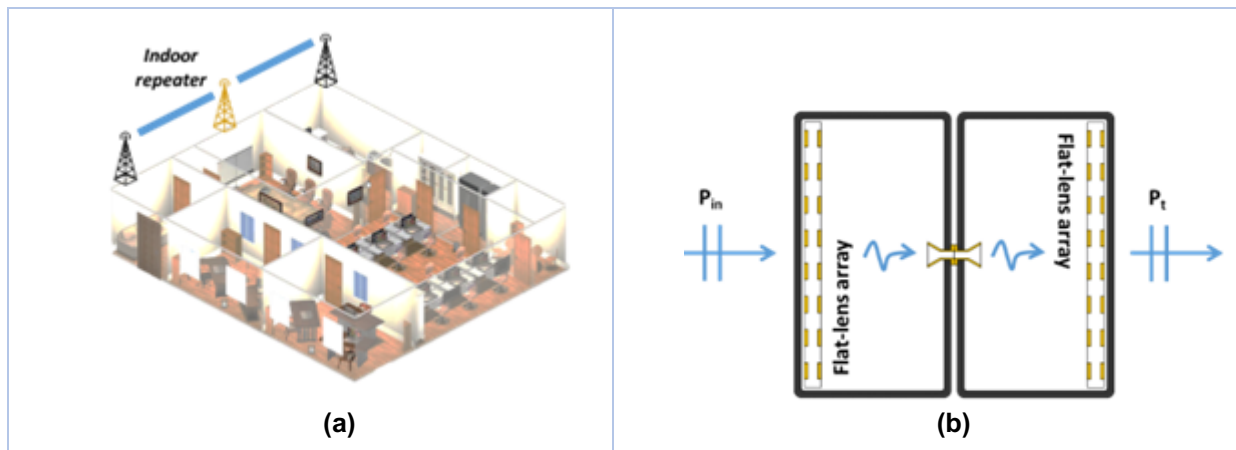


Figure 6-4 Hybrid Outdoor/Indoor RIS repeater

Network coverage can be extended by the help of radio frequency (RF) repeaters, for either outdoor or indoor applications, as they have been used in commercial deployments depicted in Figure 6-4. However, their functionality is limited since they simply operate in an amplify and forward mode with respect to the signals they receive. To overcome such limitations, RISs are capable to act as smart repeaters and provide further degrees of freedom in terms of coverage and performance, especially when LoS links between transmitters and receivers are blocked. A RIS-based repeater, Figure 6-4 (b),

can be passive (fixed beam) or reconfigurable. A passive-based repeater can be an extremely low-cost solution to allow the transmission of the sub-THz electromagnetic wave from a room to another room, or from the outdoor to the indoor without using any power amplifier. By using the antenna solution proposed in Figure 6-4(b), the incident wave is received by a first transmit array interconnected to a second transmit array, which retransmits the power in the free space direction. An electronically reconfigurable T-RIS can be also used in one or both sides of the repeater to perform beam control in near- and far-field regions.

6.4.2. Multi-Carrier/Multit-Band RIS Operation

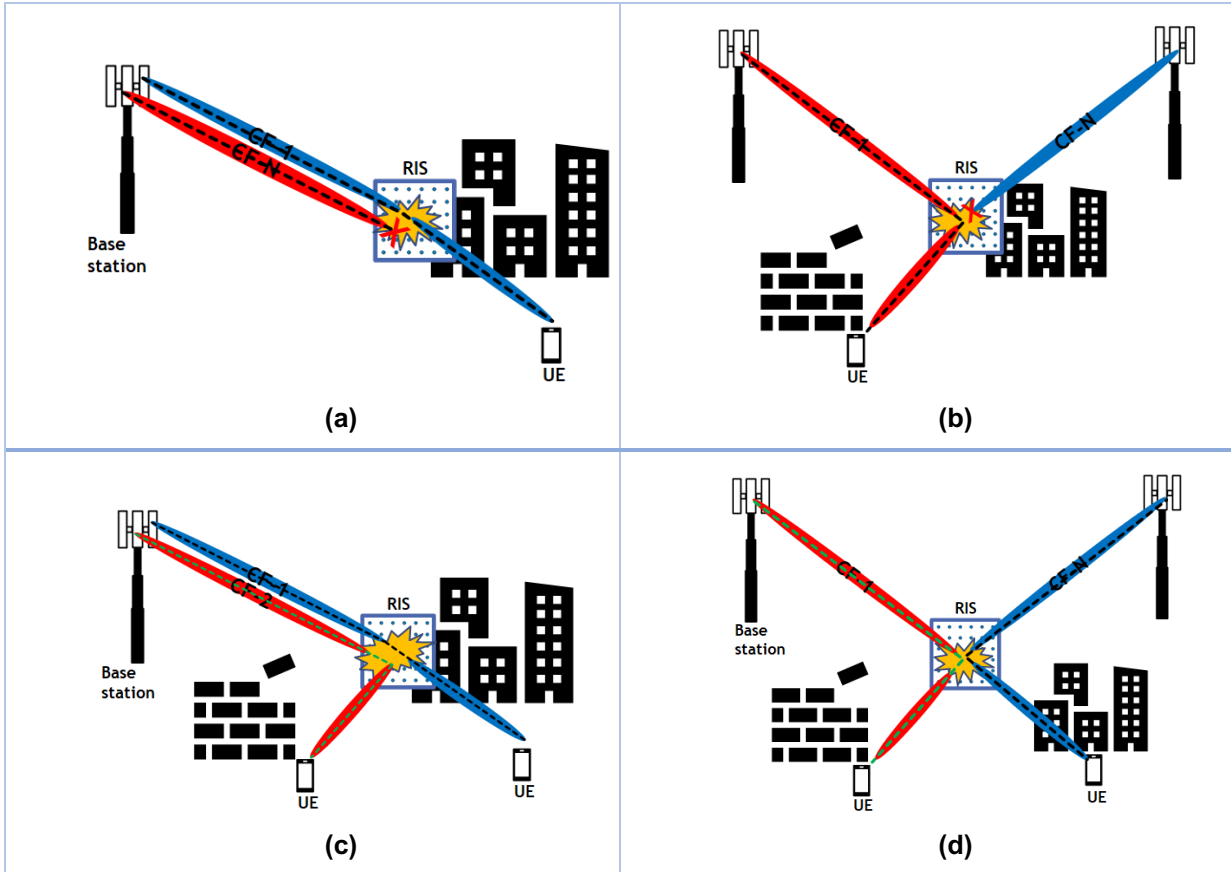


Figure 6-5 multi-carrier outdoor deployments expected with a THz RIS

A THz RIS can be modelled as a new network node for tuneable reflections, using control signalling from a 6G base station. The use cases depicted in Figure 6-5 illustrate the types of multicarrier deployments expected in an outdoor environment. Figure 6-5 (a) depicts a multicarrier 6G base station with multiple carriers where these carriers can be single operator owned or the base station can be shared by multiple operators with separate carriers where the RIS is tuned to a specific carrier transmitting to a desired UE. Figure 6-5 (b) depicts geographically separated 6G base stations, where these multi-base station deployments can be single operator owned or each base station is owned by different operators with separate carriers, where the RIS is tuned to a specific carrier transmitting to a desired UE. Like Figure 6-5 (a), Figure 6-5 (c) depicts a multicarrier 6G base station with multiple carriers where these carriers can be single operator owned or the base station can be shared with by multiple operators with separate carriers, where the RIS can transmit the desired signals to the specified UEs which are separated in the frequency domain. Like Figure 6-5 (b), Figure 6-5 (d) depicts geographically separated 6G base stations where these multi-base station deployments can be single operator owned or each base station is owned by individual operators with separate carriers, where the RIS can transmit the desired signals to the specified UEs which are separated in the frequency domain.

6.4.3. Infrastructure Sharing

Some of the key directions for 6G networks include the evolution towards a paradigm of “Networks of Networks” [URB21]. From a practical point of view this paradigm comes with the following implications:

1. First, 6G networks are expected to act as the catalyst which will bridge the gap between the human and digital world, and act as the necessary infrastructure for interconnecting the human, digital, and physical worlds. Such an evolution will allow for creating extended cyber-physical systems and enable a wide range of applications including, among others, digital twinning.
2. Second, 6G networks themselves are expected to follow the “Networks of Networks” paradigm, such as to facilitate the management of mass-scale deployments and seamless inter-operation [URB21] potentially allowing for extended infrastructure sharing, which is already discussed as a solution for reducing operational costs and increasing the energy efficiency of 5G networks [SKR20, KO23, RMG19].

Motivated from the above, and focusing on outdoor deployments, we envision as a potential use-case, the case of Base Station Sharing and RIS sharing among operators in order to combine energy efficiency with extended, reliable connectivity in RIS-assisted THz communications networks. To further understand the benefits of such deployment, in Figure 6-5, we present a first base case where no infrastructure-sharing is applied.

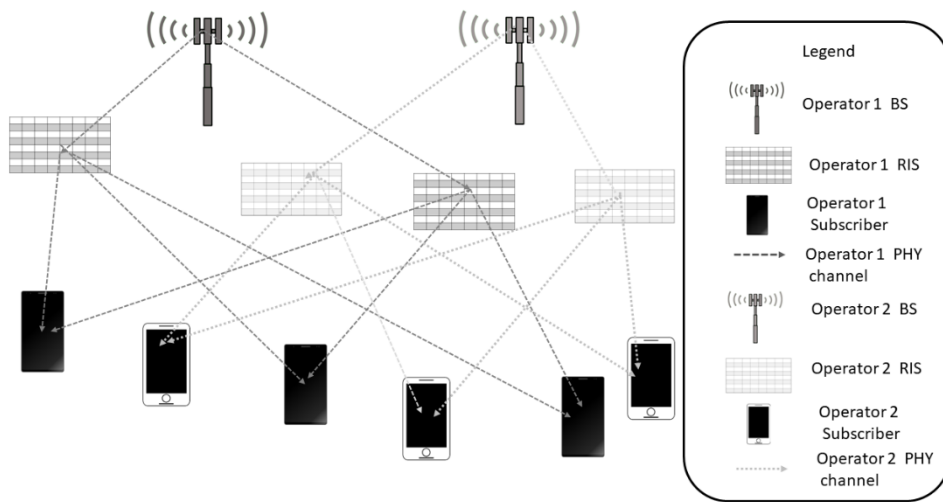


Figure 6-5 Non cooperative deployment

Within TERRAMETA we envision the following variations of the infrastructure sharing use case which can result in more efficient THz communications.

BS Sharing

BS sharing cases are designed for increased energy efficiency, reduced CapEx/OpEx and increased coverage. Figure 6-6 illustrates how the architecture of Figure 6-5 can be transformed if Base Station (BS) operation is employed (for simplicity only subscribers of Operator 1 are depicted). From Figure 6-5 we can see that such a use case can allow for ensuring better downlink conditions and result in better coverage for Operator 1 subscribers. This conclusion is also valid for subscribers of Operator 2. Moreover, by allowing BS sharing, reliable coverage can be provided for both Operator subscribers while using a smaller total number of BSs, resulting in smaller CapEx for each one of the operators and higher energy efficiency.

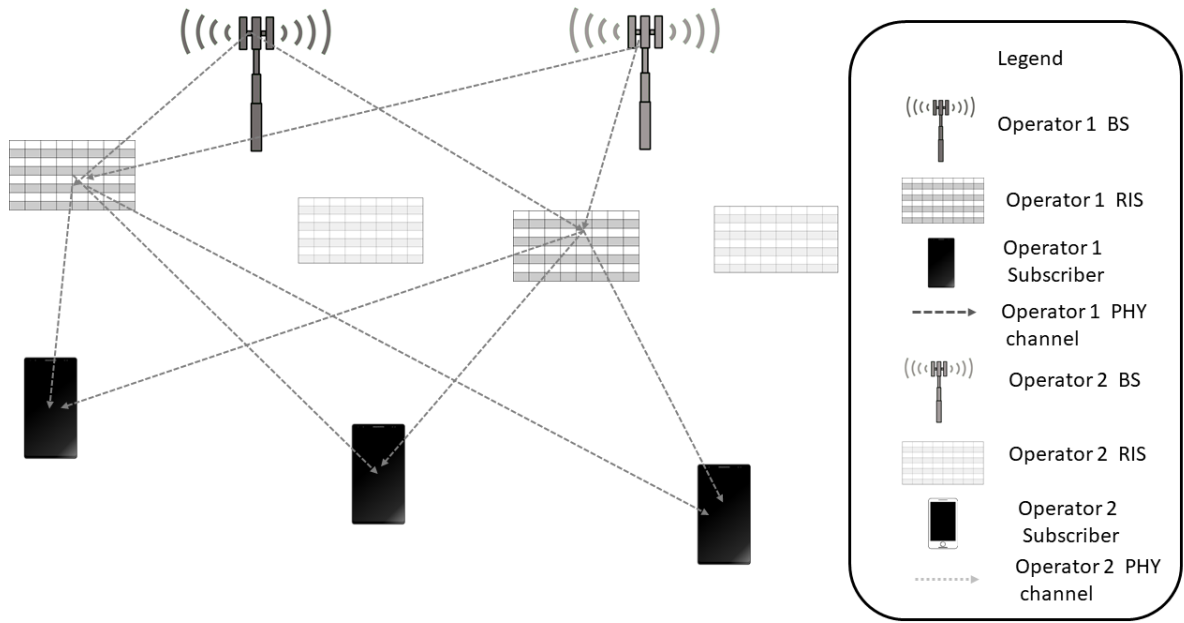


Figure 6-6 BS station sharing.

BS and RIS Sharing

Figure 6-7 illustrates full infrastructure sharing for maximizing energy efficiency and CapEx/OpEx savings. In case of full infrastructure sharing, operators do not only share their network of BSs but also their RISs. As a result, better propagation conditions can be ensured for all users.

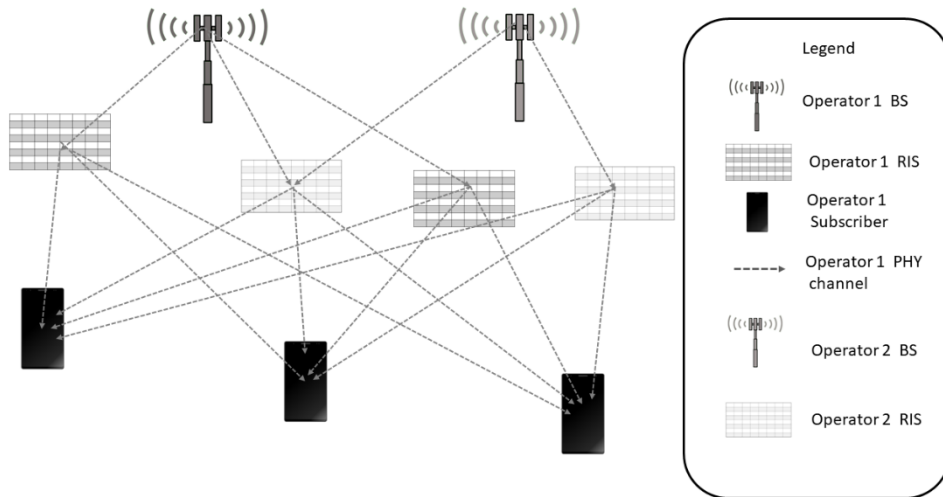


Figure 6-7 BS station and RIS sharing.

Moving Infrastructure Sharing

Figure 6-8 is an illustration of exploiting a moving infrastructure. As an example of ultimate sharing which brings us closer to the network of networks paradigm, we envision use cases where besides BS and fixed RIS sharing, we consider the presence of a network of shared aerial RIS, mounted on UAVs (for simplicity only one Unmanned Aerial Vehicle (UAV) is shown).

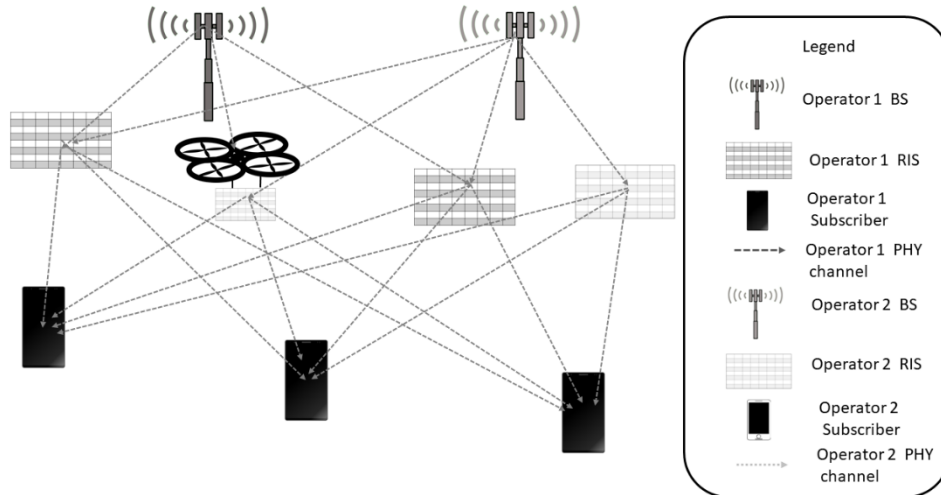


Figure 6-8 The THz network as a shared “Network of Networks” where a network of UAVs is also shared.

6.4.4. Backhaul and Integrated Access

Improved Backhaul Performance

The technology advancements in the mobile communications have been steadily driven by the increasing demand for the high data throughput, as well as the high data traffic, from the end-user devices. This led to the proliferation of base stations and this trend will continue further in the future. Each base station requires a communication channel to the core network that is known as backhaul links. Typically, backhaul links are provided over fibre connection. However, cabling fibre backhaul links is time-consuming and labour-intensive. In addition to this, installation of fibre backhaul links may not be able in some cases due to the geographical, political, and economical issues. Due to this fact research on the realization of wireless backhaul links operating at FR2 (24.25GHz-52.6GHz) and E-band (60GHz-90GHz) is one of the topics being actively investigated in 5G.

However, as the number of base stations to be deployed increases, the complexity of the backhaul planning task becomes greater since it is one of the typical non-deterministic polynomial problems, how many and which base stations shall possess wireless backhaul links in order to find an optimum solution of the backhaul network. On this account, several algorithms for the automatic planning of the wireless backhaul links have been developed by taking into account different networking constellations: star topology considering LoS [JDE19], star topology considering both LoS and NLoS [KJ21], ring topology considering LoS [JK21], and ring topology considering both LoS and NLoS [JK23].

In the context of 6G, the number of backhaul links and their capacity become a huge issue more than what being discussed in 5G. This is because that the number of base stations is expected to more densely proliferate and the backhaul links should seamlessly exchange the unprecedented amount of aggregated data at the access nodes to the core network and vice versa. The peak data rate in 6G is expected to reach 1 Tbps [SBC19]. This means that the backhaul links will have to support the data transmission of such a high data rate. By having these aspects in mind, wireless backhaul links operating at FR2, and E-band may not be enough anymore to fulfil the backhaul capacity in 6G due to the limited available bandwidth. Therefore, THz backhaul links (sub-THz) have been recently spotlighted for a

promising application scenario in 6G due to the great compromise between mmWave and Free Space Optical (FSO) backhaul links that enables to the higher data transmission rates than mmWave backhaul links due to the large available bandwidth and to the greater achievable link distance than FSO.

In THz backhaul networks, the use of RIS is expected to be a useful tool improving the performance of THz backhaul links in various aspects. First of all, the use of RIS can improve THz backhaul connectivity. The wave propagation at THz shows strong straightness and low penetrability through the materials which forces mobile communications at this frequency spectrum to be available only under LoS condition between two transceivers or a specific condition of the specular reflection by the surfaces. RIS can overcome the conditional limitation of THz backhaul connections by relaying backhaul connections over non-specular reflection. The relevant use case scenario is visualized in Figure 6-9, in which neither LoS condition between two cell sites is feasible due to a building nor a path can be found via specular reflection of the building walls. The use of RIS as a relay enables one to establish the THz backhaul link regardless of the above limitations. This can be accomplished by implementing a RIS surface on the external wall of the building, in which both paths between cell sites and RIS are in LoS. This use case is expected to be seen in most of the THz backhaul networks. Especially in this scenario where the deviation of the building height is high so that many of the LoS conditions between cell sites are obstructed.

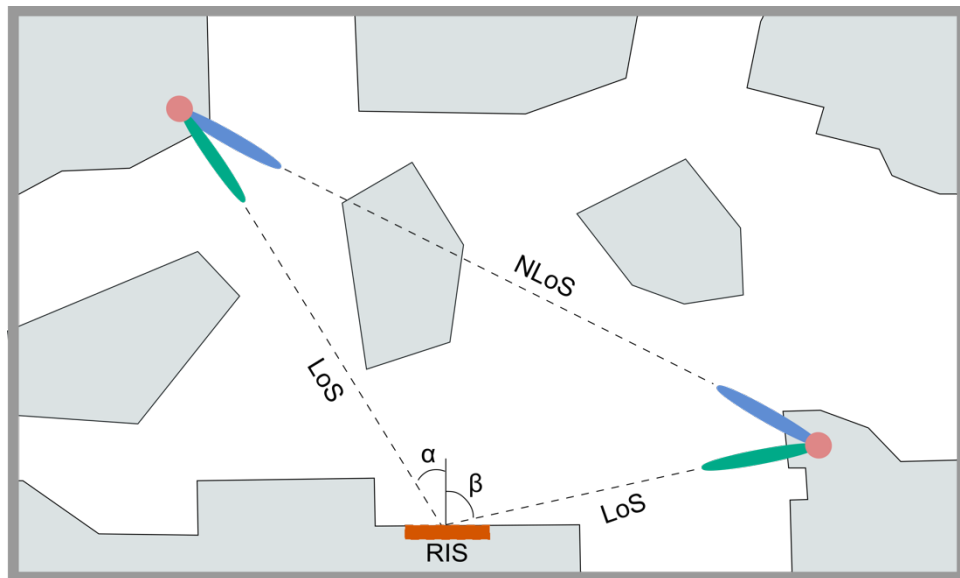


Figure 6-9 An RIS's use case of increasing THz backhaul connectivity using the relay concept.

Furthermore, in THz backhaul network, RIS can be exploited to mitigate high interference caused by undesired alignment of THz links. Considering the use of high gain antennas at both transmitter (TX) and receiver (RX), the high interference shall be generated by in-line THz backhaul links given in Figure 6-10. In this case, the cell sites are deployed at the lamp-post sites at the same height, where two THz back haul links are established one between cell 1 and 2, as well as one between cell 3 and 4. Here, cell 1 is highly interfered by cell 4 due to the undesired alignment of antennas and vice versa. This leads to the poor Signal to Interference plus Noise Ratio (SINR), which degrades the performance of data transmission. The given type of high interference can be simply alleviated by managing the direction of antennas. This can be completed by the use of RIS. In the case that if the THz link between cell 1 and cell 2 is established via RIS instead of the direct LoS link, then no antenna will be aligned anymore, which results in the low interference between cell sites 1 and 4.

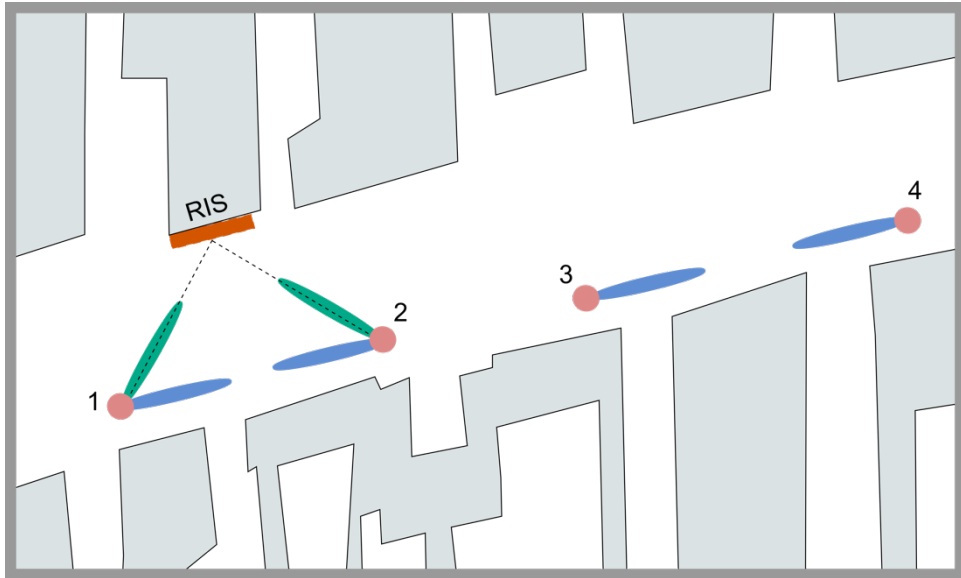


Figure 6-10 An RIS's use case of relaxing high interference caused by in-line backhaul links.

The use of RIS is not only limited in increasing network performance but RIS can be also exploited to make the maintenance work related to the antenna alignment more bearable. Due to the fact of high propagation loss in wireless channels at THz frequencies, the use of high gain antennas of 50+ dBi at both TX and RX is demanded for THz backhaul links. Note that the half power beam width of 50 dBi is not greater than 0.5 degree. Which means, even a slight misalignment of antennas can cause severe degradation of the channel quality and even result in the link failure. Many causes including impact of wind exists resulting in the antenna misalignment. This makes therefore the antenna alignment and maintenance become more challenging tasks. The use of RIS enables us however to react adaptively against antenna misalignment caused. Figure 6-11 shows a schematic visualization of the RIS's use case for this, where antenna alignment can be assured in any case by the adjustment of antenna's pointing vector with help of RIS both at TX and RX. This can be further extended to the beam management. In case that LoS condition of the link is obstructed, an alternative link instead of the obstructed link can be immediately switched on to secure the data transmission over the backhaul link, which traditionally is supposed to be completed by manual configuration and thus requires considerable time. The corresponding information related to multi paths can be supported by the real time 3D environment sensing.

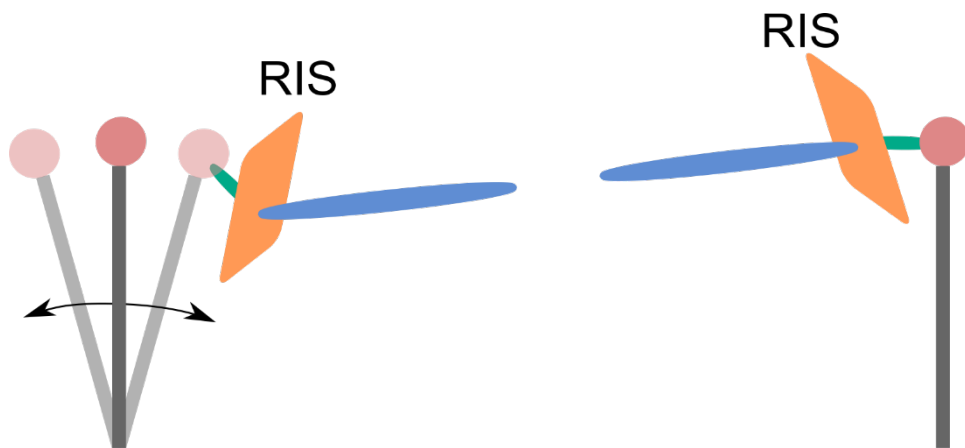


Figure 6-11 An RIS's use case of managing THz backhaul links' beam alignment.

Another RIS's use case for THz backhaul networks is to use RIS as a beam splitter. RIS is in principle an N by M array of antenna elements where the signals generated by each element are superposed to produce new desired signals. With the help of RIS, a cell site can thus simultaneously provide THz backhaul links to more than one cell site. The provision of multiple THz backhaul links can be accomplished either by spatial division multiple access approach or time division multiple access approach. In any case, it is feasible to reduce the number of antennas at the anchor cell site. At the same time, it enables one to reduce the effort of the maintenance work for the antenna alignment. An example of this can be seen in Figure 6-12.

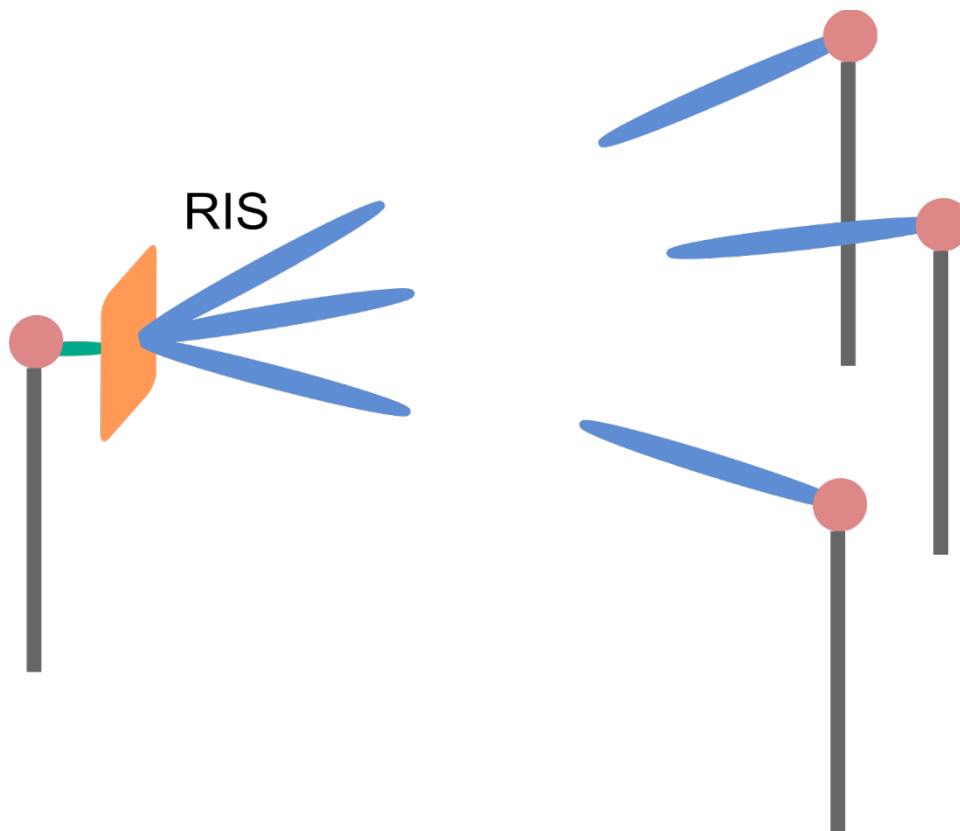


Figure 6-12 An RIS's use case of beam-splitting.

The four use cases introduced above are the typical use cases of using RIS integrated into 6G mobile networks. To identify and assess the benefits of using RIS in THz backhaul networks, what firstly should be done is to set appropriate scenarios. For that a cell deployment scenario in the city centre of Berlin visualized in Figure 6-13 will be used to represent a generic 6G mobile network. The scenario is designed within the former EU-Japan joint project ThoR [T19], where high data traffic and high data throughput is expected as the area is composed of complex city profiles containing business district, residential area, and tourist attractions.

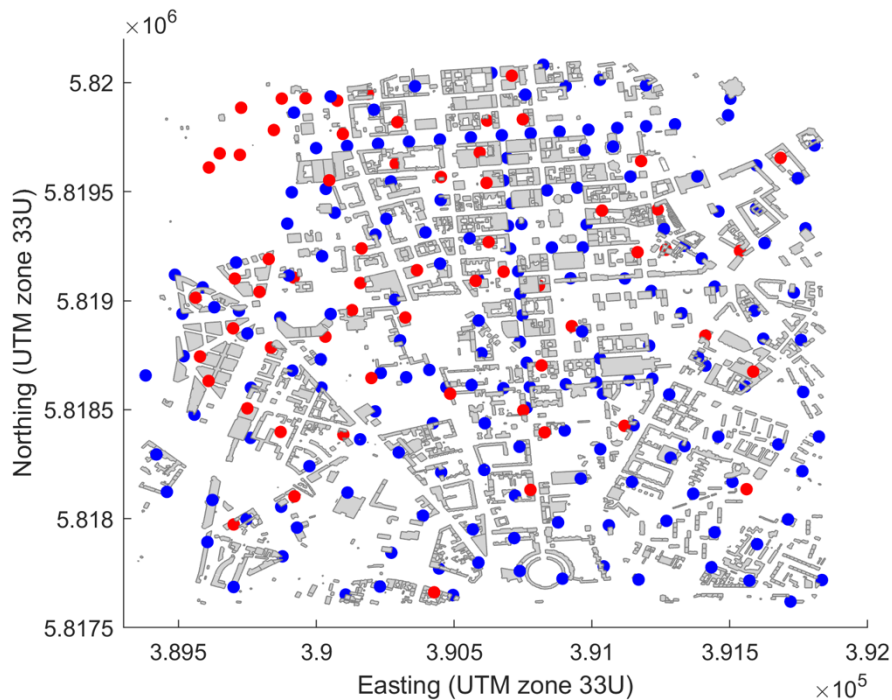


Figure 6-13 Cell deployment scenario in the city centre of Berlin

In this scenario, 62 Macro Cell Sites (MCS) are represented by red dots and deployed arbitrarily at 1m above the roof top of the buildings considering the actual cell deployment of one of the network operators. The backhaul links of MCSs are already provided over fibre connections. In addition to that a total of 176 Small Cell Sites (SCS) are represented by blue dots and assumed to be deployed as to support seamless mobile access to the end users. The 50% of SCSs are assumed to be deployed at 4m above the ground as lamp-post sites while the rest of SCSs are at 1m above the roof top of the buildings as typical base stations. Their backhaul links are to be decided and the deployment of SCSs is considered completely arbitrary.

The scenarios for integrating RISs in THz backhaul networks in 6G starts with planning of THz backhaul links in the entire scenarios exploiting four different algorithms as follows:

1. star topology considering LoS [JDE19]
2. star topology considering both LoS and NLoS [KJ21]
3. ring topology considering LoS [JK21]
4. ring topology considering both LoS and NLoS [JK23]

Each Figure 6-14 to Figure 6-17 show the automatically planned THz backhaul links using each algorithm as given above. Here the red dots represent cell sites whose backhaul links have to be provided by fibre connections in order to provide THz backhaul links to the other cell sites and the blue dots represent cell site whose backhaul links can be provided over THz backhaul links. The corresponding THz backhaul links are visualized in green lines.

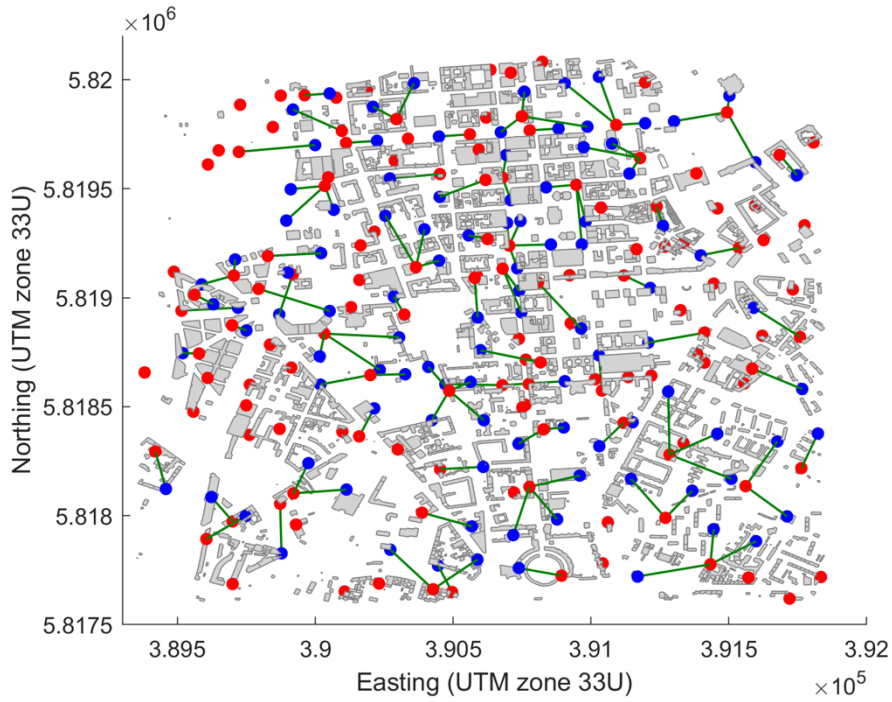


Figure 6-14 Example of a wireless backhaul network using a star topology based automatic planning algorithm considering only LoS link connectivity.

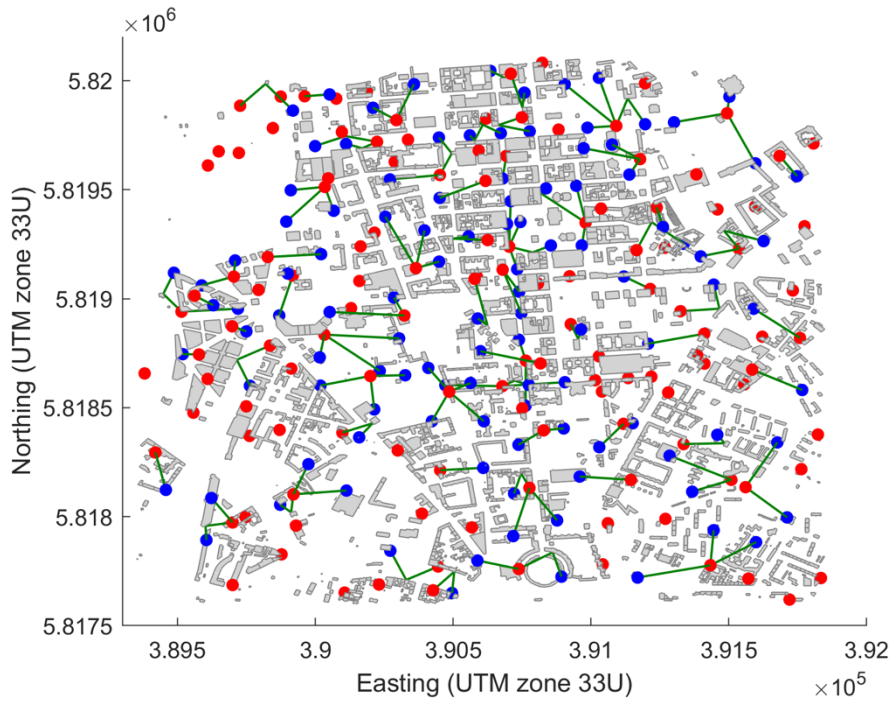


Figure 6-15 Example of a wireless backhaul network using a star topology based automatic planning algorithm considering both LoS and NLoS link connectivity.

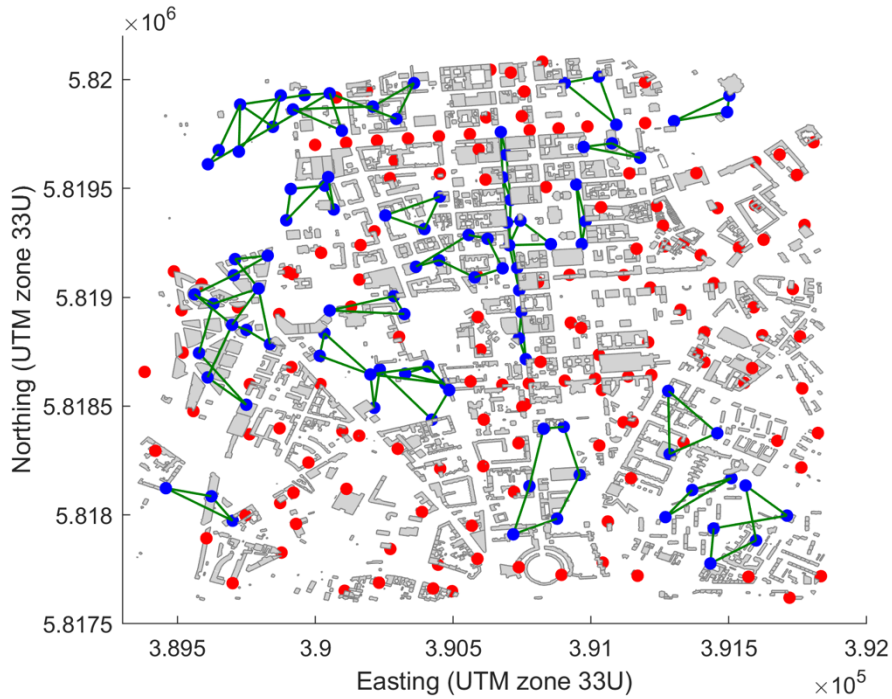


Figure 6-16 Example of a wireless backhaul network using a ring topology based automatic planning algorithm considering only LoS link connectivity.

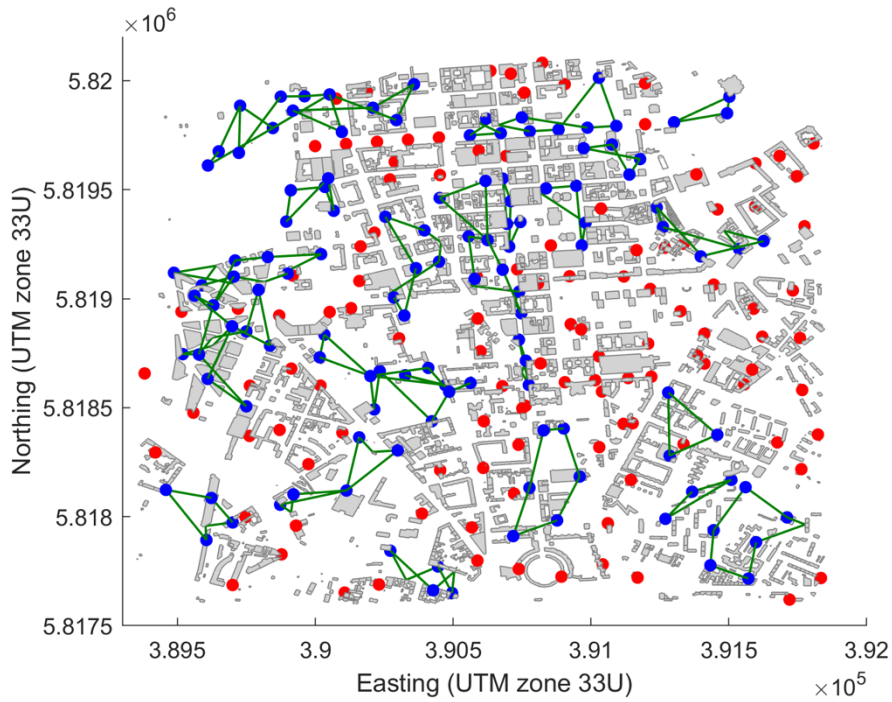


Figure 6-17 Example of a wireless backhaul network using a ring topology based automatic planning algorithm considering both LoS and NLoS link connectivity.

Integrated Access to Backhaul (IAB)

It is well known that network densification can lead to substantial enhancements in achievable rates and latencies. However, every additional Radio Access Network (RAN) node would then be required to backhaul its data to the Core Network (CN). Such backhauling can be accomplished either via the expensive and time-consuming installation of optical fibre cables, or through wireless channels (i.e. wireless backhauling). The latter is commonly known as the Integrated Access and Backhaul (IAB), since the access for UEs and the backhauling are both carried out over the wireless channels.

Two different types of IAB operations have been standardized by the Third Generation Partnership Project (3GPP): In-band (IB) and out-of-band (OB). In the OB-IAB, the access and backhaul links adopt separate frequency bands, which eliminates the interference between the two links. In contrast, at least partial frequency overlap between the access and backhaul should exist in the IB-IAB, which can potentially lead to enhanced spectrum utilization compared to the former case. However, the resultant interference for the IB-IAB must be tackled through separating the two links in time, space, or frequency (i.e., allocating orthogonal bandwidths for access and backhauling on the same frequency band). Different frequency bands in FR1 (below 7.125 GHz) and FR2 have been standardized by the 3GPP for the IAB operation in the 5G-NR.

Regarding the network architecture, an IAB network consists of an IAB donor and IAB nodes (see Figure 6-18). An IAB node is a RAN node that supports NR access links to UEs, and NR backhaul links to other IAB nodes or to the IAB donor, while the IAB donor is a gNodeB (gNB) that provides network access to UEs through a network of access and backhaul links. Specifically, the IAB donor consists of one Central Unit (CU) with both user plane and control plane functionalities, and a minimum of one Distributed Unit (DU). The DU at the IAB donor is utilized to serve child nodes, which could either be IAB nodes or UEs, while the CU connects the IAB donor to the CN via a non-IAB link (such as optical-fibre cables). On the other hand, each IAB node comprises two functionalities, namely a Mobile Termination (MT) and a DU. An IAB node connects to child IAB nodes or UEs via its DU functionality, while the MT unit connects an IAB node to parent IAB nodes or to the IAB donor. It is worth mentioning that the routing of data packets between different RAN nodes and the CN is controlled by a novel protocol known as the Backhaul Adaptation Protocol (BAP), which is a middle sublayer that supports various functions and was introduced in the 3GPP release 17. The route selection is done based on the network needs, which could include blockage minimization or load balancing.

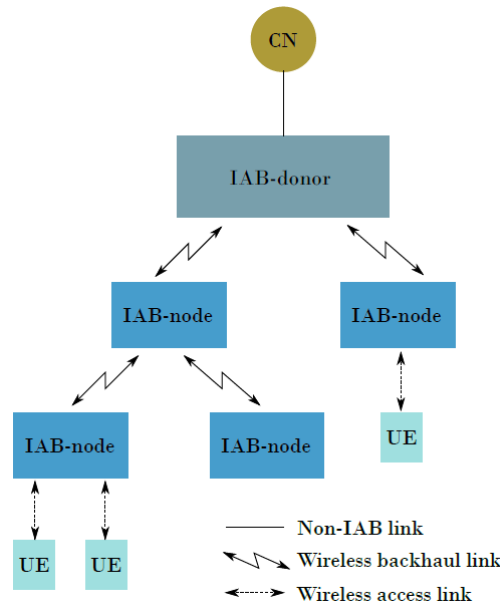


Figure 6-18 5G-NR IAB network architecture.

The application of IAB in the THz frequencies can be highly useful in situations where the RAN nodes (small cells) are highly overloaded. For example, in a concert or a large stadium where hundreds (if not thousands) of UEs aim to establish broadband connection. In such scenarios, OB-IAB with mmWave

UE access and THz RAN backhaul can be adopted for highly efficient network operation. In such scenarios, and given the considered mmWave/THz communication links, the presence of RIS is key to enable efficient IAB operation via providing high-quality virtual LoS links when the direct LoS links between RAN nodes and UEs and/or between different RAN nodes are blocked.

6.4.5. Direct Short-Range Links

We envision an open room, let say an office, where is common to have multiple interconnect devices, distributed along a desk or in nearby furniture of the room. We can think that these devices as conventional laptops, or in a more IoT approach, as elements of a distributed network organized (access points, smart glasses, etc) to provide immersive user experiences (e.g., argument reality). The common point in this use-case for these applications is that high-data rates transmission is required that cannot be deliverable by mmWave links. Hence, RIS-THz would play an important role here as it could provide LoS short-range (up to 5m) connections between devices interconnected by an extremely high-speed wireless link (up to 1 Tbps). These be achieved by considering ultra-low profile transmit array on both devices having a gain in the range 25 – 30 dBi, or one terminal with a higher gain (as an Access point install in ceiling) and other with lower gain mobile terminal as. In Figure 6-19 we depicted one possible example in a given workplace. The RIS reconfigurability would be used to maintain the link as the relative position between the terminals change. This use case in fact encompasses two RIS modes of operation: 1) far-field beam steering (conventional beam focusing); 2) near field beam focusing when the distance between the terminals become two small.



Figure 6-19 Indoor direct short-range link for immersive data analysis and exchange

6.4.6. Ultra-Directive Short Haul and Mid-Haul

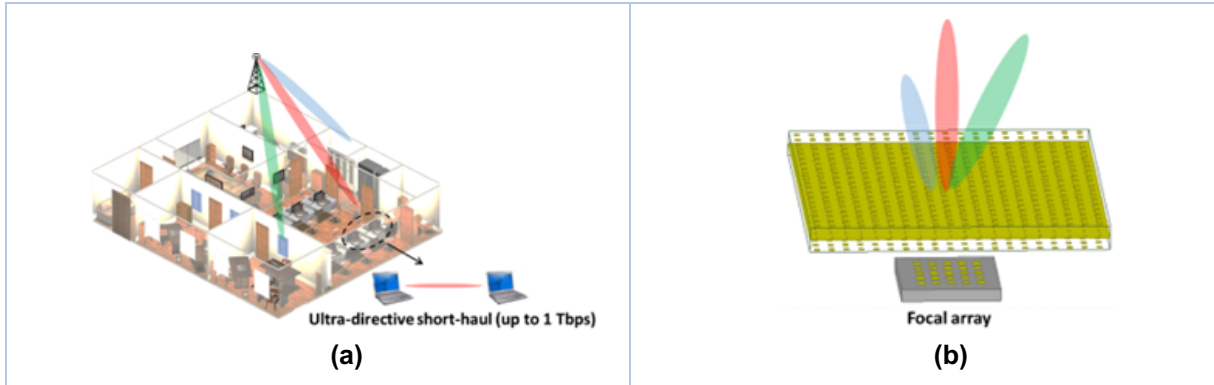


Figure 6-20 Ultra-directive short haul

Indoor short haul

The use case is presented in Figure 6-20 (a). It is dedicated to the indoor connectivity at sub-THz frequency, and it considers indoor short-range hotspots. Specifically, two objects or devices are interconnected by an extremely high-speed wireless link with a data rate up to 1 Tbps. The link distance is in the range 1 – 5 m and can be implemented by considering an ultra-low profile fixed beam transmit array Figure 6-20 (b) on both devices having a gain in the range 25 – 30 dBi.

Indoor short-range hotspot

A variation of the above use case can be furthermore considered where the indoor short-haul is acting as a hot-spot. In this case, the system is very similar to an access point with extremely high data rate (in the order of 100 Gbps). In this case, the antenna has a gain around 20 – 25 dBi. Beam-steering capability in a field of view of $\pm 45^\circ$ can be required. In this case, innovative transmit array solutions based on fixed beam architecture associated to a phased array or full reconfigurable transmit arrays are required.

Outdoor mid-haul

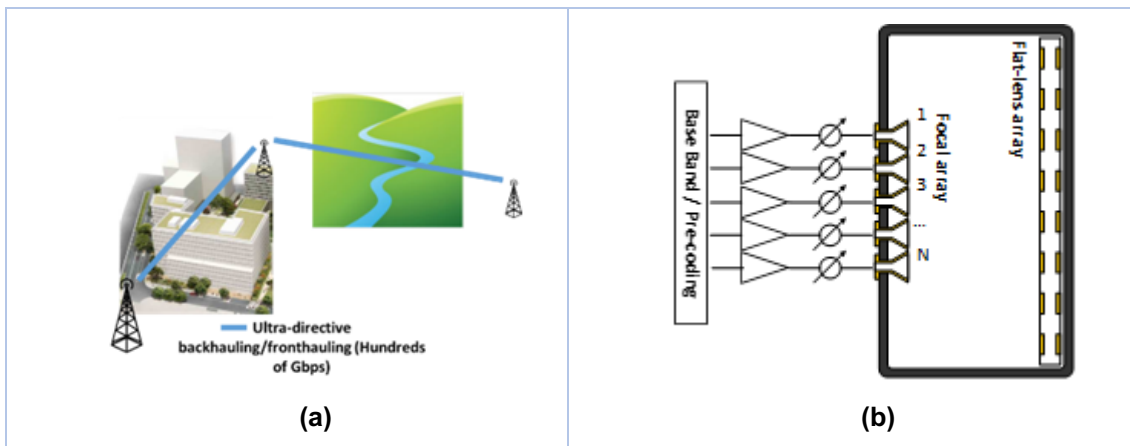


Figure 6-21 Outdoor mid-haul.

Figure 6-21 depicts a schematic view of the outdoor mid-haul deployment, and (b) illustrates a T-RIS-based solution for wireless transport at sub-THz. In order to generate the limited steering capability, the antenna architecture presented in Figure 6-21 free space. In order to control the steering direction in a limited field of view (max $\pm 15^\circ$), each focal source has a controllable power amplifier and a phase shifter. By opportunely controlling both amplitude and phase, the beam

6.5.1. RIS-aided Backhaul Link Sensing and Localisation

This use case will consider the outdoor 6G cellular networks, where the densely deployed base stations connected through the THz backhaul links to overcome the inter-base station Non-Line-of-Sight (NLoS) transmission. The fixed backhaul links can support both high throughput inter-base station communication and weather sensing as the THz wavelength is comparable or smaller than the rain drops. In addition, the reflective RIS can split the beams to achieve the dual/multi-functionality, e.g., sensing/imaging for the flying targets like UAVs in Figure 6-22.

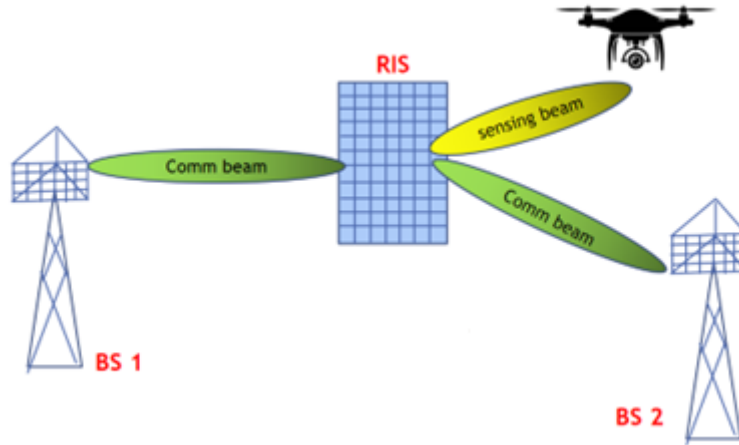


Figure 6-22 THz RIS-aided backhaul links based JSAC.

6.5.2. RIS-aided Multi-Access Sensing

This use case will consider 6G cellular networks, where the RIS is utilised to overcome the NLOS transmission between the base station and user ends. The active RIS can apply the multi-beam technique to support target sensing and high-resolution imaging and downlink transmission simultaneously, e.g., some beams to sense the targets and others for the communication, as shown in Figure 6-23. The JSAC performance balance will be investigated by JSAC resource allocation.

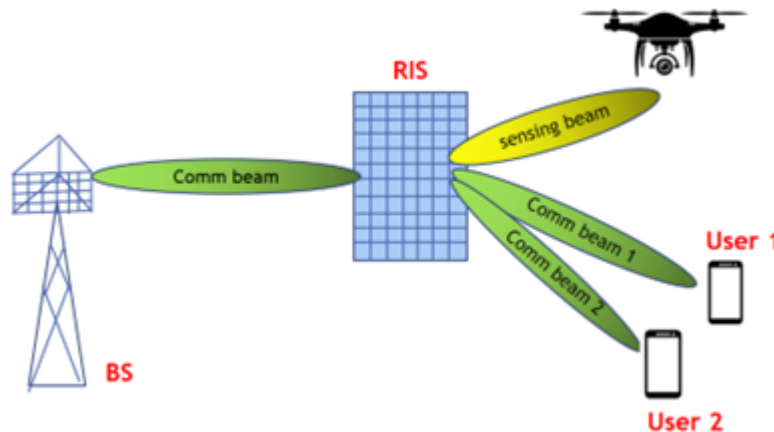


Figure 6-23 THz RIS-aided multi-access based JSAC

This use-case is also suited for indoor environments. As an example, in smart factory settings, THz RIS can be used to combat the limits of short-range communication and blockage through multi-hop transmission via one or multiple simultaneous RIS, where the RISs can serve as the virtual access points to realise the high accuracy localisation, and also the high-resolution imaging. For instance, the

9 GHz bandwidth of THz sensing can achieve cm-level ultra-high-resolution image that would be applied to detect the moving assembly robots and humans.

6.5.3. RIS-aided Outdoor-to-Indoor Sensing

This use case will consider the use of outdoor signal from 6G cellular networks to support the indoor localisation, sensing, and communication, through the star-RISs, where the signals captured at star-RIS can be transmit into the indoor environment, as shown in Figure 6-24. The star-RIS can actively split the power for both sensing and communication simultaneously, which can benefit from the advanced signalling from the outdoor cellular networks compared with the Wireless Local Area Network (WLAN).

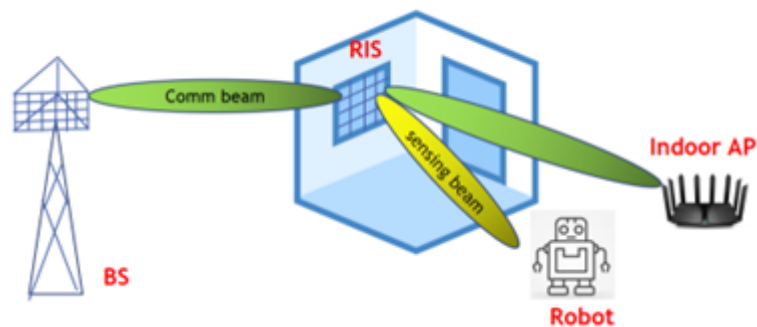


Figure 6-24 THZ RIS aided indoor localisation and sensing.

6.5.4. Full-Duplex Enabled Simultaneous Communications and Sensing

A Holographic Full Duplex DMA antenna can be implemented, as shown in Figure 6-25, operating at THz for sensing the propagation environment, and serving the users to improve their downlink rates [GIS23]. It is envisioned that in THz frequencies, where the Line-of-Sight path dominates the channel and communication usually takes place in the near field regime, it will be easier to achieve accurate and fast positioning of multiple targets at once. As a result, the holographic architecture BS will serve the users using this acquired knowledge leading to increased SNR, sum rate and space division multiple access, even at very similar angles. The BS has the dual objective of locating objects lying in its vicinity while also serving the users. This proposed system follows the Integrated Sensing and Communications (ISAC) paradigm, specifically the BS will transmit the desired signals to each user, thus serving them in the Down Link (DL), while also sensing the environment through the reflected signals as demonstrated in Figure 6-27. The RX DMA will sense the environmental reflections while also cancelling the self-interference induced by the TX DMA. A trade-off between accurate positioning of objects and downlink beamforming will be investigated as sensing the environment may require wider beams as opposed to sharp beams used for increased gain. It is instrumental to stress that the objects and users in the environment do not cooperate in the estimating process, thus making it excellent for IoT systems. This system can naturally implement tracking of the environment, by exploiting channel knowledge from previous time slots to enhance the estimation accuracy and track moving targets. Lastly, multiple object positioning can be carried out using algorithms for parameter estimation (multiple signal classification, compressive sensing, etc.).

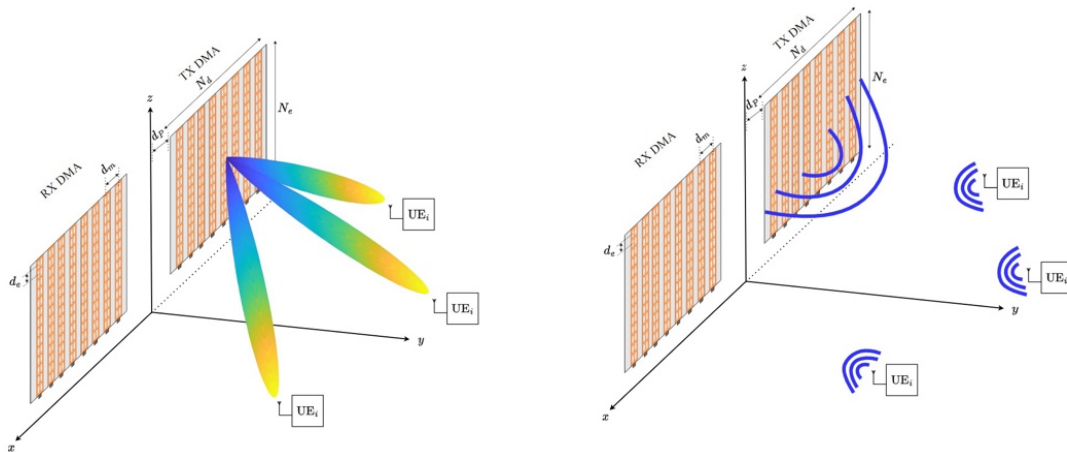


Figure 6-25 Full duplex holographic MIMO system enabling sensing and beamforming.

6.5.5. Environmental Mapping and Imaging

Holography is an innovative technology for high-fidelity 3D imaging that is envisioned to become a reality thanks to wave amplitude and phase information. Compared with the conventional geometrical optics-based photography, recording only the wave intensity, and presenting a 2D image, holography utilizes coherent light sources for recording the complete wave information and presents a 3D image. This technology can become a reality with the use of Holographic MIMO architectures [GGJ23], and THz Communications [WGG21]. Specifically, DMAs and H-RISs are some of the enablers of this new paradigm [H20] that simultaneously act as large sensors of the environment while also compensating for propagation losses in high frequencies. In futuristic 6G networks and smart cities, buildings could be partly covered by metasurface based technology surfaces, which scan the environment in an EM manner, and recreate the 3D scenery in their vicinity. This knowledge can be used to in conjunction with ray tracing simulators to determine the channel information and perform sophisticated optimization frameworks for various objectives such as sum-rate maximisation, security enhancement, and energy efficiency. Furthermore, these holographic architectures are envisioned to autonomously perform these tasks powered by AI machinery [ASH22]. Lastly, in the pursuit of an environmentally friendly environment, energy harvesting metasurface elements are being considered for deployment in these large surfaces [CGY14]. The following are some of the potential applications:

- Holographic Production: introducing holography to agricultural industries such as crop, livestock production, and aquaculture which often operate over large areas will allow them to remotely look over them.
- Holographic cultural experiences: people can entertain themselves with holographic cultural experiences such as having a hands-on experience of the customs of a country, visiting museums and monuments.
- Holographic entertainment: immersive participation in 3D extended reality video games, and movies.
- Holographic health care: holography can enable remote surgery and patient monitoring.

It should be noted that this technology is in its infancy, and in this project, we aim to evaluate its limits via simulations and theoretical analysis, not real-life scenarios, and experiments.

6.6. Industrial Environments

6.6.1. Enhancing Throughput, Localisation, and Mapping in Factory Settings

In recent years the manufacturing industry has been undergoing a digital transformation known as Industry 4.0. This new era of manufacturing is characterized by the integration of advanced technologies, such as IoT, AI, and automation, into traditional manufacturing processes. One of the key

goals of Industry 4.0 is to create a fully mobile, software-defined factory that can be quickly and easily reconfigured to meet changing customer demands and production requirements. An example of the design of a software-defined factory can be seen in Figure 6-26, which highlights a manufacturer choosing to produce a certain product. The IT and manufacturing infrastructure then autonomously reconfigures its resources in a distributed but collaborative fashion to produce this product.

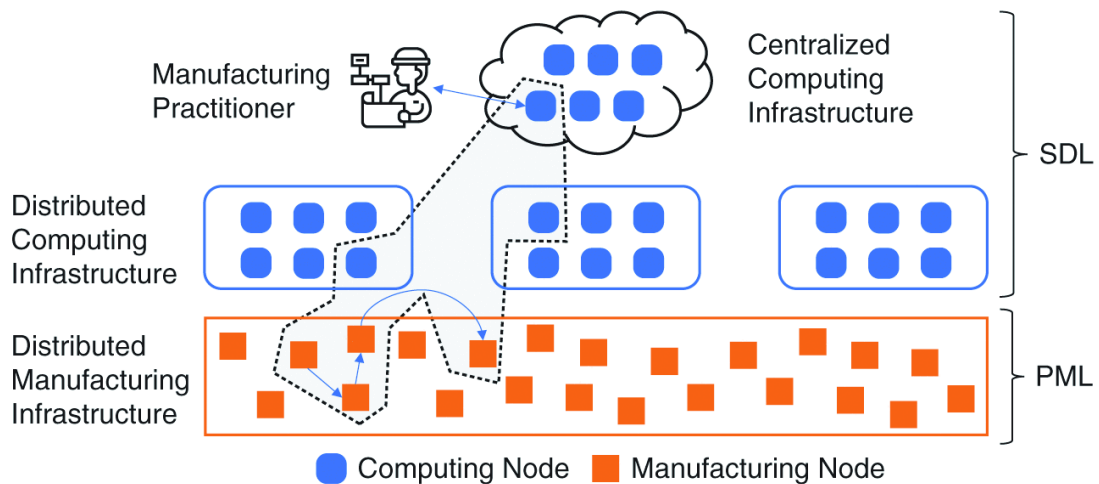


Figure 6-26 Example of a software-defined factory.

A software-defined factory offers several benefits over traditional manufacturing environments. One of the most significant advantages is flexibility. With a software-defined factory, the entire manufacturing process can be programmed and controlled through software, allowing for rapid reconfiguration and customization to meet changing customer demands or production requirements. This level of agility is essential in today's fast-paced business environment, where companies must be able to quickly respond to shifting market demands and customer preferences. Another benefit of a software-defined factory is improved efficiency. Automation and machine learning algorithms can be integrated into the manufacturing process, allowing for real-time monitoring and optimization of production processes. This not only helps to reduce waste and downtime but can also lead to increased output and quality.

However, creating a fully mobile software-defined factory also poses several challenges, particularly around mobility. Traditional factories are typically fixed in location, with machines and equipment permanently installed and connected to utilities such as electricity and copper or fibre network connections. In contrast, a software-defined factory may need to be rapidly deployed and redeployed in different locations, making it essential to ensure that all equipment and machines can be easily transported and connected to necessary utilities. To overcome these challenges, solutions such as modular designs, standardized connections, and new network architectures need to be created to create easily transportable and deployable factory units such as robotic assemblers, conveyer systems, and packaging configurations. By addressing these mobility challenges, a fully mobile, software-defined factory can be created that offers unprecedented flexibility and efficiency in the manufacturing process.

Current and future factories require a high-performance network infrastructure to operate effectively. Traditional fixed network infrastructure, such as copper wire and fibre optic cables, are not ideal for a software-defined factory due to their limited flexibility and mobility. A software-defined factory requires a network that is flexible, scalable, and reliable to support the high volume of data traffic generated by machines, sensors, and robots. Wireless technologies such as Wi-Fi and cellular networks such as Long Term Evolution (LTE) and 5G are currently not able to meet the demands of a software-defined factory due to a variety of limitations. These limitations include limited bandwidth, high latency, and susceptibility to interference and network congestion. Additionally, current-generation wireless technologies will struggle to provide high-bitrate connections to a large number of devices at scale, simply due to the limited wireless spectrum available and the often-used omni-directional broadcast method limiting spectrum re-utilization.

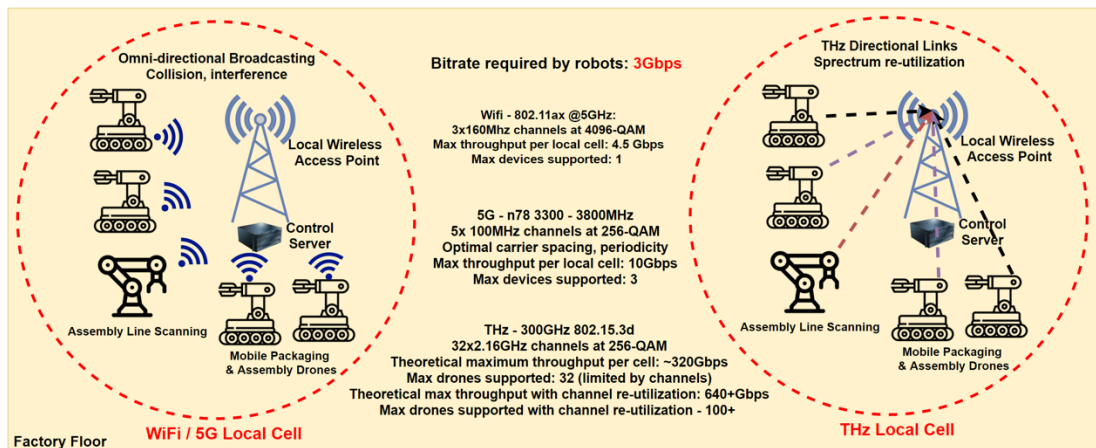


Figure 6-27 Example diagram showing the overall network throughput available per local cell for WiFi, 5G, and THz and number of high bitrate robots are supported.

To meet the network requirements of a software-defined factory, new technologies such as THz wireless links are being developed. THz wireless links offer increased bitrates, more wireless channels, and lower latency than previous generations of wireless networks, making them well-suited for the high-volume, low-latency, and large-scale data traffic generated by a software-defined factory. The use of directional antennas combined with RIS, also enables THz wireless links to re-use the same THz wireless channels more efficiently and effectively for communication between devices in the same local area. This greatly increases the total amount of throughput available for a given area and enables THz technology to provide a feasible alternative to fixed network infrastructure to meet the growing data demands of Industry 4.0 use cases. A simplified example of this advantage can be seen above in Figure 6-27.

Computer vision is an essential component of robots in Industry 4.0. It allows them to "see" and analyse their environment, which is critical for carrying out their tasks accurately and safely. Computer vision technology includes various techniques such as image processing, pattern recognition, and machine learning, which enable robots to interpret and make sense of visual information. One critical application of computer vision in robots is Simultaneous Localization and Mapping (SLAM). SLAM is a technique that enables a robot to create a map of an unknown environment while simultaneously locating itself within that environment. This technology allows robots to navigate autonomously in complex environments, which is particularly useful in manufacturing plants and warehouses.

In a software-defined factory, SLAM mapping technology is useful for creating digital twins of the manufacturing plant's physical environment. These digital twins can be used to simulate the production process, optimize the factory's layout, and improve the efficiency of material handling. However, SLAM mapping technology requires high network performance to enable the robot to transmit the mapping data to other machines for processing and analysis. These high-performance requirements are due to the large amounts of data being generated by the robot's sensors and the need for real-time data transmission and feedback. As such, having a high bitrate and low latency network infrastructure is crucial for implementing SLAM mapping technology in Industry 4.0.

In addition to SLAM mapping, current trends in robotics are incorporating object detection technology to enable mobile robots to interact with machines and objects in a software-defined factory. Object detection technology uses computer vision techniques to identify and locate specific objects in an image or video feed. In a software-defined factory, object detection technology allows mobile robots to interact with machines and objects in the factory environment autonomously. For example, a mobile robot equipped with object detection technology could identify and locate a specific machine on the factory floor, then interact with that machine to carry out a particular task. This technology can be particularly useful for tasks such as material handling and logistics, where mobile robots need to locate and interact with specific objects and machines in the factory environment. By incorporating object detection technology, mobile robots can operate more efficiently and effectively, reducing the need for human intervention and improving overall factory productivity.

This use case scenario focuses on testing THz wireless links using RIS to provide a high-speed wireless connection between a mobile or semi-mobile robot and the local Edge server which will be processing its information in order to provide an overall SLAM map of the factory environment. These robots will connect to the processing server using THz wireless links and the THz RIS to provide mobility tracking and maintaining a connection in a NLoS environment. The robots and processing servers are designed to be deployed in a scalable local cell architecture design, meaning the local processing servers operate as part of a distributed software-defined architecture and collaborate together to build a complete map of the factory floor and all of the objects and machines contained within it. These control servers can communicate to each other using fixed optical links (as for this use case they can be considered static), or by utilizing THz MIMO as a local backhaul, to increase the available bitrate for server-server communication for SLAM map sharing. An example of this architecture and implementation can be seen in Figure 6-28.

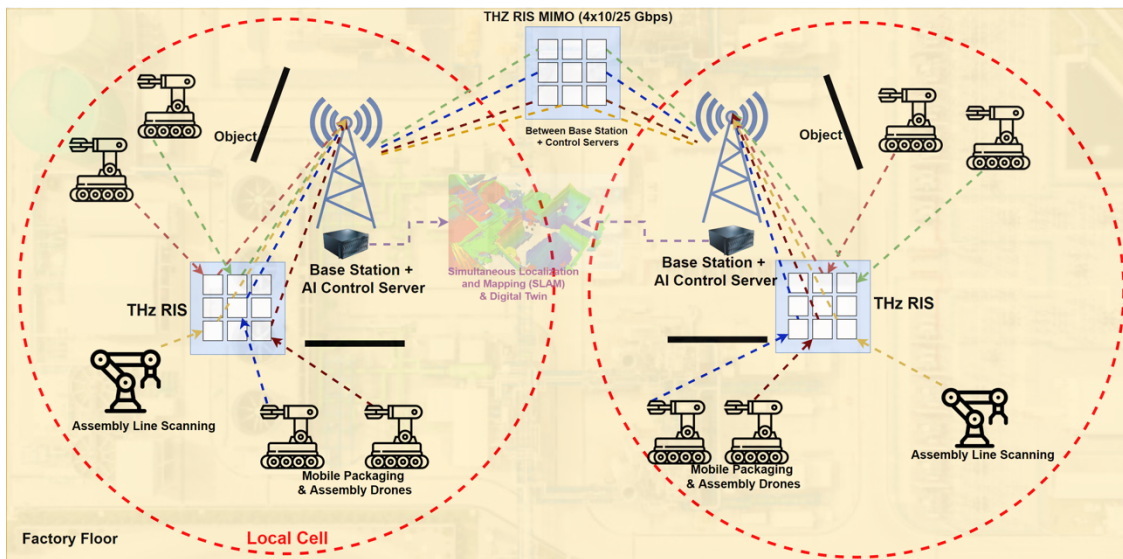


Figure 6-28 Diagram showing robot to server communication utilizing a THz RIS and server-server connection between local cells using THz RIS MIMO

In terms of the local factory environment that this use case is based on, a section of the factory can be seen below in Figure 6-29. Note that the manufacturing machines are not present in the image but are marked with a blue outline on the floor. It can be seen from this figure that the overall general layout of the factory features consistent rows and columns of pillars approximately 10 meters apart.



Figure 6-29 Factory floor design

These pillars (in addition to possible supplemental RIS' mounted on the ceiling) serve as a good location from which to mount THz RIS devices in order to cover the vast majority of the factory floor. This RIS deployment strategy can be seen below in Figure 6-30, where RISs could be mounted on each side of the pillar at an angle that maximizes the total area of coverage. This angle could change depending on the type of RIS being deployed.

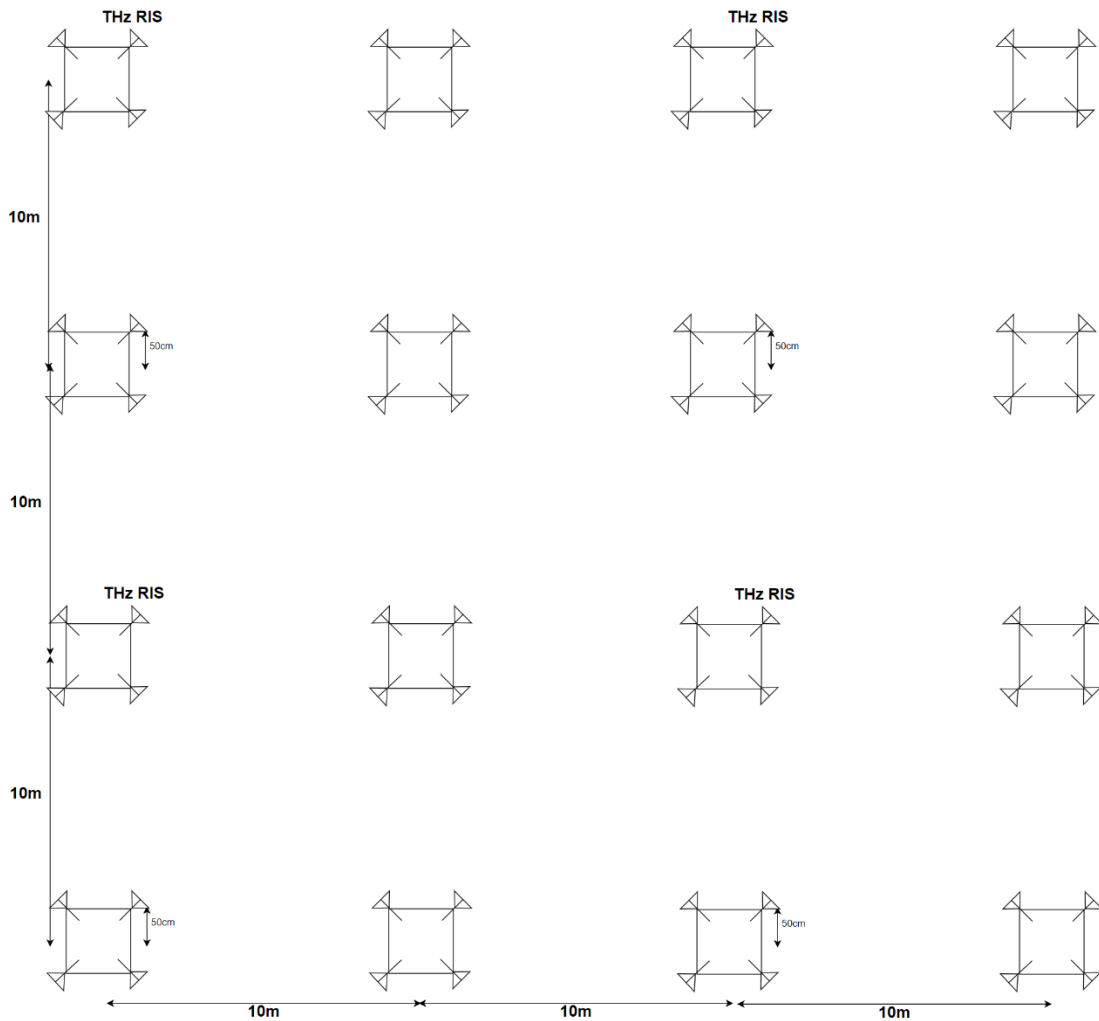


Figure 6-30 Possible THz RIS deployment strategy

This RIS deployment strategy will be further refined in future deliverables but serves as the basis for defining minimum requirements and KPI's in order for the use case to implement a successful demonstration and determine the use cases viability via link budget calculations and system simulations in subsequent sections and Work Packages.

6.6.2. Software Defined Networking Enhancement in Data Centres

RIS technologies represent a transformative and promising technology capable of fundamentally redefining communication in many environments, including datacentres. Operating in the THz spectrum, they hold the potential to significantly enhance datacentre communications, integrating with Software-Defined Networking (SDN) to dynamically boost the capacity of optical links and offer a multitude of other benefits. RISs' ability to dynamically reconfigure waves and thus wireless links dynamically can be exploited to improve the communication channels in data centres significantly. As data centres generate large volumes of data, they demand networks with high capacity and efficiency. Operating in the THz spectrum, RIS can enhance wireless communication within datacentres, providing ultra-high bandwidth, low latency, and high energy efficiency.

One significant way RIS can be used in datacentres is through integration with SDN to dynamically augment the capacity of optical links. SDN decouples the control and data planes of a network, allowing for programmable, adaptive, and flexible network management. This means network administrators can shape traffic from a centralized control system and Quality of Service (QoS) policies without touching individual switches. In the case of optical communication, the bandwidth can be adjusted dynamically based on the current load and demands but is ultimately limited by the fixed point-to-point nature of wired links, and the static maximum bandwidth for any given link.

By incorporating RIS into this setup, we can further increase the flexibility and adaptability of the network. The RIS can be programmed to dynamically adjust the available bandwidth between communicating servers on-demand. This can be to increase the total available bitrate between two servers during high traffic events, avoid traffic congestion that can occur in the traditional wired network leaf-spine topology, or any number of reasons. As a result, the overall capacity of the network during periods of peak demand can be significantly boosted. This dynamic management of capacity optimizes network performance, allowing data centres to handle larger volumes of data more efficiently. An example diagram of this can be seen in Figure 6-31, showing a set of THz RIS links connecting between server H6 and server H3, augmenting the total bitrate between these servers and also bypassing the potentially traffic congested core switch.

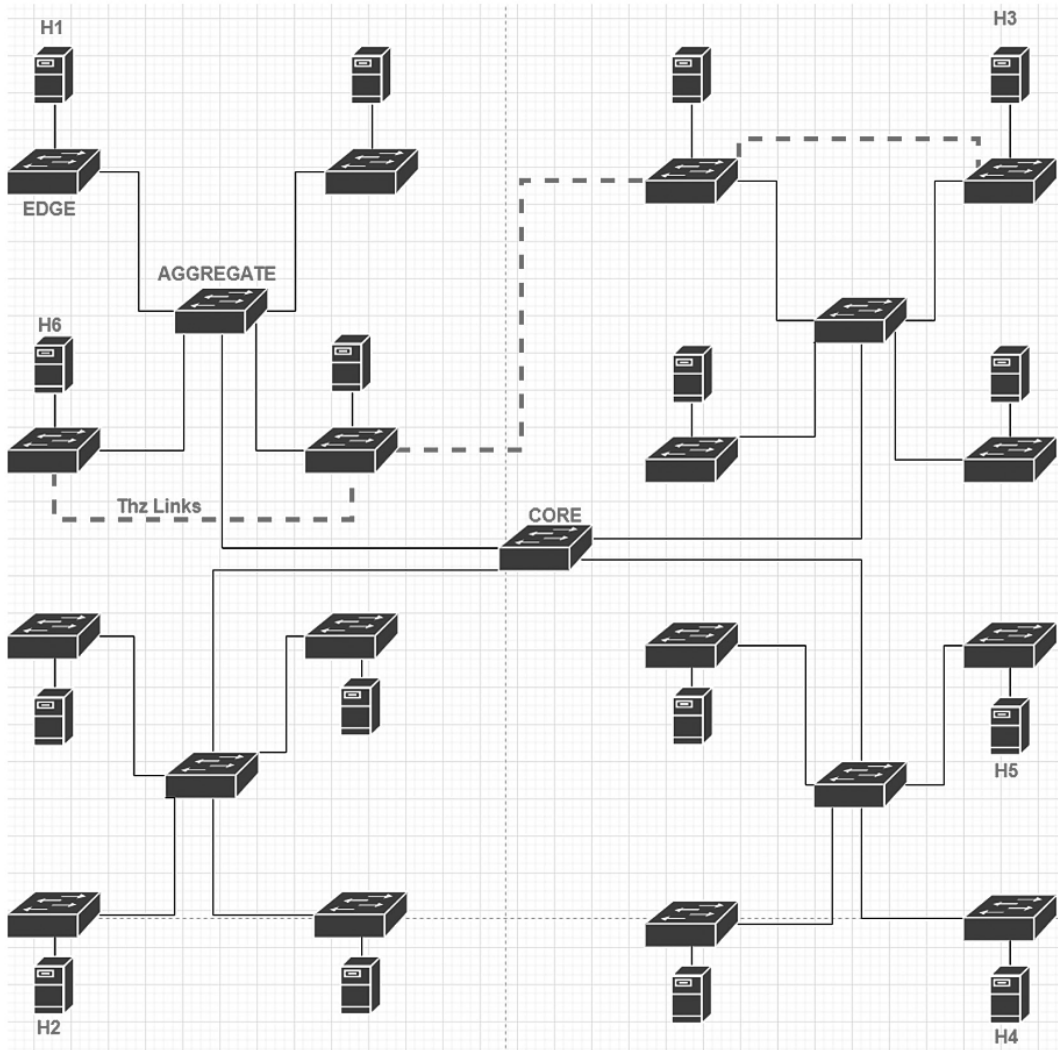


Figure 6-31 Using THz RIS links to augment optical network throughput.

RIS also holds potential in improving the resilience and reliability of datacentre communications. If a particular communication link is disrupted, the RIS can be reconfigured to establish alternative communication paths, thereby enhancing the overall network resilience. This can be particularly beneficial in mission-critical datacentre applications where maintaining high levels of uptime and reliability is paramount.

RISs' unique attributes also open up the possibility of new network designs in datacentres. Traditional datacentres typically deploy a fixed point-to-point wired infrastructure, which is often expensive and inflexible. By utilizing RIS-based wireless datacentres, it is possible to design more flexible and cost-

effective network infrastructures. One other key feature in the implementation of RIS and THz wireless networking in the datacentre would be the ability to use point-to-multipoint communications. This would enable communications links within a datacentre to have a level of flexibility far greater than what is physically possible with wired optical links and can create new types of SDN features or overall datacentre network infrastructures or designs that are a paradigm shift from the way datacentre networks are designed today. Figure 6-32 shows an example implementation of such a design, using Time Division Multiple Access (TDMA) to enable point-to-multipoint communication between racks in a datacentre that would be physically impossible with wired links. Other 5G/6G technologies could also be integrated into the THz wireless network, bringing the greater flexibility, performance, and efficiency of those technologies to a new demanding area of network infrastructure.

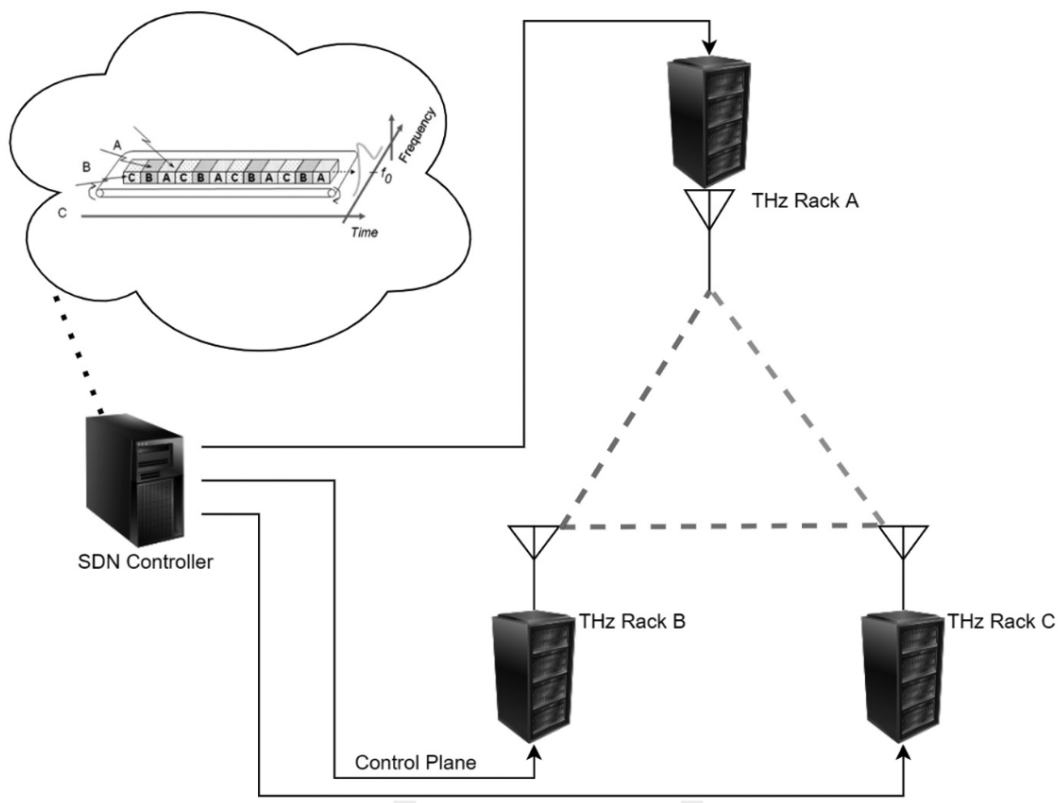


Figure 6-32 THz communications using TDMA and RIS

A RIS's capabilities of manipulating electromagnetic waves can hold great promise in various applications, including sensing in factory environments. In a factory scenario, the use of RIS-based sensing can bring numerous advantages in terms of precision, flexibility, efficiency, and more. At its core, a RIS is a programmable metasurface that can alter the properties of electromagnetic waves, such as their amplitude, phase, and polarization. This ability can be used in sensing applications to achieve superior performance over traditional sensing approaches. When an electromagnetic wave interacts with an object, it can undergo changes in its properties. By capturing these changes, a RIS-based sensor can extract valuable information about the object, including its presence, location, shape, and material properties.

6.6.3. Large-Scale Distributing Sensing in Factory Environments

One key advantage of RIS-based sensing in a factory environment lies in its high precision. By effectively controlling and shaping electromagnetic waves, RIS can achieve a high resolution in sensing, which is essential in many industrial applications, like detecting tiny defects in manufactured products

or monitoring subtle changes in machine performance. This high precision can significantly enhance quality control in factories and prevent costly machine failures. Another advantage is flexibility. Given that the RIS is software-defined and programmable, it can adapt to various sensing requirements dynamically. For instance, in a software-defined factory environment where different machines are mobile, modular, and re-programmable, a RIS sensor can be programmed to focus on specific areas or objects, or switch between different targets swiftly. This flexibility can make RIS-based sensing a powerful tool for real-time factory monitoring and control.

A unique advantage of RIS-based sensing is its potential to support large-scale and distributed sensing. In a large factory, hundreds or even thousands of objects or machines may need to be monitored simultaneously. Conventional sensing systems may struggle to cope with such a scale due to limited coverage and potential interference issues. RIS, on the other hand, can control the direction of signal propagation, allowing it to cover a large area with much less interference in comparison to traditional sensor systems. As a result, it can support large-scale sensing and provide a comprehensive view of the factory's operation. RIS-based sensing can also enhance the security and safety of factories. By monitoring the factory environment continuously and accurately, it can detect potential safety risks promptly, such as overheating machines, hazardous gas leaks, or nearby humans entering a dangerous path. An example of this can be seen in Figure 6-33.

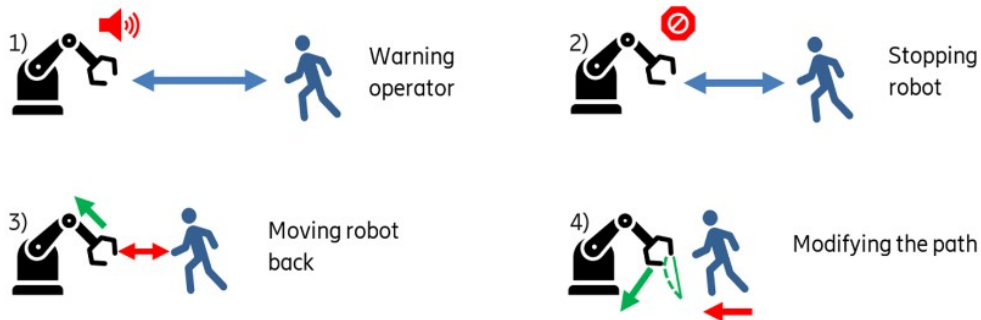


Figure 6-33 using a RIS for human detection [ESN21].

7. KPI Definitions and Requirements for THz

To evaluate the performance and usability of the use-cases and scenarios envisioned in this deliverable, as well as of the results that will be delivered throughout the TERRAMETA project, it is important to define the Key Performance Indicators (KPIs) as well as the intended requirements that are expected to be covered. To that end, the current section provides a clarification of those concepts under the prism of 6G/THz/RIS networks. Specifically, Section 7.1 contains the definitions of functional and non-functional KPI requirements, and Section 7.2 gives illustrative values for the most relevant KPIs.

7.1. KPI definitions

The following table contains definitions of the main communication performance objectives that are addressed in THz RIS networks. Each of the use-cases presented in the previous section may focus on the satisfaction of different sets of KPIs.

Table 3 - KPI Definitions

Definition	Description
Minimum Bitrate	The minimum rate of data transfer between two devices with the link established at the PHY layer. Measured in Gigabits per second (Gbps).
Minimum Range	The minimum range between two devices which is deemed acceptable to be useful/viable for the use case. Measured in metres.
Signal-to-Noise Ratio (SNR)	The minimum signal level necessary for detection and recovery of a transmitted signal by the receiver compared to background noise. Measured in decibels (dB).
Bandwidth Utilization	For a given established link between two devices, the bandwidth is the amount of frequency spectrum dedicated for that link for communication. Measured in Gigahertz (GHz).
Frequency Band	The area of the electromagnetic spectrum used for communications. Measured in GHz.
Modulation & Coding Schemes	The methods available with which to encode and decode the binary bits of a data transmission in order to reduce bandwidth usage and reduce errors with Forward Error Correction (FEC).
Bit Error Rate	The probability of an error occurring during transmission and reception of data, measured in 1 per x number of bits.
Packet Loss	NET layer KPI which represents the number of data packets discarded due to too many errors occurring during transmission and reception. Measured in percent of the overall data stream.
Throughput	The actual bitrate which is usable by the applications when a link is established after all other network overheads. Measured in Gbps.
Latency	The amount of time taken for a transmitting application to send a data packet and have it be received and acknowledged by the receiver. Measured in milliseconds (ms).

Jitter	For an active and ongoing data link between two devices, jitter is the variance in latency between the devices over time. Measured in ms.
Spectral efficiency (SE)	Using agreed measured or standard radio propagation models. Measured in bits per second per Hertz [bps/Hz].
Area spectral efficiency (ASE)	Combined measure of capacity and coverage. Measured in bits per second per Hertz per square kilometre [bps/Hz/sq.km].
Spectral and energy efficiency (SEE)	Combined measure of capacity and energy efficiency. Measured in bits per second per Hertz per Joule [bps/Hz/Joule].
Coexistence with legacy radio access technologies (COEX)	Measure of performance impact when new techniques are deployed in spectrum shared with other technologies.
Position accuracy	Measure of how close the true position of a UE is when compared to an estimated position provided by the deployment system. Measured in metres.

Note that minimum bitrate and distance are the minimum performance parameters required to enable the use case to be viable. This will be investigated in the following section containing link budget calculations. Improvements to bitrate and distance over time will enable new features and improved overall use case performance.

The above requirements are classified as functional, since concrete numerical target values or ranges can be set to effectively evaluate the performance of the systems under question. Nevertheless, non-functional requirements are of equal importance. This term refers to expected behaviour of the system that is not easily precisely quantifiable, but must be taken into consideration when designing, implementing, and evaluating communication systems in general. In the following table, we present the most relevant qualifiers for THz RIS networks.

Table 4 Non-Functional Requirements

KPIs/ Requirements	Description
Reliability/ Availability	The THz wireless link should be able to guarantee an uptime of 99.999% (also known as five-nines). This is crucial in a manufacturing environment where any downtime can result in substantial costs.
Interference Resistance	The THz wireless link should be robust to physical and electromagnetic interference common in manufacturing settings, including from machinery and other wireless devices.
Environmental Considerations	Consideration of the harshness of the manufacturing environment, including temperature, humidity, and vibration. The wireless devices should be robust enough to withstand such conditions.
Scalability	The THz RIS system should be able to support an increasing number of devices without significant degradation in performance.

Energy Efficiency	Especially for battery-powered robots, the wireless technology should aim for maximum data rates with minimal power consumption.
Mobility	In case devices or machinery need to move around, the wireless link should maintain consistent performance and connectivity.
Backward Compatibility	The THz RIS technology should be compatible with existing network devices and infrastructure to enable seamless integration with existing network technologies on the factory floor

7.2. 6G Requirements

To realise the benefits brought under the 6G vision (see also Section 5.3), the community has set to establish realistic yet ambitious target values for the considered KPIs that go beyond of what it currently technologically plausible. This effort is still ongoing (with the TERRAMETA Consortium being an active participant via its Standardisation and Dissemination efforts), therefore target KPI values are not yet final. Nevertheless, some indicative proposed requirement values that concern general 6G networks are presented in Table 5 below.

7.2.1. Generic Requirements

Table 5 - 6G Requirements [HSD21]

KPI	6G requirement
Peak data rate	1 Tbps
User experienced data rate	1 Gbps
Peak spectral efficiency	60 b/s/Hz
User experienced spectral efficiency	3 b/s/Hz
End-to-End latency	1 ms
Radio-only latency	100 microseconds
Block Error Rate (BLER)	$10e^{-9}$
Connection density	$10e^7$ devices/Km ²
Network energy efficiency	1 pJ/b
Position accuracy	0.1 m
Maximum frequency	10 THz
Maximum bandwidth	100 GHz

It should be noted that the values provided in Table 5 are only speculative as the 6G requirements have not been agreed upon via standardisation bodies. Additionally, some KPIs may not be relevant in some WPs.

7.2.2. Requirements and KPIs for Manufacturing Use-Cases

Furthermore, it is important to stress that multiple scenarios may require even higher requirements and KPIs. As an example, such settings may arise in manufacturing use-case, where ultra-high reliability and throughput may be expected. Since the TERRAMETA project specifically addresses such cases (as presented in Section 6), indicative values for manufacturing use-cases are additionally presented in Table 6 below. Let is again be noted that the link budget analysis (Section 8) to be carried out through the lifetime of the Project aims to better clarify such target KPIs.

Table 6 Manufacturing requirements and KPIs

KPIs/Requirements	Description
Minimum Bitrate	3 Gbps
Minimum Range	10 m
Signal-to-Noise Ratio (SNR)	5 dB
Bandwidth Utilization	Approx. 2 GHz
Frequency Band	140-300 GHz
Modulation & Coding Schemes	Based on IEEE 802.15.3d (300 GHz), OOK, BPSK, QPSK, 8-PSK, 8-APSK, 16-QAM, 64-QAM, FEC 14/15, 11/15 LDPC
Bit Error Rate	Less than $10e^{-9}$
Packet Loss	Less than 1%
Throughput	Approx. 2.8 Gbps
Latency	Less than 10 ms end-to-end
Jitter	Less than 2ms

8. THz Link Budget Analysis and System Design Challenges

8.1. Preliminary Link Budget Analysis for THz

This section presents link budgets formulas under idealized conditions and corresponding calculation examples for different use cases. This academic exercise is useful for providing an upper bound for the system performance, which already shows some of the challenging tan need to be tackled in the design of THz RIS.

8.1.1. Models and Definitions

We can divide the link budget analysis in two groups corresponding to different scenarios: i) the RIS and the primary feed (e.g., base station antenna) are placed nearby behaving as single antennas; ii) the RIS collects partially the environmental incoming signal, acting as a dynamic target.

In the first scenario, it is assumed that the energy from the primary source is mostly captured by the RIS (as in conventional reflect-arrays and transmit-arrays) and transmitted (Figure 8-1) or reflected according to a prescribed pattern (pencil beam, multibeam, etc). This description applies when the RIS is placed nearby the primary source (i.e. the ratio focal between focal distance d_2 and the RIS aperture dimension D is in the same order of magnitude). The upper bound of the link budget of case i) is established in this case by the Friis Formula [B16], meaning that path loss attenuation depends on the distance by the factor of $(1/d_2)^2$, where d_2 distance between the RIS aperture and the receiving terminal and the RIS gain is measured relative to the power emitted by the primary source:

$$\left(\frac{P_L}{P_{in}}\right)_{dB} = G_{RIS}^{dBi} + G_{BS}^{dBi} + 20 \log\left(\frac{\lambda}{4\pi d_2}\right)$$

This can be applied to the use cases like THz backhaul links' beam alignment, Transmissive RIS: Conformal Array, holographic MIMO.

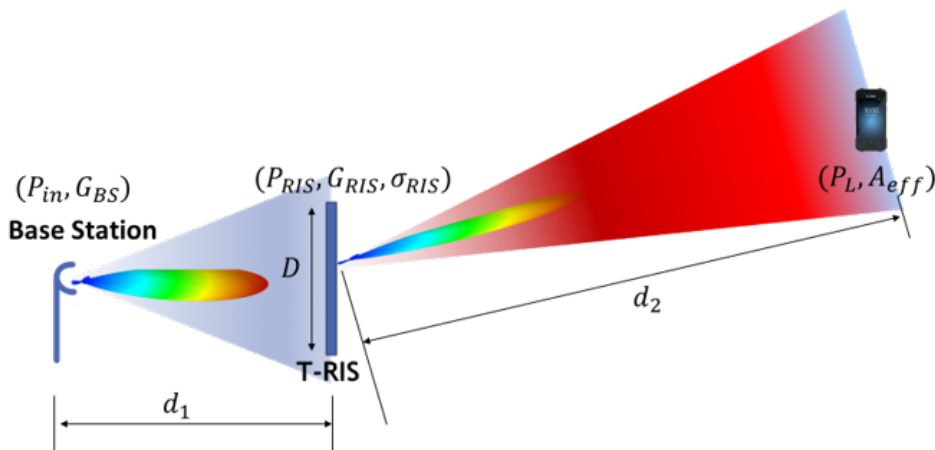


Figure 8-1 T-RIS and the primary source (Base Station) acting as an antenna (case i).

In the second scenario the energy impinging the RIS corresponds only to a part of the energy collected from the environment acting in the form of a plane wave (as depicted in Figure 8-2). From the electromagnetic point of view this problem is analogous to a bi-static radar problem, where the radar cross section of the RIS can be controlled dynamically for directing the beam towards the terminal. The path loss distance dependence is given by term $(1/d_2)^2(1/d_1)^2$, where d_1 is the distance between the base station and the RIS. In this scenario the path loss is even more critical that in case i) as we will show in the next section for some of the scenarios of this proposal.

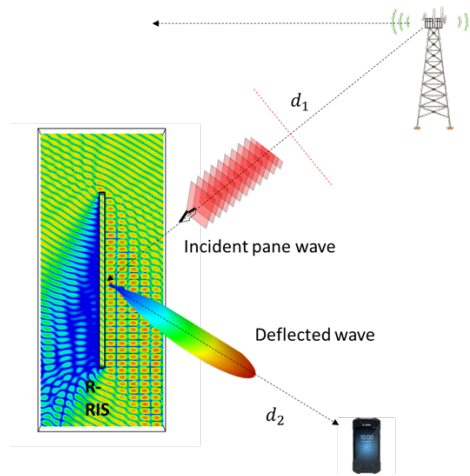


Figure 8-2 RIS acting as a dynamic target (case ii)

$$\left(\frac{P_L}{P_{in}}\right)_{dB} = G_{BS}^{dB} + G_T^{dB} + \sigma_{RCS}^{dB} + 10 \log\left(\frac{1}{(4\pi)^3} \left(\frac{\lambda}{d_1 d_2}\right)^2\right)$$

The fundamental concept capturing the redirect energy is the radar cross section of the RIS instead of gain as in case i). An upper limited can be defined based on the know formular for the radar cross section of a perfect electric conductor plane under specular reflection.

$$\sigma_{RCS} \leq \frac{4\pi}{\lambda^2} D^4 \cos(\theta_t) \cos(\theta_{des})$$

The accurate calculation of this quantity requires a specific RIS model, which will be achieve only at latter stages of the project. Herein, we assume a more idealize approach based on the analysis presented in [WT2021]. In fact, it can be shown that this radar formulation is equivalent to the free-space path loss models of [WT2021], according to Figure 8-3.

$$P_r^{MAX} = P_t \frac{G_t G_r G M^2 N^2 d_x d_y \lambda^2 F(\theta_t, \varphi_t) F(\theta_{des}, \varphi_{des}) A^2}{64\pi^3 d_1^2 d_2^2} L_Q$$

Where $\sigma_{RCS} = G M^2 N^2 d_x d_y A^2 F(\theta_t, \varphi_t) F(\theta_{des}, \varphi_{des}) L_Q$. The L_Q term was added to account the phase quantization loss (e.g., 1-bit or 2-bit phase quantization). In the case of 1-bit phase quantization, the reported maximum aperture efficiency of the RIS is approximately 40% [WT2021]. The remaining parameters are explained in Table 7. For the following examples we assume that: i) the RIS elements have a period of half-wavelength at the center frequency; ii) The gain of each RIS element is 6 dBi (cosine pattern).

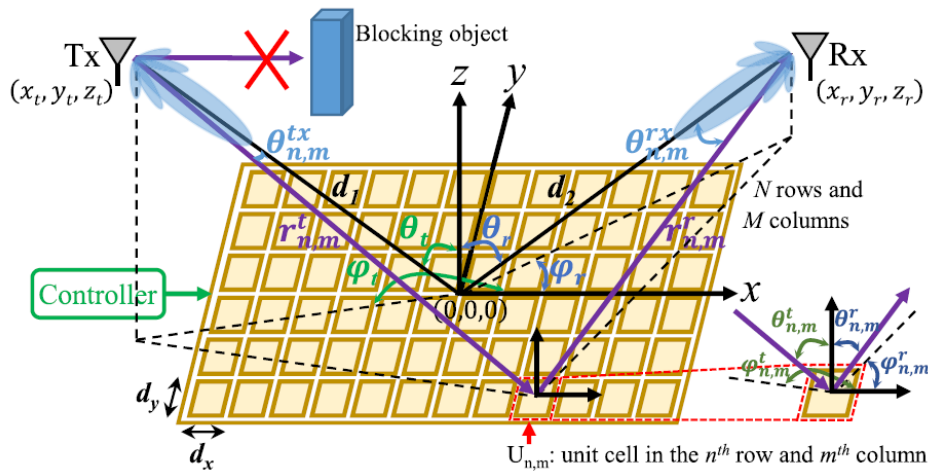


Figure 8-3: The coordinate system used for link budget calculation. Cited from [WT2021].

Table 7: Parameter list for the link budget calculation

P_r^{MAX}	Received max. power	M	Number of columns of the RIS
P_t	Transmit power	N	Number of rows of the RIS
G_t	Gain of the transmit antenna	d_x	The size of RIS unit cell along the X axis
G_r	Gain of the receive antenna	d_y	The size of RIS unit cell along the Y axis
G	Gain of the RIS	$F(\theta, \varphi)$	Normalized power radiation pattern of the RIS element
λ	Wavelength of the operating frequency	A	Reflection amplitude of the RIS element
d_1	Distance between the transmitter to RIS	(θ_t, φ_t)	Incident beam angle of the transmitter (use RIS as the reference)
d_2	Distance between the UE to RIS	$(\theta_{des}, \varphi_{des})$	Reflected beam angle of the RIS (use RIS as the reference)

8.1.2. Example 1 - Outdoor Use Case

For the outdoor use case, the transmitter is the BS, and the receiver is the UE. Both transmit antenna (BS) and receive antenna (UEs) are assumed to be in the far-field range of the RIS.

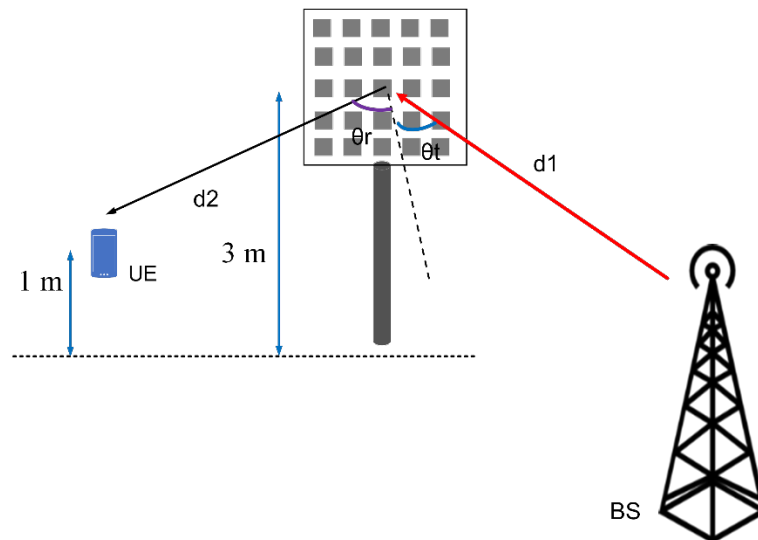


Figure 8-4 Telcom outdoor use case

Figure 8-5 shows the calculated UE received power and the SNR ($f=140\text{GHz}$) when the UE's distance from the RIS is varied. We assume that:

- The incident wave from the BS to RIS is 20 degrees and then the RIS reflected the wave to 30 degrees towards the opposite direction.
- The RIS consists of 40×40 elements, and its electrical size is $20\lambda \times 20\lambda$. For this configuration, its far-field range ($(2D^2) \div \lambda$) is 800λ . At $f = 140\text{GHz}$, this corresponds to $D=1.7$ meters.
- The remaining parameters are $P_t=30$ dBm, $G_t=30$ dBi, $G_r=12$ dBi, $d_r=100\text{m}$, $M=N=40$, and $A=0.4$.
- Phase quantization loss is not considered.
- For SNR calculation, the RX noise figure =7, $BW=2\text{GHz}$, and 4QAM modulation are used.

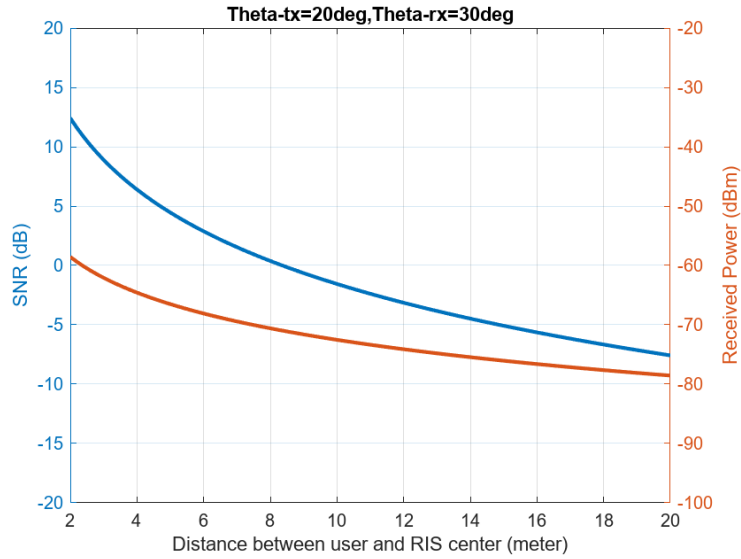


Figure 8-5: Calculated UE received power and SNR (f=140GHz) at varied distances (d_2) between UE and RIS.

Using Shannon-Hartley’s equation, with 2GHz bandwidth and SNR=0dB or 1, the theoretical maximum data rate capacity is

$$C = B \times \log_2(1 + \text{SNR}) = 2 \text{ [Gpbs]}$$

Figure 8-6 shows the SNR at UEs with varied incident and reflection angles to/from the RIS when the UE is located 5 meters ($d_2=5\text{m}$) away from the RIS. As the RIS element has a cosine radiation pattern, when either the incident or reflection angle is larger than 50-degree the SNR reduces significantly.

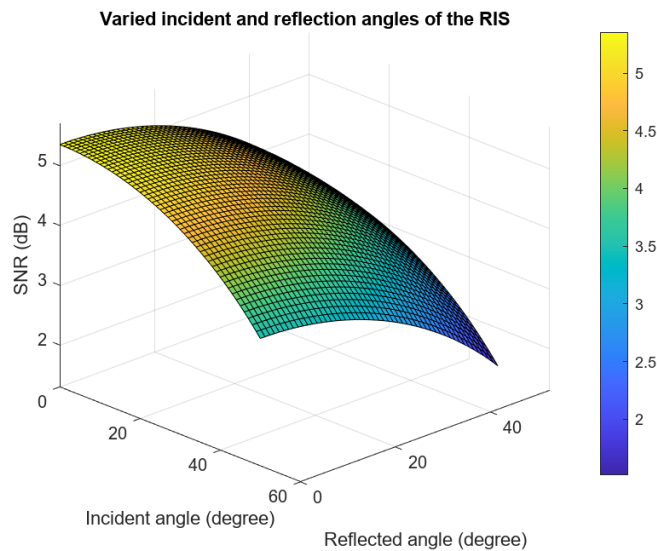


Figure 8-6: SNR at UEs with varied incident and reflection angles to/from the RIS

In the calculations, the attenuations from different weather conditions are not considered. This would affect the link budget of the outdoor use case. For example, considering a propagation distance of 100 mm, the RF signal attenuations due to the environment are given in Table 8.

Table 8: Attenuation due to the environment (Calculated by using MATLAB's Propagation and Channel Models)

f (GHz)	140GHz
Distance	100 m
Rainfall (rain rate=4 mm/hr)	0.96 dB
Atmospheric gases (T = 15-deg; P = 101300 Pa *Atmospheric water vapor density=0 g/m ³)	0.002 dB
Fog and clouds (T = 15-deg; cloud liquid water density= 0.5 g/m ³)	0.34 dB

8.1.3. Example II – Industrial Factory Use Case

For the factory floor use case (Figure 8-7), the transmitter is located within the machine or robot, whereas the receiver is located on the data server.

Figure 8-8 shows the calculated received power and SNR of the data server when the machine/robot is in different locations regarding the RIS. It is assumed that:

- The data server has a fixed position, which is 20 meters from the RIS, and to have the beam towards the server, the reflected wave of RIS is steered to 30 degrees.
- The RIS consists of 30x30 elements, and its electrical size is $15\lambda \times 15\lambda$. For this configuration, its far-field range ($(2D^2)\lambda$) is 450λ . At $f=140\text{GHz}$, this corresponds to $D=0.96\text{m}$. By placing the machine/robot and the server at least 1 meter from the RIS ensure that both transmit antenna and receive antenna are in the far-field range of RIS.
- The remaining parameters are $P_t=30\text{ dBm}$, $G_t=25\text{ dBi}$, $G_r=20\text{ dBi}$, $d_2=20\text{m}$, $M=N=30$, and $A=0.4$.
- Phase quantization loss is not considered. For SNR calculation, the Rx noise figure =7, $BW=2\text{GHz}$, and 4QAM modulation is used.

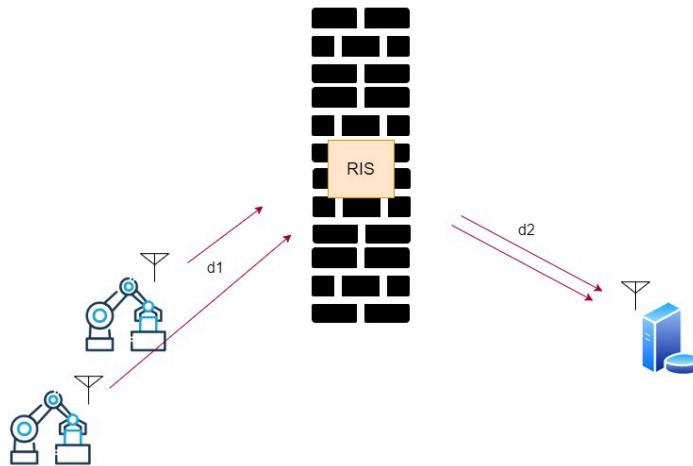


Figure 8-7: Factory floor use case

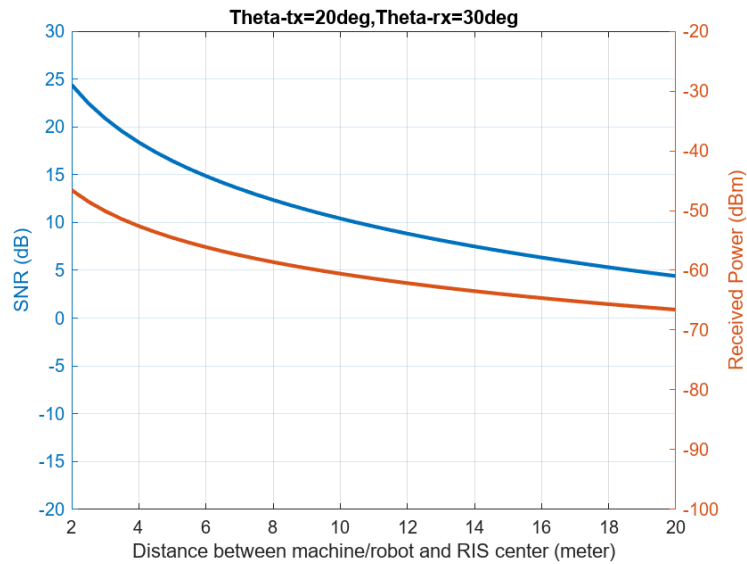


Figure 8-8: Calculate the SNR and received power at the data server with the machine or robot in different locations (d_1).

Using Shannon-Hartley’s equation, with 2 GHz bandwidth and SNR = 5 dB or 3.16, the theoretical maximum data rate capacity is

$$C = B \times \log_2(1 + \text{SNR}) = 3.3 \text{ [Gpbs]}$$

Figure 8-9 shows the SNR at the server when the machine is in various locations, in other words, the distance between the machines and RIS is different, as well as the incident wave from machine to RIS. In this calculation, the location of the server with reference to the RIS is fixed. As shown in this figure, when the incident angle is smaller and/or the machine is closer to the RIS, the SNR at the server is higher.

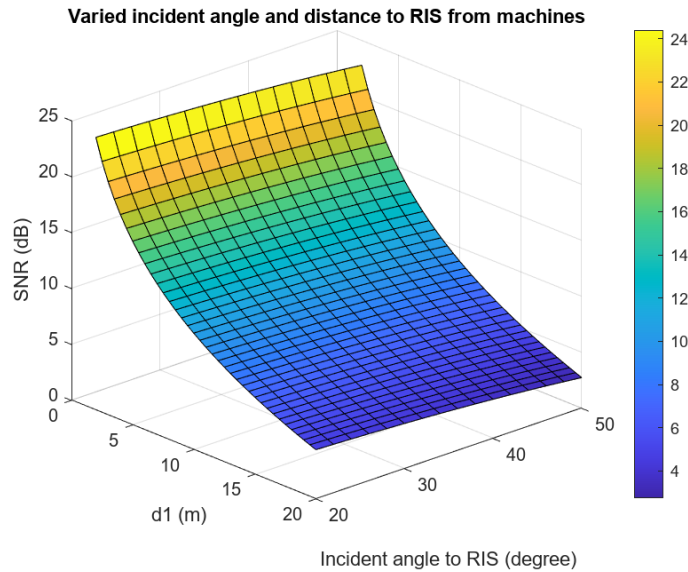


Figure 8-9: The SNR at the server when the machine is in various locations.

8.2. RIS Beamforming Challenges

Beamforming with metasurfaces at millimetre waves, e.g., transmit-arrays, reflect-arrays, and phase arrays, has been studied in detail by the antenna community. Each technology has its own advantages and disadvantages which translate into a balance among complexity, cost, and RF performance. Phased-arrays are a key technology for electronic reconfigurable antennas for mm-wave (Kymeta, ViaSat). However, as we scale in frequency, the complexity and efficiency of the feeding network limits the use of this technology in THz range in terms of cost and power consumption. For RIS to become viable for the wide range of scenarios proposed in literature, it must be composed of mostly passive components without requiring high-cost active components such as power amplifiers to result in low implementation cost and energy consumption.

The current main challenge is to find proper reconfigurable THz technologies, which will be one of the aims of this project. Another challenge of operating in the THz regime are the high path losses that limit the link range of these surfaces (as shown in the link budget calculation examples). To counteract this effect, two approaches must be followed: i) increase the source power; ii) increase the gain of the RIS. The power available by the state-of-the-art transmitters of THz modulated signals are still limited in many applications, further extending the need for hardware development (which is also a topic to be addressed in this project). For increasing the aperture gain, this implies the use of very large panels in terms of wavelengths that add additional stress to the energy consumption and cost requirements. Moreover, working with very narrow (directive) beams imposes additional challenges regarding the alignment and frequency stability. This project will also address the problem of scalability. As planar aperture the visibility region of RIS is limited by the cosine law, which impose additional limitation for the deployment scenarios. For instance, 60-degree beam scanning relative to the RIS boresight direction, implies a reduction of 3dB of effective area. Finally, the number of available phase states, that depends on the RIS hardware implementation, introduces additional performance degradation (corresponding L_Q factor used in link budget calculation). In this project these hardware related limitations will be included in the high-level models that will be used for channel characterization, allowing a more realistic assessment of the THz RIS.

For better illustrating some of these challenges, we present the performance of an idealized RIS aperture of size 32 mm operating at 140 GHz. This was obtained using the classical geometric and physical optics framework and considering analytical amplitude and phase distribution that represent the RIS outgoing radiated fields of a tilted plane wave at 45 degrees. Even in this idealize case, we can

see in Figure 8-10 how beam point direction dependence with frequency (effect designated as beam squint) can affect the directivity for a given position. In Figure 8-11, we show that the number of phase bits can play an important role to increase the aperture efficiency.

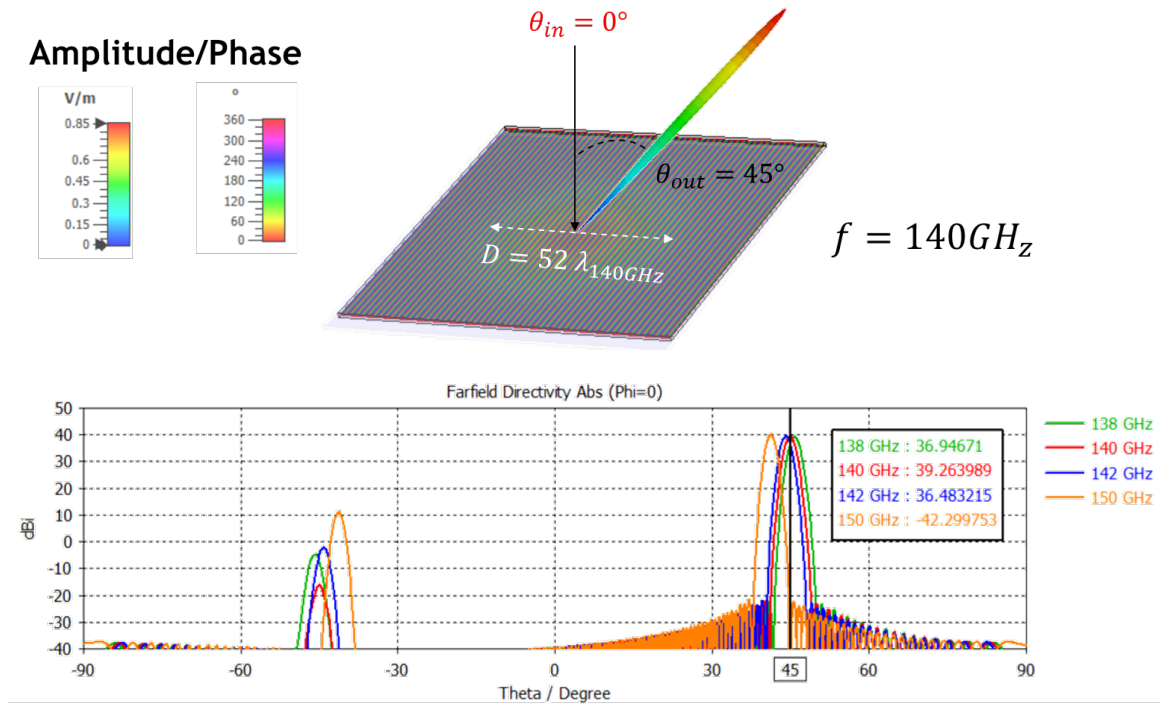


Figure 8-10: Directivity of an idealized RIS aperture that redirects the incoming beam (considered as plane wave) to a 45-degree plane wave as function of frequency.

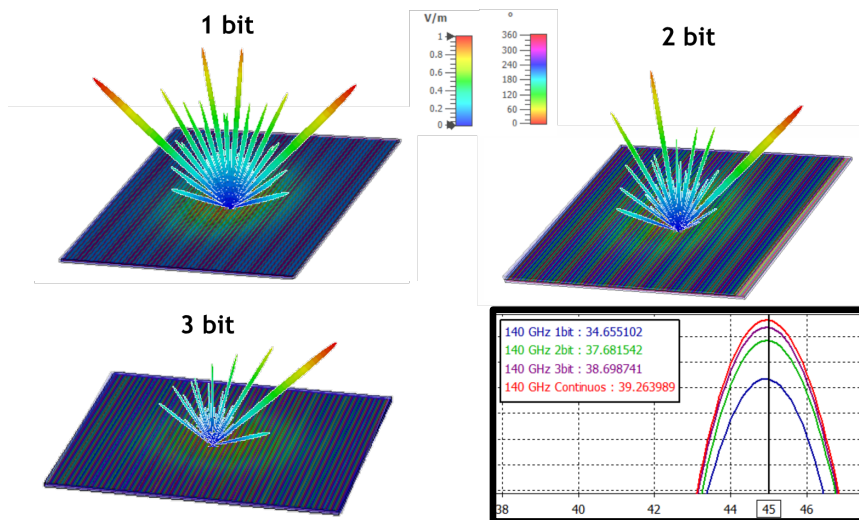


Figure 8-11: Directivity of an idealized RIS aperture that redirects the incoming beam (considered as plane wave) to a 45-degree plane wave for different phase quantization steps (1 to 3 bit).

8.3. THz Hardware Components

8.3.1. RIS Element and Structure Design

The type of RIS, from hardware point of view, is more related to the tuning technology that is applied to fabricated RIS. It is worth noting that the choice of the most suitable tuning technology to be adopted is highly dependent on the target frequency of each application. As shown in Figure 8-12, most of popular approaches using pin diodes or varactors is suitable for microwave band up to 10 GHz, meanwhile some techniques using graphene or nonlinear materials are more suitable for higher frequency band above 1 THz. For RIS implementation, TERRAMETA mainly focuses on using CMOS-based and microfluidic-based tuning technologies.

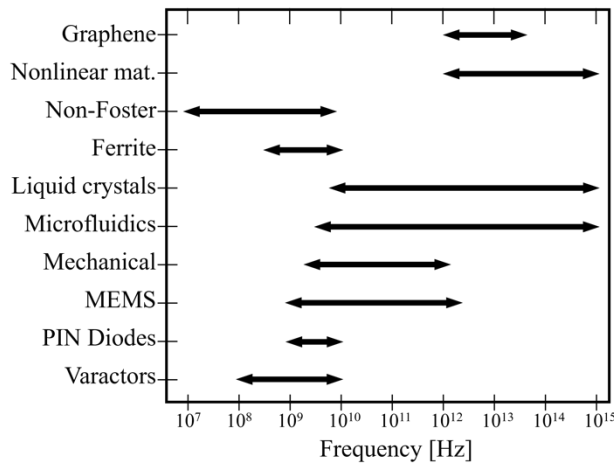


Figure 8-12 Reconfigurable technologies for implementing RIS versus operating.

8.3.1.1. CMOS-based Technology for THz

The enhancement of THz RIS performance will derive from careful choice of silicon technologies and, from novel wideband meta-atom designs (also called unit cell or element) with integrated switches. Meta-atom designs using both silicon wafer substrates and low-loss laminates will be investigated to increase the degrees of freedom and improve the maximum achievable performance. Most passive elements of the meta-atom are likely to be realized on the laminate to mitigate the narrowband behaviour due to the high permittivity on silicon, while switches and related circuits, and a few passive elements requiring very high processing accuracy can be integrated on the wafer. Radio-frequency silicon-on-insulator (RF-SOI) CMOS technology on 45 nm is associated with the use of high-resistivity substrates (resistivity of about 7.5 kΩ×cm), which is expected to enable the integration, at affordable costs, of antenna elements and low-loss MOS-based switches with R_{on} and C_{off} properties suitable for operation up to at least 300 GHz. Additionally, Silicon-Germanium (SiGe) BiCMOS technology, a simpler and cheaper alternative to RF-SOI will also be considered to achieve at least 140 GHz. Using this type of technology, local bias circuitry can be realized within each meta-atom. Therefore, each switch in each meta-atom can be individually controlled, offering unparalleled flexibility in the configuration of the RIS. Moreover, MOS-based switches lead to extremely low power consumption (in the order of tens of μW per meta-atom), as opposed to diodes (several mW per meta-atom). Indeed, they dissipate power only when changing or refreshing their logic state, but do not require a constant bias to hold the state. The outcome of this study in TERRAMETA will lead to the lowest loss and power consumption design compared to the state of the art. A relatively fine phase resolution over the entire 360° range (e.g., a 3-bit uniform quantization) will be targeted, leveraging on the possibility to integrate several switches in each meta-atom. The successful demonstration of such a RIS would outperform state-of-the-art designs, which mostly rely on coarse phase quantization or do not cover the entire phase ranges [HYJ19].

8.3.1.2. Microfluidic-based technology for THz

Besides implementing meta-atom designs using wafer technology, another promising technology pursued in this project is the microfluidic-based technology. This technology is expected to provide high speed phase changes in the THz band due to the smaller required displacements using smaller amounts of liquid metal to result in phase change of these meta-atoms. It is expected that liquid displacement speeds of between 10 and 100 mm/s can be maintained (and is frequency independent). This translates to a high liquid displacement speed of between 3 λ /s to 30 λ /s in the THz band. The proposed technology features individual unit-cell control using low power consumption (e.g., piezoelectric actuators). Liquid metal will be embedded into channels integrated in low loss polymeric substrates (e.g., polyamide) and will be moved within these channels. Low power consumption actuators integrated within the structure to tune/switch phases will provide low power and fine resolution to enable comprehensive and continuous phase changes at the meta-atom level, potentially resulting in a truly holographic beamforming ability. The envisioned liquid-based reconfiguration will significantly extend the tuning range due to its extensive structural reshaping capability, a property which is unique to this technology for the THz band.

8.3.1.3. A High-power THz Transceiver Option

The advantages of the use of THz together with RIS to provide a solution to different use cases have been shown in previous sections, clearly proving their superiority in comparison to already existing standards, like Wi-Fi or 5G. In the scope of beyond 5G and 6G development, the frequency range between 100 GHz and 300 GHz is targeted, enabling the needs of a series of novelties in terms of hardware development. The THz transmitter required for the demonstration of THz RIS relies on the know-how in THz high-power sources and THz detection technology, which should be capable to support the previously calculated link budgets, providing solutions to some of the proposed use cases. In particular, the THz sources at 150 GHz are required to provide 20 dBm as typical transmitted output power, whereas in the range of 285 GHz 18 dBm are available. The typical performance of these high-power THz sources are depicted in Figure 8-13 and Figure 8-14.

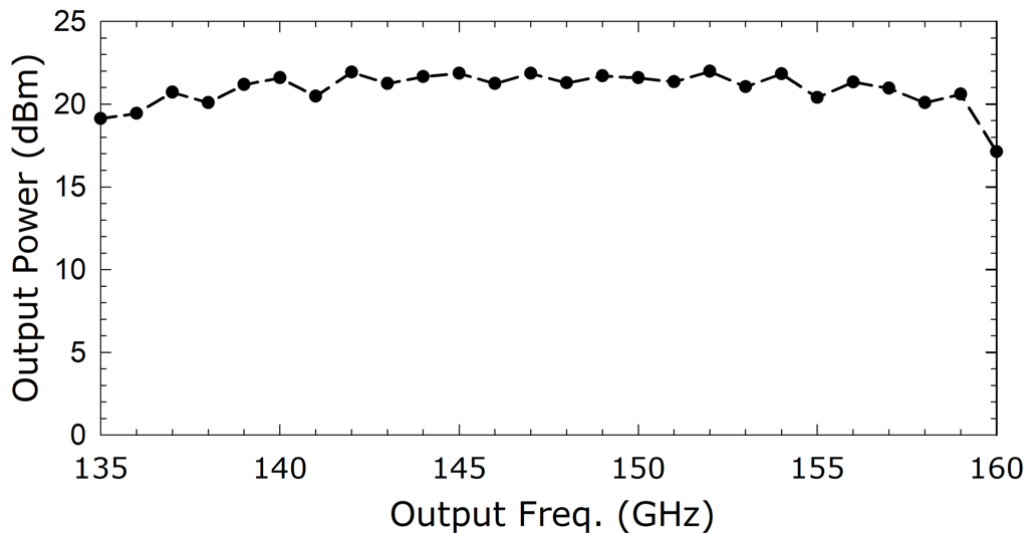


Figure 8-13 Output Power @150 GHz

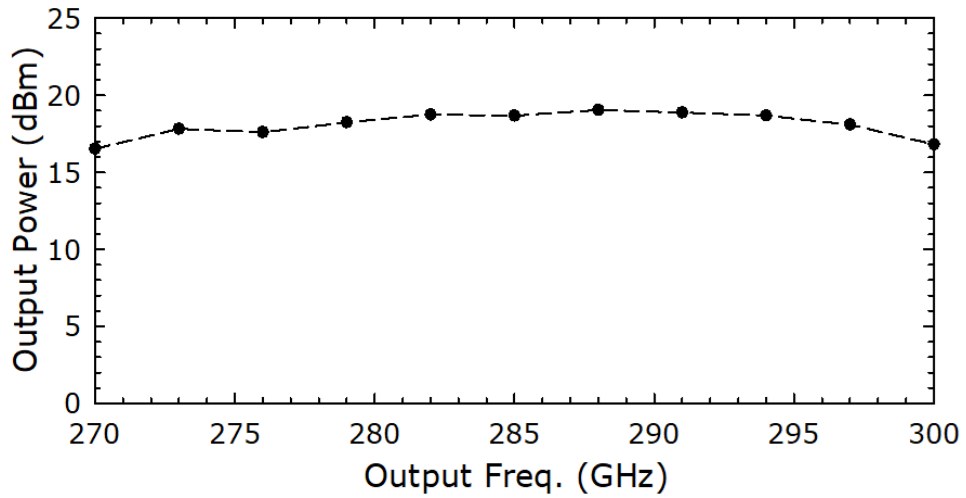


Figure 8-14 Output Power @285 GHz

Furthermore, the specified THz transmitters have large available bandwidths at both 150 GHz and 285GHz are clearly beneficial to achieve higher throughput levels. More detailed specifications for the sources at these frequency ranges are detailed in Table 9.

Table 9 Specifications of ACST’s sources between 110 GHz and 370 GHz

	@150 GHz	@285 GHz	Full D-Band	Full WR-3.4	Full WR-4.3
Output Frequency (GHz)	140 – 158	270 – 300	110 – 170	220 – 330	250 – 370
Typical Output Power (dBm)	21	18	10	4	4
Input Frequency (GHz)	11.5 – 13.12	11.25 – 12.5	13.75 – 21.25	12.22 – 18.33	13.88 – 20.55
Input Power (dBm)	0	0	4	4	4
Antenna Gain (dBi)	24	24	24	24	24

The use of a modulator is expected to reduce the transmitted output power by approximately 3 dB due to its insertion losses. However, this should not be a limiting factor in order to achieve the proposed link budgets for the targeted performance described in Section 8.1.

8.3.2. BBU Architecture for THz Communications

A common characteristic of several of the use-cases presented earlier (e.g., THz based backhauling, hybrid outdoor/indoor repeaters, outdoor deployments, short-hauling) is that they are expected to require transmission rates of the order of hundreds of Gbps while, particularly for the case of short-hauling and 6G THz backhauling (where the transport networks should

be able to support 6G peak data rates) transmission rates reaching 1 Tbps should be potentially supported. Achieving such target data rates calls for the use of spectrally efficient modulation schemes, e.g., Quadrature Amplitude Modulation (QAM) and the exploitation of Adaptive Coding and Modulation (ACM) such as to take advantage of favourable propagation conditions.

Taking into account the above, the research efforts will be on the implementation of a baseband unit leveraging on mmWave communications, using QAM and ACM and employing appropriate signal processing techniques, with capability to mitigate the impairments caused by the THz channel. The schematic diagram of the BBU is depicted in Figure 8-15.

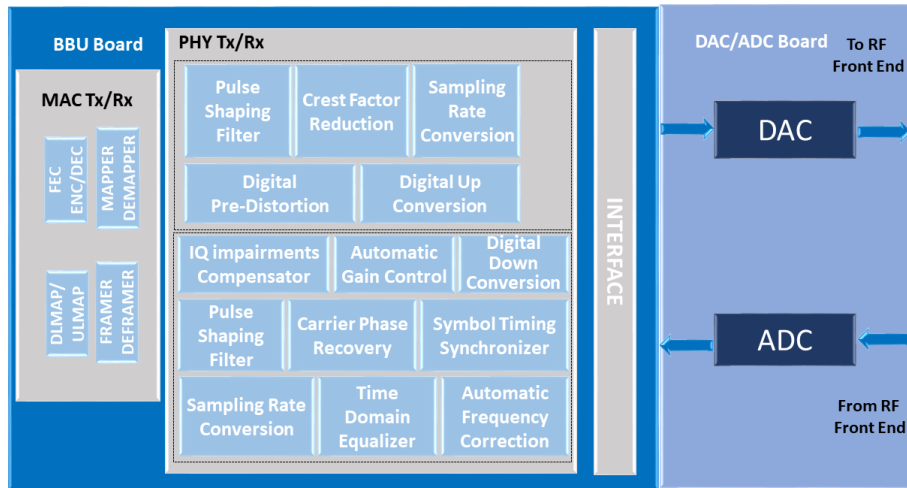


Figure 8-15 The architecture of BBU.

As it can be seen from Figure 8-15, the BBU will be based on a dedicated FPGA board. The operations applied at the transmitter side will include the encapsulation of Ethernet packets inside wireless transmission frames and the coding of these frames using Forward Error Correction (FEC) codes and formats up to 256-QAM. The signal processing applied at the receiver will include clock recovery, equalization, impairment cancellation, phase recovery, symbol recovery, FEC decoding, and the extraction of the Ethernet packets. Some key characteristics of the BBU which will be developed are summarized in the following table, where it is seen that a bandwidth of 2 GHz will be employed, identical to the value used for link-budget calculations. Moreover, the adoption of QAM is aligned with the methodology applied during link-budget calculations, where the use of 4-QAM has been assumed.

Table 10 - Expected TERRAMETA BBU characteristics

<i>Expected TERRAMETA BBU characteristics</i>	
<i>Signal Bandwidth</i>	2 GHz
<i>Constellations</i>	M-QAM (up to M=256)
<i>Forward error correcting codes</i>	LDPC/Reed Solomon

8.4. RISs in Existing Network Architectures

8.4.1. Integration in O-RAN

The Open Radio Access Network (O-RAN) alliance aims to expand diversity and competition in the mobile infrastructure ecosystem by improving multi-vendor interoperability and enabling

hardware/software disaggregation. These changes help diversify technology supply chains and have a role to play in diversifying deployment models. This allows for the deployment of networks that are vendor-agnostic and also deployer-agnostic.

In [APK23], an O-RAN architecture was proposed for RIS-empowered systems, according to which the RAN elements are split into a Central Unit (CU), a Distributed Unit (DU), and a Radio Unit (RU). The proposed RAN controller can integrate with third-party applications which control specific RAN functions in an automatic manner, thus leading to various implementations for representative use cases. Additionally, the benefits of RAN disaggregation, is that disaggregation solutions allow for flexibility, that will be required based on the use-case. One such benefit is the ability to switch a low frequency RU to a THz RU. Such a deployment can be enhanced with new protocols that can be optimised to include different types of RISs, such as reflective, transmissive, and hybrid in terms of simultaneous reflecting and sensing, operating in THz frequencies with their actuators responding within few milliseconds.

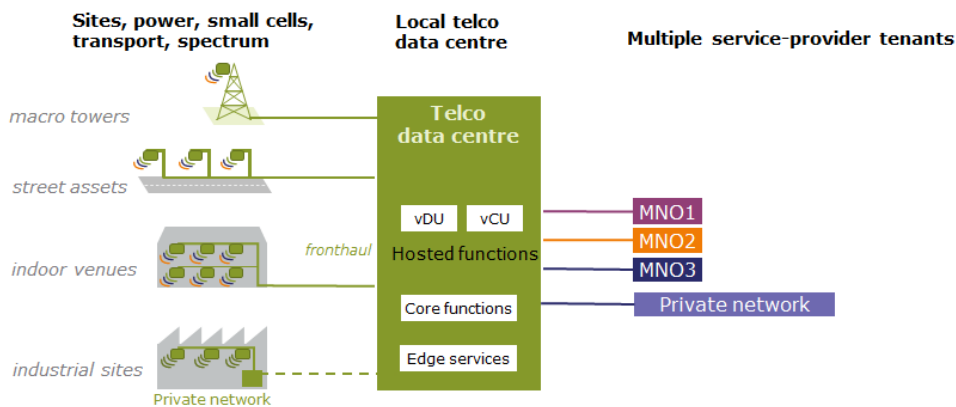


Figure 8-16 Hosted O-RAN solution for Neutral Hosts [SCF22].

Figure 8-16 presents an architectural framework for a flexible and modular platform to host MNOs, private networks, and other tenants. Sharing of common elements improves affordability for both the enterprise customer and the service provider. Hosted RAN is a 4G, 5G, and 6G small cell network architecture for neutral host operators and those that deliver services over a shared infrastructure. There are many options for service delivery which can become complicated, making it difficult to describe a network architecture or a system of networks. This is a conceptual model that simplifies the process and should help neutral host and shared network providers in 6G environments.

8.4.2. Integration in Industrial Networks

The network architecture for the industrial use case will align in general with IEEE 802.15.3d, meaning the design and implementation of the use case scenario and architecture will have more in common with WLAN networks as opposed to O-RAN networks. The 802.15.3d definitions are quite flexible, allowing many different types of THz RIS and hardware to be used as part of the network architecture. An example of the proposed architecture can be seen below in Figure 8-17. This figure shows an expanded view of the THz RIS system deployed across the factory floor. A “local cell” consists of an edge server providing 3D SLAM mapping and other processing services for the THz RIS-enabled devices in its locality, with connections to its adjacent local cells. This is to enable the creation of a fully realized semantic map of the entire factory floor in a distributed computing fashion, with mobile robots able to move seamlessly across the factory, transmitting their sensor information to the closest (or nearest visible) edge control server. The grid nature of the diagram aims to represent the use of pillars as the primary THz RIS deployment strategy mentioned in the use case section. A more detailed description of the architecture, including its integration with the hardware to be developed in the other WP’s of the project will be presented in the next WP2 deliverable.

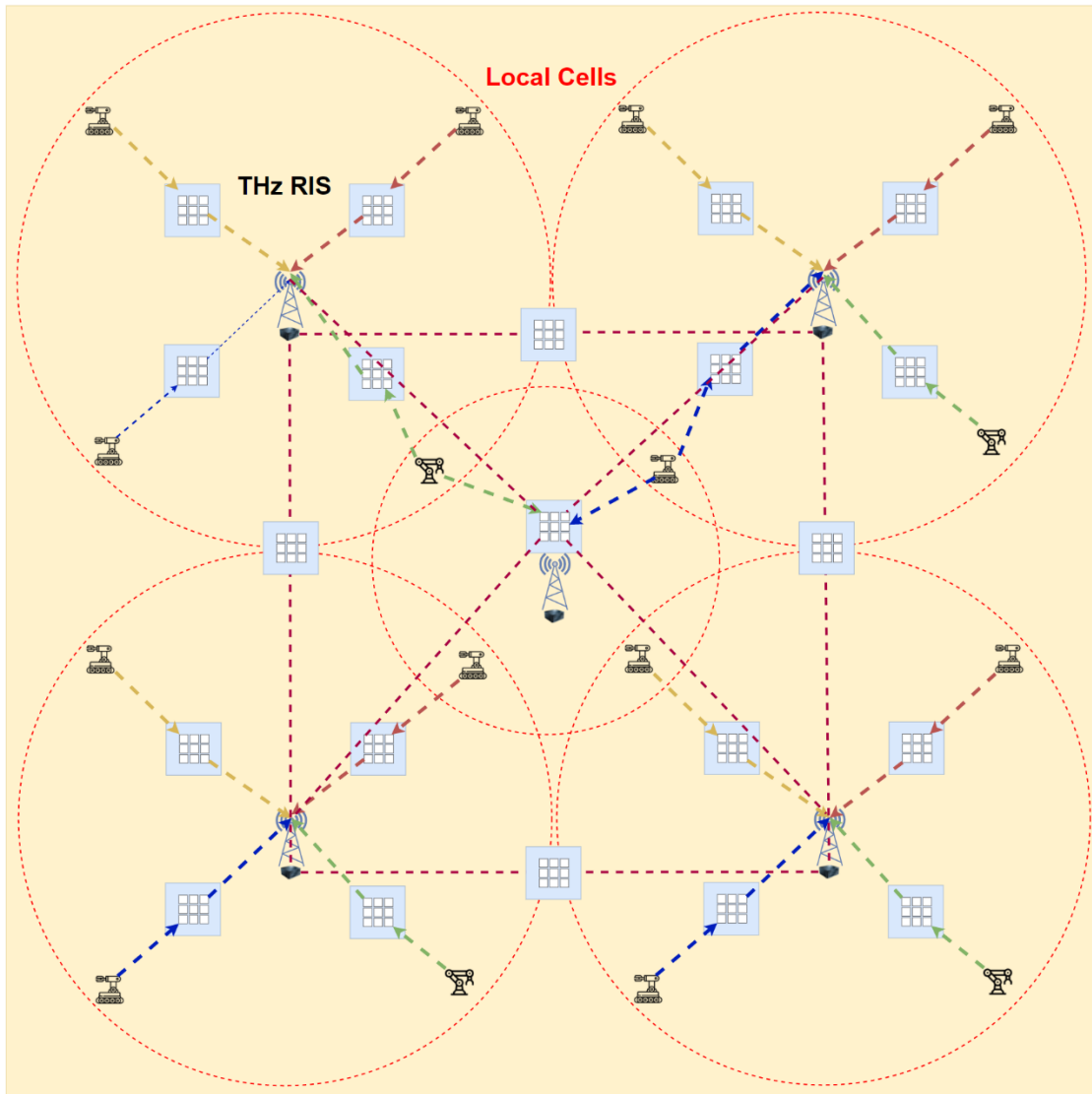


Figure 8-17 Possible Network architecture using pillar RIS deployment strategy.

9. Conclusion

This deliverable provides stable results collected in the first project months. In particular, the deliverable is aimed at identifying reference scenarios and use cases where THz RIS can play a role. In addition, relevant use-cases are also discussed. Such use cases are collected within different categories according to the expected achievable performance. We have illustrated the viability of both indoor industrial and outdoor radio access for 6G via the link budget calculations and the SNR for the established data rate requirements. The results of the link budget analysis prove that the minimum system SNR threshold for acceptable service is achievable for both indoor and outdoor use cases. This justifies their execution as part of WP6 and supporting technical work in the other WP's. Field-trial demonstrations will be performed based on WP2 outputs within WP6, with experienced problems, expected solutions, and achievable KPIs to be listed in the next WP2 deliverable to further validate all selected project proposed solutions.

This deliverable introduces the initial set of project scenarios and use cases that will provide the deployment options which we view as most promising in terms of the potential value and benefits they can bring to 6G mobile networks. The descriptions of the scenarios and use cases in this document are intended to be top level. This document represents the first version of the proposed project use cases. Updates and revisions on the use cases will be implemented through further releases of this document based on the progress of the TERRAMETA project.

10. References

- [AAS21] I. Alamzadeh, G. C. Alexandropoulos, N. Shlezinger, and M. F. Imani, "A reconfigurable intelligent surface with integrated sensing capability," *Nature Scientific Reports*, vol. 11, no. 20737, pp. 1–10, Oct. 2021.
- [AAI23] I. Alamzadeh, G. C. Alexandropoulos, and M. F. Imani, "Intensity-only OMP-based direction estimation for hybrid reconfigurable intelligent surfaces," *IEEE International Symposium on Antennas and Propagation and USNC-URSI Radio Science Meeting*, Portland, USA, 23–28 July 2023.
- [ACL21] S. Abadal, T. -J. Cui, T. Low and J. Georgiou, "Programmable Metamaterials for Software-Defined Electromagnetic Control: Circuits, Systems, and Architectures," in *IEEE Journal on Emerging and Selected Topics in Circuits and Systems*, vol. 10, no. 1, pp. 6-19, March 2020, doi: 10.1109/JETCAS.2020.2976165.
- [AKP21] C. D. Alwis et al., "Survey on 6G Frontiers: Trends, Applications, Requirements, Technologies and Future Research," in *IEEE Open Journal of the Communications Society*, vol. 2, pp. 836-886, 2021, doi: 10.1109/OJCOMS.2021.3071496.
- [AKX21] A. Araghi, M. Khalily, P. Xiao and R. Tafazolli, "Holographic-Based Leaky-Wave Structures: Transformation of Guided Waves to Leaky Waves," in *IEEE Microwave Magazine*, vol. 22, no. 6, pp. 49-63, June 2021, doi: 10.1109/MMM.2021.3064118.
- [APK23] G. C. Alexandropoulos *et al.*, " RIS-Enabled Smart Wireless Environments: Deployment Scenarios, Network Architecture, Bandwidth and Area of Influence," arXiv preprint arXiv: 2303.08505, 2023.
- [AV20] G. C. Alexandropoulos and E. Vlachos, "A hardware architecture for reconfigurable intelligent surfaces with minimal active elements for explicit channel estimation," in *Proc. IEEE International Conference on Acoustics, Speech, and Signal Processing*, Barcelona, Spain, 4–8 May 2020, pp. 9175–9179.
- [AVA17] A. Díaz-Rubio, V. S. Asadchy, A. Elsakka, S. A. Tretyakov, "From the generalized reflection law to the realization of perfect anomalous reflectors." *Science Advances*, vol. 3, no. 8), e1602714, 2017.
- [ASH22] G. C. Alexandropoulos, K. Stylianopoulos, C. Huang, C. Yuen, M. Bennis and M. Debbah, "Pervasive Machine Learning for Smart Radio Environments Enabled by Reconfigurable Intelligent Surfaces," in *Proceedings of the IEEE*, vol. 110, no. 9, pp. 1494-1525, Sept. 2022, doi: 10.1109/JPROC.2022.3174030.
- [B16] C. A. Balanis, "*Antenna theory: analysis and design*". John wiley & sons, 2016.
- [BDD19] E. Basar, M. Di Renzo, J. De Rosny, M. Debbah, M. -S. Alouini and R. Zhang, "Wireless Communications Through Reconfigurable Intelligent Surfaces," in *IEEE Access*, vol. 7, pp. 116753-116773, 2019.
- [BDS21] E. Björnson, Ö. T. Demir and L. Sanguinetti, "A Primer on Near-Field Beamforming for Arrays and Reconfigurable Intelligent Surfaces," 2021 55th Asilomar Conference on Signals, Systems, and Computers, Pacific Grove, CA, USA, 2021, pp. 105-112, doi: 10.1109/IEEECONF53345.2021.9723331.
- [BÖL20] E. Björnson, Ö. Özdogan and E. G. Larsson, "Reconfigurable Intelligent Surfaces: Three Myths and Two Critical Questions," in *IEEE Communications Magazine*, vol. 58, no. 12, pp. 90-96, December 2020, doi: 10.1109/MCOM.001.2000407.
- [BS20] E. Björnson and L. Sanguinetti, "Power Scaling Laws and Near-Field Behaviors of Massive MIMO and Intelligent Reflecting Surfaces," in *IEEE Open Journal of the Communications Society*, vol. 1, pp. 1306-1324, 2020, doi: 10.1109/OJCOMS.2020.3020925.
- [CGY14] Z. Chen, B. Guo, Y. Yang, and C. Cheng, 'Metamaterials-based enhanced energy harvesting: A review', *Physica B: Condensed Matter*, vol. 438, pp. 1–8, Apr. 2014.

- [CLN23]** Y. Cui, T. Lv, W. Ni and A. Jamalipour, "Digital Twin-Aided Learning for Managing Reconfigurable Intelligent Surface-Assisted, Uplink, User-Centric Cell-Free Systems," arXiv preprint arXiv:2302.05073, 2023.
- [CLS20]** S. Chen, Y. -C. Liang, S. Sun, S. Kang, W. Cheng and M. Peng, "Vision, Requirements, and Technology Trend of 6G: How to Tackle the Challenges of System Coverage, Capacity, User Data-Rate and Movement Speed," in *IEEE Wireless Communications*, vol. 27, no. 2, pp. 218-228, April 2020, doi: 10.1109/MWC.001.1900333.
- [CSA20]** M. Z. Chowdhury, M. Shahjalal, S. Ahmed and Y. M. Jang, "6G Wireless Communication Systems: Applications, Requirements, Technologies, Challenges, and Research Directions," in *IEEE Open Journal of the Communications Society*, vol. 1, pp. 957-975, 2020, doi: 10.1109/OJCOMS.2020.3010270.
- [CYZ23]** T. Chen, M. You, Y. Zhang, G. Zheng, J. B. Gros, G. Lerosey, Y. Nasser, F. Burton and G. Gradoni, "Model-free Optimization and Experimental Validation of RIS-assisted Wireless Communications under Rich Multipath Fading," arXiv preprint arXiv:2302.10561, 2023.
- [DDP19]** M. Di Renzo, M. Debbah, D.-T. Phan-Huy, A. Zappone, M.-S. Alouini, C. Yuen, V. Sciancalepore, G. C. Alexandropoulos, J. Hoydis, H. Gacanin, J. de Rosny, A. Bounceu, G. Lerosey, and M. Fink, "Smart radio environments empowered by AI reconfigurable meta-surfaces: An idea whose time has come," *EURASIP Journal on Wireless Communications and Networking*, 129, pp. 1–20, May 2019.
- [DMG23]** Demmer, David, Francesco Foglia Manzillo, Samara Gharbieh, Maciej Śmierzchalski, Raffaele D'Errico, Jean-Baptiste Doré, and Antonio Clemente. 2023. "Hybrid Precoding Applied to Multi-Beam Transmitting Reconfigurable Intelligent Surfaces (T-RIS)" *Electronics* 12, no. 5: 1162. <https://doi.org/10.3390/electronics12051162>.
- [dH20]** P. del Hougne, 'Robust position sensing with wave fingerprints in dynamic complex propagation environments', *Physical Review Research*, vol. 2, p. 043224, Nov. 2020.
- [EC19]** European Commission, "The European Green Deal", *Communication From The Commission To The European Parliament, The European Council, The Council, The European Economic And Social Committee And The Committee Of The Regions* (COM(2019) 640 final), Brussels, 11.12.2019.
- [ESN21]** Ericsson white paper, "Joint communication and sensing in 6G networks", Oct 2021, <https://www.ericsson.com/en/blog/2021/10/joint-sensing-and-communication-6g>
- [ETSI15]** ETSI white paper n. 10, "Maturity and field proven experience of millimeter wave transmission", Sept. 2015.
- [ETSI23]** ETSI white paper, "Reconfigurable Intelligent Surfaces (RIS); Use Cases, Deployment Scenarios and Requirements," – ETSI GR RIS 001, Apr. 2023.
- [GGJ23]** T. Gong, P. Gavrilidis, R. Ji, C. Huang, G. C. Alexandropoulos, L. Wei, Z. Zhang, M. Debbah, H. V. Poor, and C. Yuen, "Holographic MIMO communications: Theoretical foundations, enabling technologies, and future directions," under review, 2023.
- [GIS23]** I. Gavras, M. A. Islam, B. Smida, and G. C. Alexandropoulos, "Full duplex holographic MIMO for near-field integrated sensing and communications," under review, 2023.
- [H20]** C. Huang *et al.*, "Holographic MIMO Surfaces for 6G Wireless Networks: Opportunities, Challenges, and Trends," in *IEEE Wireless Communications*, vol. 27, no. 5, pp. 118-125, October 2020, doi: 10.1109/MWC.001.1900534.
- [HAC16]** Hasan, Mehdi & Arezoomandan, Sara & Condori, Hugo & Sensale, Berardi. (2016). Graphene terahertz devices for communications applications. *Nano Communication Networks*. 10. 10.1016/j.nancom.2016.07.011.
- [HSD21]** H. Tataria, M. Shafi, A. F. Molisch, M. Dohler, H. Sjöland and F. Tufvesson, "6G Wireless Systems: Vision, Requirements, Challenges, Insights, and Opportunities," in *Proceedings of the IEEE*, vol. 109, no. 7, pp. 1166-1199, July 2021, doi: 10.1109/JPROC.2021.3061701.

- [HWL22]** C. Han et al., "Terahertz Wireless Channels: A Holistic Survey on Measurement, Modeling, and Analysis," in *IEEE Communications Surveys & Tutorials*, vol. 24, no. 3, pp. 1670-1707, thirdquarter 2022, doi: 10.1109/COMST.2022.3182539.
- [HY2017]** H. Yang et al., "A Study of Phase Quantization Effects for Reconfigurable Reflectarray Antennas," in *IEEE Antennas and Wireless Propagation Letters*, vol. 16, pp. 302-305, 2017, doi: 10.1109/LAWP.2016.2574118.
- [HYJ19]** S. He, H. Yang, Y. Jiang, W. Deng, and W. Zhu, "Recent advances in MEMS metasurfaces and their applications on tunable lens," *Micromachines*, vol. 10, no. 8, 2019, doi: 10.3390/mi10080505.
- [HYM22]** L. Han, H. Yin and T. L. Marzetta, "Coupling Matrix-based Beamforming for Superdirective Antenna Arrays," *ICC 2022 - IEEE International Conference on Communications*, Seoul, Korea, Republic of, 2022, pp. 5159-5164, doi: 10.1109/ICC45855.2022.9838533.
- [HZA19]** C. Huang, A. Zappone, G. C. Alexandropoulos, M. Debbah and C. Yuen, "Reconfigurable Intelligent Surfaces for Energy Efficiency in Wireless Communication," *IEEE Transactions on Wireless Communications*, vol. 18, no. 8, pp. 4157-4170, Aug. 2019.
- [ITU-P.676]** ITU, "Attenuation by atmospheric gases and related effects", Report – P.676, Aug. 2022.
- [ITU-P.838]** ITU, "Specific attenuation model for rain for use in prediction methods", Report – P.838, Mar. 2005.
- [JAB22]** M. Jian *et al.*, "Reconfigurable intelligent surfaces for wireless communications: Overview of hardware designs, channel models, and estimation techniques," in *Intelligent and Converged Networks*, vol. 3, no. 1, pp. 1-32, March 2022, doi: 10.23919/ICN.2022.0005.
- [JDE19]** B. K. Jung, N. Dreyer, J. M. Eckhard and T. Kürner, "Simulation and Automatic Planning of 300 GHz Backhaul Links," *2019 44th International Conference on Infrared, Millimeter, and Terahertz Waves (IRMMW-THz)*, Paris, France, 2019, pp. 1-3, doi: 10.1109/IRMMW-THz.2019.8873734.
- [JA11]** J. M. Jornet and I. F. Akyildiz, "Channel Modeling and Capacity Analysis for Electromagnetic Wireless Nanonetworks in the Terahertz Band," in *IEEE Transactions on Wireless Communications*, vol. 10, no. 10, pp. 3211-3221, October 2011, doi: 10.1109/TWC.2011.081011.100545.
- [JHH21]** W. Jiang, B. Han, M. A. Habibi and H. D. Schotten, "The Road Towards 6G: A Comprehensive Survey," in *IEEE Open Journal of the Communications Society*, vol. 2, pp. 334-366, 2021, doi: 10.1109/OJCOMS.2021.3057679.
- [JK21]** B. K. Jung and T. Kürner, "Automatic Planning Algorithm of 300 GHz Backhaul Links Using Ring Topology," *2021 15th European Conference on Antennas and Propagation (EuCAP)*, Dusseldorf, Germany, 2021, pp. 1-5, doi: 10.23919/EuCAP51087.2021.9411010.
- [JK23]** B. K. Jung and T. Kürner, "Simulation and Automatic Planning of NLoS Backhaul Links at 300 GHz using Ring Topology," *2023 17th European Conference on Antennas and Propagation (EuCAP)*, Florence, Italy, 2023, pp. 1-5, accepted.
- [KCW23]** S. Kosulnikov, F. S. Cuesta, X. Wang and S. A. Tretyakov, "Simple Link-Budget Estimation Formulas for Channels Including Anomalous Reflectors," in *IEEE Transactions on Antennas and Propagation*, doi: 10.1109/TAP.2023.3264982.
- [KJ21]** T. Kürner and B. K. Jung, "Automatic Planning of NLOS Backhaul Links at 300 GHz arranged in Star Topology," *2021 XXXIVth General Assembly and Scientific Symposium of the International Union of Radio Science (URSI GASS)*, Rome, Italy, 2021, pp. 1-3, doi: 10.23919/URSIGASS51995.2021.9560305.
- [KO23]** S. K. A. Kumar and E. J. Oughton, "Infrastructure Sharing Strategies for Wireless Broadband," in *IEEE Communications Magazine*, doi: 10.1109/MCOM.005.2200698.
- [LKT23]** F. Liu, D. -H. Kwon and S. Tretyakov, "Reflectarrays and Metasurface Reflectors as Diffraction Gratings: A tutorial," in *IEEE Antennas and Propagation Magazine*, vol. 65, no. 3, pp. 21-32, June 2023, doi: 10.1109/MAP.2023.3236278.

- [LLM21]** Y. Liu *et al.*, "Reconfigurable Intelligent Surfaces: Principles and Opportunities," in *IEEE Communications Surveys & Tutorials*, vol. 23, no. 3, pp. 1546-1577, thirdquarter 2021.
- [LLP21]** R. Long, Y. -C. Liang, Y. Pei and E. G. Larsson, "Active Reconfigurable Intelligent Surface-Aided Wireless Communications," in *IEEE Transactions on Wireless Communications*, vol. 20, no. 8, pp. 4962-4975, Aug. 2021, doi: 10.1109/TWC.2021.3064024.
- [LMX21]** Y. Liu *et al.*, "STAR: Simultaneous Transmission and Reflection for 360° Coverage by Intelligent Surfaces," in *IEEE Wireless Communications*, vol. 28, no. 6, pp. 102-109, December 2021, doi: 10.1109/MWC.001.2100191.
- [OWM15]** G. Oliveri, D. H. Werner, and A. Massa, "Reconfigurable electromagnetics through metamaterials—a review," *Proceedings of the IEEE*, vol. 103, no. 7, pp. 1034–1056, 2015.
- [PKH20]** V. Petrov, T. Kurner and I. Hosako, "IEEE 802.15.3d: First Standardization Efforts for Sub-Terahertz Band Communications toward 6G," in *IEEE Communications Magazine*, vol. 58, no. 11, pp. 28-33, November 2020, doi: 10.1109/MCOM.001.2000273.
- [RMG19]** J. -L. Romero-Gázquez, F. -J. Moreno-Muro, M. Garrich, M. -V. Bueno-Delgado, P. S. Khodashenas and P. Pavón-Mariño, "A Use Case of Shared 5G Backhaul Segment Planning in an Urban Area," *2019 21st International Conference on Transparent Optical Networks (ICTON)*, Angers, France, 2019, pp. 1-4, doi: 10.1109/ICTON.2019.8840257.
- [RPB23]** K. Rasilainen, T. D. Phan, M. Berg, A. Parssinen, and P. J. Soh, "Hardware Aspects of Sub-THz Antennas and Reconfigurable Intelligent Surfaces for 6G Applications" to be appeared in *IEEE Journal on Selected Areas*, 2023.
- [SAI21]** N. Shlezinger, G. C. Alexandropoulos, M. F. Imani, Y. C. Eldar and D. R. Smith, "Dynamic Metasurface Antennas for 6G Extreme Massive MIMO Communications," in *IEEE Wireless Communications*, vol. 28, no. 2, pp. 106-113, April 2021, doi: 10.1109/MWC.001.2000267.
- [SAW21]** E. C. Strinati *et al.*, "Reconfigurable, Intelligent, and Sustainable Wireless Environments for 6G Smart Connectivity," in *IEEE Communications Magazine*, vol. 59, no. 10, pp. 99-105, October 2021, doi: 10.1109/MCOM.001.2100070.
- [SBC19]** W. Saad, M. Bennis and M. Chen, "A Vision of 6G Wireless Systems: Applications, Trends, Technologies, and Open Research Problems," in *IEEE Network*, vol. 34, no. 3, pp. 134-142, May/June 2020, doi: 10.1109/MNET.001.1900287.
- [SCF22]** Small Cell Forum, "SCF245: Neutral Host Requirements", 2022.
- [SJ17]** K. T. Selvan and R. Janaswamy, "Fraunhofer and Fresnel Distances: Unified derivation for aperture antennas," in *IEEE Antennas and Propagation Magazine*, vol. 59, no. 4, pp. 12-15, Aug. 2017, doi: 10.1109/MAP.2017.2706648.
- [SKR20]** N. Slamnik-Kriještorac, H. Kremó, M. Ruffini and J. M. Marquez-Barja, "Sharing Distributed and Heterogeneous Resources toward End-to-End 5G Networks: A Comprehensive Survey and a Taxonomy," in *IEEE Communications Surveys & Tutorials*, vol. 22, no. 3, pp. 1592-1628, thirdquarter 2020, doi: 10.1109/COMST.2020.3003818.
- [SSK22]** U. Saeed *et al.*, "Intelligent Reflecting Surface-Based Non-LOS Human Activity Recognition for Next-Generation 6G-Enabled Healthcare System," *Sensors*, vol. 22, no. 19, p. 7175, Sep. 2022, doi: 10.3390/s22197175.
- [URB21]** M. A. Uusitalo *et al.*, "6G Vision, Value, Use Cases and Technologies From European 6G Flagship Project Hexa-X," in *IEEE Access*, vol. 9, pp. 160004-160020, 2021, doi: 10.1109/ACCESS.2021.3130030.
- [WGG21]** Z. Wan, Z. Gao, F. Gao, M. D. Renzo and M. -S. Alouini, "Terahertz Massive MIMO With Holographic Reconfigurable Intelligent Surfaces," in *IEEE Transactions on Communications*, vol. 69, no. 7, pp. 4732-4750, July 2021, doi: 10.1109/TCOMM.2021.3064949.
- [WHD20]** H. Wymeersch, J. He, B. Denis, A. Clemente and M. Juntti, "Radio Localization and Mapping With Reconfigurable Intelligent Surfaces: Challenges, Opportunities, and Research Directions," in *IEEE Vehicular Technology Magazine*, vol. 15, no. 4, pp. 52-61, Dec. 2020, doi: 10.1109/MVT.2020.3023682.

[WT21] W. Tang et al., "Wireless Communications With Reconfigurable Intelligent Surface: Path Loss Modeling and Experimental Measurement," in *IEEE Transactions on Wireless Communications*, vol. 20, no. 1, pp. 421-439, Jan. 2021, doi: 10.1109/TWC.2020.3024887.

[XCG20] L. Xu, L. Chen, Z. Gao, H. Moya and W. Shi, "Reshaping the Landscape of the Future: Software-Defined Manufacturing" in *Computer*, vol. 54, no. 07, pp. 27-36, 2021.

[ZDB22] H. Zhang, B. Di, K. Bian, Z. Han, H. V. Poor and L. Song, "Toward Ubiquitous Sensing and Localization With Reconfigurable Intelligent Surfaces," in *Proceedings of the IEEE*, vol. 110, no. 9, pp. 1401-1422, Sept. 2022, doi: 10.1109/JPROC.2022.3169771.

[ZFW19] B. Zong, C. Fan, X. Wang, X. Duan, B. Wang and J. Wang, "6G Technologies: Key Drivers, Core Requirements, System Architectures, and Enabling Technologies," in *IEEE Vehicular Technology Magazine*, vol. 14, no. 3, pp. 18-27, Sept. 2019, doi: 10.1109/MVT.2019.2921398.

[ZLX23] Z. Zhang et al., "Active RIS vs. Passive RIS: Which Will Prevail in 6G?," in *IEEE Transactions on Communications*, vol. 71, no. 3, pp. 1707-1725, March 2023, doi: 10.1109/TCOMM.2022.3231893.